Title
Novel Functions for Reelin Signaling in Mammary Gland Development and Breast Cancer Progression

Author
Khialeeva, Elvira R.

Publication Date
2016

Peer reviewed|Thesis/dissertation

UNIVERSITY OF CALIFORNIA

Los Angeles

Novel Functions for Reelin Signaling in Mammary Gland Development and Breast Cancer Progression

A dissertation submitted in partial satisfaction of the requirements for the degree Doctor of Philosophy in Molecular Biology

by

Elvira Radikovna Khialeeva

2016

ABSTRACT OF THE DISSERTATION

Novel Functions for Reelin Signaling in Mammary Gland Development and Breast Cancer Progression

by

Elvira Radikovna Khialeeva

Doctor of Philosophy in Molecular Biology

University of California, Los Angeles, 2016

Professor Ellen M. Carpenter, Chair

The reelin signaling pathway is a critical regulator of cell migration and positioning throughout the central nervous system. Recent studies identified non-neuronal functions for reelin, and reported alterations in reelin expression in cancers. It is not known whether the reelin signaling pathway plays a role in the development of the mammary gland or in progression of breast cancer. Using mice with mutations in *reelin* and *Disabled-1* (Dab1), the intracellular adaptor protein activated in response to the reelin signal, we showed that the reelin signaling pathway is required for correct ductal patterning during mammary gland morphogenesis. Reelin and Dab1 are expressed in the developing and the mature mammary duct in a complementary pattern. Mutations in *reelin* or *Dab1* resulted in delayed ductal elongation and disorganized mammary epithelium in mice. Mammary epithelial cells exhibited decreased migration in response to exogenous reelin in a Dab1-dependent manner *in vitro*. Using a syngeneic mouse mammary tumor transplantation model, we examined the effect of host-derived reelin on breast cancer progression. We found that transplanted tumors grew and metastasized more slowly in

reelin-deficient mice. Tumors grown in reelin-deficient animals had fewer blood vessels and increased macrophage infiltration. Loss of host-derived reelin altered the balance of M1- and M2-associated macrophage markers in primary tumors, suggesting that reelin may influence the polarization of tumor-associated macrophages. These results indicated an important function for the reelin protein in progression of breast cancer. Furthermore, we found that several alternatively spliced variants of Dab1 exist in the developing and the mature mammary gland. In addition, we showed that alternative splicing of Dab1 is spatially and temporally regulated during puberty, pregnancy, and lactation. Taken together, our findings suggest that the reelin signaling pathway is an essential regulator of mammary gland development and has critical functions in progression of breast cancer.

The dissertation of Elvira Radikovna Khialeeva is approved.

Karen M. Lyons

Patricia E. Phelps

Ellen M. Carpenter, Committee Chair

University of California, Los Angeles

2016

DEDICATION

To Joe

Parents Lala and Larry

Grandmother Bibinour

Uncle Rashit and Aunt Nela

TABLE OF CONTENTS

LIST OF FIGURES AND TABLES

ACKNOWLEDGMENTS

The work for this dissertation was performed under the direction of Dr. Ellen M. Carpenter. I would like to acknowledge Dr. Carpenter for providing me with outstanding mentorship throughout my graduate studies. In addition, I would like to thank my committee members Dr. Timothy F. Lane, Dr. Karen M. Lyons, Dr. Anna M. Wu, and Dr. Patricia E. Phelps for their guidance and support.

I am thankful to Dr. Cristina A. Ghiani, Dr. Steven J. Bensinger, and Dr. Steven M. Dubinett for guidance and helpful discussions.

I sincerely thank the undergraduate students whom I had the pleasure to work with since I joined the laboratory: Denise Allen, Joan Chou, Alec Chiu, Michelle Han, Cassandra Gonzalez, Kimberly Bui, and Diane Anthony.

I would like to acknowledge the UCLA Molecular Biology Interdepartmental Program and the Whitcome Predoctoral Training Program for providing me with financial assistance.

Chapter One

Chapter one is adapted with permission from Khialeeva, E., Lane, T. F., and Carpenter, E. M. (2011). Disruption of reelin signaling alters mammary gland morphogenesis. *Development.* **138**:767-776.

We thank Dr. John J. Colicelli and Dr. Patricia E. Phelps for helpful discussions and critical reading of the manuscript. We thank Diane Anthony for assistance with immunohistochemistry and cell counting, Jessie Philipps and Kimberly Bui for assistance with cell counting; Cassandra Gonzalez and Erin Kirkbride for assistance with RT-PCR; J. Han, Jennifer Stevens and Jenny Huang for assistance with immunohistochemistry; and Donna Crandall for assistance with figure preparation. This research was supported by the UCLA Stein/Oppenheimer Endowment and by grants from the NIH (HD061815) and the California Breast Cancer Research Program (161B-0110) to Dr. Ellen M. Carpenter.

Chapter Two

Chapter two is adapted from Khialeeva *et al*. Reelin deficiency delays mammary tumor growth and metastatic progression. This manuscript has been submitted and is currently under review. The full list of authors is as follows: Elvira Khialeeva, Joan W. Chou, Denise E. Allen, Alec M. Chiu, Steven J. Bensinger, Ellen M. Carpenter.

We thank Dr. Patricia E. Phelps, Dr. Cristina A. Ghiani, Dr. Catalina Abad Rabat and Dr. Diana Moughon for kindly providing reagents and for thoughtful discussion. We are thankful to Donna Crandall for assistance with figure preparation and Joseph Argus for critical reading of the manuscript. These studies were supported by the National Institute of Child Health and Development R03 HD075840 - https://www.nichd.nih.gov/Pages/index.aspx, and the California Breast Cancer Research Program 161B-0110 - http://www.cbcrp.org/ to Dr. Ellen M. Carpenter. Elvira Khialeeva was supported by the Whitcome Fellowship of the UCLA Molecular Biology Institute. The funders had no role in study design, data collection and analysis, decision to publish, or preparation of the manuscript.

Chapter Three

We thank Dr. Roseline Godbout and Dr. Mitsuharu Hattori for kindly providing reagents. We thank Denise Allen for assistance with cell isolation and RT-PCR, and the UCLA Sequencing Core for assistance with sequencing. These studies were supported by the National Institute of Child Health and Development R03 HD075840 to Dr. Ellen M. Carpenter. Elvira Khialeeva was supported by the Whitcome Fellowship of the UCLA Molecular Biology Institute.

VITA

Education

B.S., Bioengineering, UCLA. June 2008.

Experience

Graduate Student Researcher, University of California, Los Angeles (2010 – Present)
Advisor: Dr. Ellen M. Carpenter

- Established a crucial role for the reelin signaling pathway in proper development of the mammary gland using mice with mutations in *reelin* and the adaptor in the reelin pathway, *Disabled-1*.
- Discovered a role for reelin in progression of breast cancer using *in vivo* mammary tumor models. Found a novel function for reelin in regulating the tumor microenvironment by modulating tumor-associated macrophage activation.

Laboratory Assistant, University of California, Los Angeles (2008 – 2010)
Supervisor: Dr. Ellen M. Carpenter

- Evaluated the influence of reelin signaling on migration of mouse mammary epithelial cells.

Undergraduate Assistant, University of California, Los Angeles (2007 – 2008)
Supervisor: Dr. Jack W. Judy

- Performed *in vitro* experiments designed to assess feasibility of a MEMS-enabled catheter for hydrocephalus

Publications

B.R. Mullen, **E.Khialeeva**, D.B. Hoffman, C.A. Ghiani, E.M. Carpenter. (2013). Decreased reelin expression and organophosphate pesticide exposure alters mouse behavior and brain morphology. *ASN Neuro*. **5**: 27-42

S.A. Lee, H. Lee, J.R. Pinney, **E. Khialeeva**, M. Bergsneider, J.W. Judy. (2011). Development of microfabricated magnetic actuators for removing cellular occlusion. *J. Micromech. Microeng.* **21**:54006.

E. Khialeeva, T.F. Lane, E.M. Carpenter. (2011). Disruption of reelin signaling alters mammary gland morphogenesis. *Development.* **138**:767-776.

S.A. Lee, J.R. Pinney, **E. Khialeeva**, M. Bergsneider, J.W. Judy. (2008). Functional evaluation of magnetic microactuators for removing biological accumulation: An in vitro study. *Conf. Proc. IEEE Eng. Med. Biol. Soc*. **2008**:947-950.

E. Khialeeva, J.W. Chou, D.E. Allen, A.M. Chiu, S.J. Bensinger, E.M. Carpenter. Reelin deficiency delays mammary tumor growth and metastatic progression. *Manuscript submitted, under review.*

Presentations

E. Khialeeva, J. Chou, E.M. Carpenter. "Reelin deficiency in reeler Orleans mice delays mammary tumor growth and metastasis". Poster presentation at AACR Annual Meeting, Philadelphia, PA, April 2015.

E. Khialeeva, J. Chou, E.M. Carpenter. "Reelin signaling in the tumor microenvironment is required for metastasis of mammary carcinoma cells". Poster presentation at AACR Cellular Heterogeneity in the Tumor Microenvironment Conference, San Diego, CA, February 2014.

E. Khialeeva. "Reelin signaling in tumor microenvironment promotes metastatic behavior of mammary carcinoma cells". Oral presentation at Gordon Research Seminar on Mammary Gland Biology, Stowe, VT, June 2013.

E. Khialeeva, E.M. Carpenter. "Reelin signaling in tumor microenvironment promotes metastatic behavior of mammary carcinoma cells". Poster presentation at Gordon Research Conference on Mammary Gland Biology, Stowe, VT, June 2013.

E. Khialeeva. "Reelin signaling in tumor microenvironment promotes metastasis of breast cancer cells". Oral presentation at MBIDP Student Seminar, UCLA, Los Angeles, CA, June 2013.

E. Khialeeva. "Reelin – from development to breast cancer". Oral presentation at Embryology Club, UCLA, Los Angeles, CA, May 2013.

E. Khialeeva, E.M. Carpenter. "Functions of reelin signaling in mammary gland morphogenesis and breast cancer progression". Poster presentation at Gordon Research Conference on Mammary Gland Biology, Lucca (Barga) Italy, June 2012.

E. Khialeeva. "Role of reelin signaling in mammary gland development". Oral presentation at Embryology Club, UCLA, Los Angeles, CA, January 2012.

E. Khialeeva, E.M. Carpenter. "Mammary gland morphogenesis is altered following disruption in reelin signaling". Poster presentation at Society for Developmental Biology 69th Annual Meeting, Albuquerque, NM, August 2010.

Honors

- AACR Scholar-In-Training Award, supported by Aflac, Inc, 2014.
- Paul D. Boyer Outstanding Teaching Award, UCLA, 2013.
- Honorable Mention, National Science Foundation Graduate Research Fellowship Program, 2012.

INTRODUCTION

The reelin signaling pathway

The discovery of a mutation that caused impaired balance and side-to-side swaying in mice spurred intensive studies of what is currently known as the reelin signaling pathway (Falconer, 1951). The spontaneous mutation was termed '*reeler*', and resulted in a vast array of behavioral abnormalities, which include tremors, ataxia, and a 'reeling' gait, along with morphological alterations, including cerebellar hypoplasia, and disruption of neuronal layers in the cortex and the hippocampus (Falconer, 1951; D'Arcangelo, 2014). The *reelin* gene was cloned when molecular biology techniques became available, and the current understanding of reelin and other components of the signaling pathway stems mainly from neurobiological studies conducted in the last two decades (D'Arcangelo et al., 1995; Rice and Curran, 2001; Herz and Chen, 2006; D'Arcangelo, 2014).

Reelin is a large extracellular matrix glycoprotein, and functions via several mechanisms. Canonically, reelin binds to low-density lipoprotein receptors Apo E receptor 2 (ApoER2) and very low-density lipoprotein receptor (VLDLR) (Rice and Curran, 2001; Herz and Chen, 2006). The signal is relayed via the adaptor protein Disabled-1 (Dab1), which binds to the NPXY motifs on the intracellular portion of the reelin receptors. Binding of reelin to ApoER2 and VLDLR leads to phosphorylation of Dab1 by the Src family kinases Fyn and Src on specific tyrosine residues. Phosphorylated Dab1 then recruits downstream effectors such as Crk, Crk-like (CrkL), and phosphatidylinositide 3-kinase (PI3K), resulting in activation of several signaling cascades (Bock and Herz, 2003; Kuo et al., 2005; Honda et al., 2011). Mutations in genes involved in canonical reelin signaling result in identical deficits in the nervous system, and both *Dab1* mutants and the *ApoER2*/*Vldlr* double mutants display severe errors in cortical layering, loss of Purkinje cells with cerebellar hypoplasia, and ataxia (Rice and Curran, 2001). Recent evidence suggests that

reelin can function independently from the lipoprotein receptors and Dab1, but the alternative pathways are not well understood (Jossin et al., 2004; Lutter et al., 2012; Lee et al., 2014).

Given the prominence of the *reeler* phenotype in the central nervous system, it is not surprising that the initial studies of the reelin signaling pathway primarily focused on its importance in nervous system development. However, several investigators reported expression of reelin in non-neuronal tissues. Northern blot, RT-PCR, and *in situ* hybridization studies revealed expression of *reelin* mRNA in the spleen, liver, kidney, testis, and the interstitial region of the ovary (D'Arcangelo et al., 1995; Hirotsune et al., 1995, Ikeda and Terashima, 1997). Assessment of reelin expression in peripheral tissues by Western blot reported the presence of reelin protein in the plasma of humans, mice, and rats. Immunohistochemical studies showed that reelin protein was also present in the adrenal medulla, the pituitary, and in the adult liver (Smalheiser et al., 2000). These earlier studies did not detect gross morphological abnormalities in the organs outside of the nervous system in *reeler* $^{-/-}$ mice (Ikeda and Terashima, 1997). However, the expression of reelin protein in non-neuronal organs raised the possibility that the reelin signaling pathway was functional during the development of these tissues. In recent years, multiple studies have addressed the role for reelin signaling outside of the central nervous system, and provided evidence for distinct functions of the reelin signaling pathway in the development of the lymphatics, the small intestine, submandibular gland, cartilage, and bone. Reelin has been implicated in liver fibrosis and rheumatoid arthritis, and alterations in reelin levels are observed in multiple cancers. The subsequent sections of this introduction serve to summarize the evidence for the functions of reelin signaling in development and disease of non-neuronal tissues.

Reelin signaling in development of non-neuronal tissues

Lymphatics

Several studies identified reelin as a marker of lymphatic endothelial cells (LEC) (Hong et al., 2004; Samama et al., 2005; Norgall et al., 2007; Lutter et al., 2012). In contrast, blood endothelial cells do not express reelin. While the expression of reelin is specific to LECs in lymphatic arteries and more mature collecting lymphatic vessels, only the LECs of the latter secrete reelin into the extracellular matrix, suggesting that reelin signaling may be active in matured collecting vessels (Lutter et al., 2012).

Dermal lymphatic vessels of *reeler* $^{-/-}$ mice have a reduction in coverage by smooth muscle cells (SMC), and display irregular vessel diameters. On the contrary, *reeler* $^{-/-}$ mice have normal large collecting vessels of the mesentery, and the defects are thought to be specific to dermal collecting vessels. These defects lead to impaired lymphatic function, as the uptake of dyes injected intradermally is reduced in *reeler* $^{-/-}$ mice (Lutter et al., 2012). These data suggest that reelin is important for development of the lymphatic vasculature. Interestingly, *ApoER2* and *Vldlr* double mutants, as well as *Dab1* hypomorphs have normal lymphatic vessels (Lutter et al., 2012). Therefore, reelin is thought to promote lymphatic vessel development via non-canonical mechanisms.

The reduction in SMC coverage of lymphatic vessels in *reeler* $^{-/-}$ mice prompted the investigation of the possibility that reelin is involved in recruitment of SMCs to developing lymphatic vessels. In agreement with this hypothesis, contact of LECs with SMCs stimulated secretion of reelin into the extracellular matrix of collecting lymphatic vessels. In turn, reelin induced expression of monocyte chemoattractant protein-1 (*MCP1*) in SMCs. MCP1 recruits SMCs to lymphatic vessels, and therefore reelin acts by an autocrine mechanism in LECs to promote SMC recruitment (Lutter et al., 2012).

Studies of Kaposi's sarcoma and lymphangioma further confirmed the specificity of reelin expression in LECs. Kaposi's sarcomas are caused by infections with Kaposi's sarcoma-

associated herpesvirus (KSHV). The neoplastic cells display characteristics of the lymphatic endothelium and express several lymphatic lineage markers. KSHV infection of human umbilical vein endothelial cells resulted in lymphatic reprogramming of these cells with induction of lymphatic-specific genes, including *RELN* (Hong et al., 2004). Lymphangiomas are benign malformations of the lymphatic vessels, and LECs from lymphangiomas have higher levels of reelin than blood endothelial cells (Norgall et al., 2007). It is currently not known whether reelin functionally contributes to these pathologies.

Submandibular gland

Expression of the reelin receptor *Vldl*r was reported in the end buds of the submandibular gland. The end buds contain highly proliferative cells and contribute to branching morphogenesis. Although *reelin* is normally expressed at low levels in the end buds, studies of miR-200c, a micro-RNA that targets VLDLR and reelin, uncovered a possible role for the reelin signaling pathway in modulating epithelial cell proliferation during the development of the submandibular gland (Rebustini et al., 2012).

MiR-200c is downregulated in invasive cancers, and normally functions to inhibit epithelial to mesenchymal transition and cell proliferation. MiR-200c is expressed in the end buds of the submandibular gland along with VLDLR. Loss of miR-200c results in higher number of end buds, an increase in FGF10-dependent proliferation of epithelial cells, and elevated expression of the target genes *Vldlr* and *reelin*. Treatment of the end buds with reelin stimulated branching morphogenesis and epithelial cell proliferation, mimicking miR-200c loss-of-function phenotypes. Interestingly, Akt phosphorylation was unaffected by treatment of submandibular gland epithelial cells with reelin, but an increase in mitogen-activated protein kinase (MAPK) phosphorylation was observed instead. Reelin signaling via VLDLR is proposed to help regulate proliferation and differentiation of epithelial end bud cells in the submandibular gland (Rebustini et al., 2012).

Small intestine

The epithelium of the small intestine has a high turnover rate, and is subject to rapid renewal. The proliferating stem cells are located in the crypts, and differentiation occurs once the progenitor cells reach the villus. Reelin is expressed in the myofibroblasts located beneath the intestinal epithelium. Dab1 and VLDLR are expressed in crypt and villus cells, while ApoER2 is found in the upper half of the villi, but is absent from the crypt cells (García-Miranda et al., 2010).

Microarray analysis of intestinal epithelial cells from *reeler* $^{-/-}$ mice revealed alterations in expression of genes associated with metabolism, membrane transport, and the inflammatory response (García-Miranda et al., 2012). *Reeler* $^{-/-}$ mice exhibit reduced cell proliferation in the crypts, leading to slower cell migration along the villi. The *reeler* $^{-/-}$ intestinal epithelium has fewer apoptotic cells and fewer differentiated Paneth cells, while the numbers of goblet cells remain unchanged. The length and number of villi are unaffected in the absence of reelin, and the tight junctions remain intact (García-Miranda et al., 2013). Analysis of the small intestine of *Dab1* hypomorph mice revealed alterations that were similar to those observed in *reeler* $^{-/-}$ mice (Vázquez-Carretero et al., 2014). These data suggest that the canonical reelin signaling pathway may function to support stem cell proliferation and the stability of the crypt-villus unit in the small intestine.

Cartilage and bone

Recent studies showed that the reelin signaling pathway plays a role in limb development. Reelin and Dab1 are expressed in the undifferentiated limb mesoderm, and their levels decrease prior to interdigital cell death, which is necessary for digit formation (Díaz-Mendoza et al., 2013). The reelin receptors *ApoER2* and *Vldlr* are also expressed in the developing limb cartilage and tendons (Díaz-Mendoza et al., 2014).

Analysis of the reelin signaling pathway components in micromass cultures of limb skeletogenic progenitors by qPCR showed that levels of *reelin*, *Dab1* and *ApoER2* decrease as the cartilage undergoes differentiation, while expression of *Vldlr* follows the opposite pattern (Díaz-Mendoza et al., 2014). Reelin expression in the limb is upregulated in response to fibroblast growth factor 2 (FGF2), a cell survival factor, and downregulated in response to bone morphogenetic protein 7 (BMP7), which induces apoptosis. *Dab1* silencing in micromass cultures reduced chondrogenesis and induced cell death, with decreased phosphorylation of Akt and lower levels of focal adhesion kinase (FAK) (Díaz-Mendoza et al., 2013; Díaz-Mendoza et al., 2014). In addition, silencing of *Dab1* in limb ectoderm-mesoderm recombinants resulted in the absence of cartilage and tendon differentiation. Together, these data suggest that the reelin signaling pathway in the embryonic limb is involved in interdigital cell death, and may regulate chondrogenesis in the developing limb. These functions of reelin may be redundant with other pathways regulating limb development, since reelin signaling pathway mutants are not known to have syndactyly or other limb abnormalities (Díaz-Mendoza et al., 2013; Díaz-Mendoza et al., 2014).

Reelin expression in cartilage increases upon injury and in diseased tissue. Patients with rheumatoid arthritis have increased serum and synovial fluid reelin compared to patients with other joint pathologies (Magnani et al., 2010). Reelin is upregulated in the chondrocytes of the injured cartilage following surgically induced osteoarthritis in rats, as well as in differentiating chondrocytes (Appleton et al., 2007). The authors suggested possible involvement of reelin in mechanisms that are responsible for hypertrophic differentiation of chondrocytes in osteoarthritis, but additional studies are needed to confirm this hypothesis.

In addition to its role in the development of cartilage, reelin signaling may be active in bone cells. Reelin is secreted in the mouse inner ear, and *RELN* transcripts have been detected in the human stapes footplate (Schrauwen et al., 2009). Osteocytes, the mechanosensing cells of the bone, express higher levels of reelin than osteoblasts (Paic et al., 2009; Ma et al., 2014).

Moreover, reelin is differentially expressed in appendicular and axial skeletons. Elevated expression of *reelin* is observed in ulnar limb bones compared to parietal skull bone, and may contribute to mechanosensory adaptation mechanisms of the limb (Rawlinson et al., 2009).

Corticosterone is a hormone produced in response to stress and has been shown to induce bone loss. Treatment of a murine osteocyte cell line MLO-Y4 with corticosterone resulted in elevated reelin expression (Ma et al., 2012). In addition, several single nucleotide polymorphisms (SNPs) in the *RELN* gene are associated with otosclerosis, a form of hearing loss due to abnormal bone remodeling in the otic capsule (Schrauwen et al., 2009). Thus, reelin may be associated with mechanosensory properties of the bone, and may have roles in bone-related pathologies, but the mechanisms of reelin signaling in bone development and homeostasis are not known.

Odontoblasts

Reelin and *Dab1* mRNA are expressed during different stages of odontogenesis. Dab1 expression declines after embryonic day 13.5 (E13.5), while reelin expression persists in differentiating odontoblasts through E18.5 (Heymann et al., 2001). Human secretory odontoblasts also express reelin (Buchaille et al., 2000; Bleicher et al., 2001; Maurin et al., 2004). VLDLR and Dab1 are expressed in the dental pulp and in the trigeminal ganglion, which innervates the odontoblast region during tooth development (Maurin et al., 2004; Magloire et al., 2009). In co-cultures of rat trigeminal ganglion and human odontoblasts, reelin was colocalized with nerve fiber endings, indicating that reelin may be involved in dentine innervation by signaling to the receptors and Dab1 in the trigeminal ganglion (Maurin et al., 2004; Magloire et al., 2009).

Reelin signaling activity in non-neuronal tissues

Blood

Initially, liver cells secreting reelin into the circulation were proposed as the major source of reelin found in the blood plasma (Smalheiser et al., 2000). Further studies defined *RELN* as an erythroid-enriched gene, and confirmed that blood cells, such as erythrocytes and platelets, also produce reelin protein (Jacquel et al., 2003; Redmond et al., 2008; Tseng et al., 2010; Redmond et al., 2011; Chu et al., 2014).

In heterozygous *reeler* $^{+/-}$ mice, levels of circulating reelin are half of those found in wild type littermates, and the protein is absent from the plasma of *reeler* $^{-/-}$ mice (Smalheiser et al., 2000). Interestingly, *reeler* $^{-/-}$ mice have higher red blood cell (RBC) counts compared to wild type controls, without changes in spleen size. Higher RBC numbers are also observed in the *reeler* $^{-/-}$ bone marrow, concomitant with attenuation of phosphorylated Akt (Chu et al., 2014). In addition, *reeler* $^{-/-}$ mice display impaired hemostasis, evidenced by prolonged bleeding time and a higher tendency to re-bleed in bleeding time assays, along with abnormalities in thrombin clot formation (Tseng et al., 2014).

The alterations in the blood of *reeler* $^{-/-}$ mice suggested novel roles for reelin in erythrocyte differentiation and the coagulation cascade. The importance of reelin in hemostasis was further evidenced by studies of the human chronic myelogenous leukemia (CML) cell line K562. Treatment of K562 cells with imatinib or sodium butyrate, both of which induce erythroid differentiation, increased expression of *RELN* mRNA and reelin protein (Jacquel et al., 2003; Chu et al., 2014). In line with findings of enhanced erythropoiesis in *reeler* $^{-/-}$ mice, knockdown of *RELN* enhanced erythroid differentiation of K562 cells. These data suggest that reelin negatively regulates erythroid differentiation (Chu et al., 2014). Additional evidence suggesting the involvement of reelin in erythropoiesis comes from studies of Krüppel-like factor 2 (KLF2), a transcription factor necessary for primitive erythroid development. KLF2 was found to directly

and positively regulate *reelin* expression. Moreover, *reelin* mRNA expression is downregulated in *KLF2* $^{-/-}$ embryonic erythroid cells (Redmond et al., 2011).

Reelin is also expressed by the platelets, and reelin-platelet interaction can enhance platelet spreading on fibrinogen (Tseng et al., 2010). Reelin is thought to stabilize binding of thrombin and factor Xa (FXa) to phosphatidylserine on the surface of activated platelets (Tseng et al., 2014). Together, these data suggest that reelin in the blood plasma functions to sustain hemostasis and may be involved in the coagulation cascade. It is not yet clear whether reelin elicits these functions via the canonical signaling cascade or employs alternative mechanisms.

Immune system

Possible effects of reelin on the immune response were initially proposed in earlier studies of mice with the *reeler* mutation. Modest hyperexpression of *IL-1β* mRNA was observed in peripheral macrophages from *reeler* $^{-/-}$ mice upon stimulation with lipopolysaccharide (LPS) (Kopmels et al., 1990; Bakalian et al., 1992). In addition, suppressed T cell and macrophage function were reported in *reeler* $^{-/-}$ mice following immunization of mice with sheep red blood cells (Green-Johnson et al, 1995). T cells from *reeler* $^{-/-}$ mice had attenuated proliferative responses to stimulation with anti-CD3 antibody, and produced lower levels of IL-2, IL-4, and interferon-γ (IFNγ) (Green-Johnson et al., 1995).

Recent *in vitro* studies of the RAW 264.7 mouse macrophage cell line implicated the reelin receptors ApoER2 and VLDLR in cholesterol transport. Treatment of RAW 264.7 cells overexpressing VLDLR and ApoER2 with reelin or ApoE, another ligand for these lipoprotein receptors, increased ATP binding transporter A1 (ABCA1) expression, which functions to export cholesterol. Reelin or ApoE treatment increased phosphorylation of Dab1 and PI3K, and silencing of *Dab1* in RAW macrophages prevented upregulation of ABCA1 (Chen et al., 2012). Moreover, the C-terminal region (CTR) of reelin is not required to generate these effects, as

treatment of cells with the receptor-binding reelin repeats lacking the CTR was sufficient to increase ABCA1 expression and cholesterol efflux (Okoro et al., 2015). Whether reelin contributes to macrophage cholesterol transport *in vivo* is unknown; this question remains to be addressed in future studies.

A microarray analysis of terminally differentiated plasma cells revealed higher levels of *reelin* than those observed in B cells (Underhill et al., 2003). Moreover, blood lymphocytes from *reeler* $^{-/-}$ mice displayed alterations in serotonin transporter (SERT) clustering. SERT clusters in these cells were more dispersed and larger in size than in the heterozygous or wild type controls. Thus, reelin was proposed to have a role in clustering of SERT in blood lymphocytes (Rivera-Baltanas et al., 2010).

Liver

The primary source of reelin in the liver is the hepatic stellate cell (HSC) population (Kobold et al., 2002, Samama et al., 2005; Botella-López et al., 2008; Mansy et al., 2014), while hepatocytes normally express low levels of reelin protein (Botella-López et al., 2008). Livers from *reeler* $^{-/-}$ mice do not display morphological abnormalities (Ikeda and Terashima, 1997). However, recent studies suggest possible roles for reelin in response to liver injury and fibrosis.

Upregulation of reelin expression was reported in activated murine HSCs (Magness et al., 2004), and in a rat liver fibrosis model (Botella-López et al., 2008). Levels of reelin in hepatocytes do not change in response to injury (Botella-López et al., 2008). Despite this, when hepatocyte proliferation was blocked by deletion of *damage specific DNA-binding protein 1* (*DDB1)*, *reelin* expression was upregulated in proliferating oval cells, the progenitor cell population in the liver (Endo et al., 2012).

Several lines of evidence suggest that reelin may be involved in liver fibrosis. Blood plasma from cirrhotic patients has higher levels of reelin (Botella-López et al., 2008). Reelin was proposed as a useful marker for progression of hepatic fibrosis in patients infected with hepatitis

C virus (HCV). Serum reelin levels of patients correlate with stages of hepatic fibrosis and with serum levels of hyaluronic acid, which is a marker of advanced fibrosis (Mansy et al., 2014). Activated HSCs in fibrotic human livers express reelin, and the number of reelin-positive HSCs is positively correlated with Knodell's score of histological activity. Dab1 in the liver is expressed by Ductular Reaction cells (DR). This expression pattern prompted the authors to propose that reelin may mediate activation of DR cells by HSCs (Carotti et al., 2015).

Endometrium and the ovarian follicle

Reelin expression was reported in the bovine endometrium and in the theca layer of the bovine follicle (Fayad et al., 2007; Cerri et al., 2012), while the reelin receptor ApoER2 is expressed in the granulosa cell layer (Fayad et al., 2007). A similar expression pattern is observed in the chicken follicle, where reelin is expressed in the theca layer, and the receptors VLDLR and ApoER2, as well as the adaptor Dab1 are expressed in granulosa cells of the chicken follicle (Eresheim et al., 2014).

Reelin expression is upregulated in the theca layer as the follicle approaches the end of the growth phase (Nivet et al., 2013). Moreover, chicken VLDLR and ApoER2 bind to murine reelin protein, and addition of mouse reelin to granulosa cell cultures results in activation of Dab1, phosphorylation of Akt, and increases proliferation of granulosa cells. Addition of receptor-associated protein (RAP), which blocks reelin binding to VLDLR and ApoER2, inhibits the effect on proliferation (Eresheim et al., 2014). Thus, reelin signaling may function between the theca and granulosa layers of the endometrium to stimulate proliferation and growth of the developing oocyte. Interestingly, *reelin* mRNA is downregulated in the endometrium of lactating pregnant cows compared to lactating cyclic (non-pregnant) cows (Cerri et al., 2012), but the functional significance of endometrial reelin in pregnancy and lactation is not known.

Reelin in cancer

The processes involved in tumorigenesis and cancer progression often employ the same pathways that are required for normal development. During organ development, the signaling pathways responsible for cell proliferation and epithelial to mesenchymal transition (EMT) are tightly regulated. In cancers, these mechanisms are altered and used to the advantage of the disease, supplying it with the tools necessary for cancer cells to grow and spread to distant organs. Thus, alterations in developmental pathways such as Notch, Wnt, Hedgehog, and TGF-beta often accompany tumorigenesis, EMT of epithelial tumors, and metastasis (reviewed in Bailey et al., 2007; Massagué, 2008; Barakat et al., 2010; Izrailit and Reedijk, 2012). As described above, the reelin signaling pathway is involved in cellular migration and cell proliferation during the development of multiple organs. In addition, reelin activates PI3K/Akt signaling, which is often hyperactivated in cancers (reviewed in Larue and Bellacosa, 2005; Thorpe et al., 2015). Similar to other developmental pathways, alterations in reelin expression are observed in cancers of neuronal and non-neuronal origin, as summarized in Table 1.

Reelin expression is reduced in cancers of many different tissues, and the downregulation is primarily due to hypermethylation of the *RELN* gene. This trend is observed in hepatocellular carcinoma, breast, gastric, and pancreatic cancers. Micro-RNAs have also been implicated in regulation of reelin levels in cancer. One known example is miR-128, which may contribute to loss of reelin expression in neuroblastoma. MiR-128 targets reelin, and overexpression of miR-128 reduced reelin protein levels in a neuroblastoma cell line (Evangelisti et al., 2009). *RELN* is frequently mutated in non-small cell lung cancer, and in T-cell precursor acute lymphoblastic leukemia, and these mutations may reduce the amount of functional reelin protein.

On the contrary, upregulation of reelin is observed in esophageal carcinoma, high-grade prostate cancer, and retinoblastoma. In addition, comparisons of metastatic colorectal lesions to

primary tumors, or invasive melanoma cells to a congenic non-invasive cell line show an increase in *RELN* expression in metastatic tumors and invasive cells. These data indicate that in some cancers upregulation of reelin may be necessary for metastatic progression.

Reelin signaling may be coupled with other signaling pathways employed in metastasis. For example, reelin was linked to TGFβ-induced cell migration in a human esophageal carcinoma cell line (Yuan et al., 2012). TGFβ treatment of these cells reduced *RELN* levels, and knockdown of *RELN* increased the rate of cell migration. Reelin was proposed to negatively regulate TGFβ-induced migration, but it remains to be seen whether similar events happen *in vivo* (Yuan et al., 2012).

Recent studies identified potential roles for reelin in progression of breast cancer. Several SNPs in the *RELN* gene were proposed as susceptibility loci for sporadic post-menopausal breast cancer (Barnholtz-Sloan et al., 2010). Further studies indicated certain SNPs in the *RELN* gene to be associated with breast cancer risk in Hispanic, but not non-Hispanic white women (Fejerman et al., 2013). Reelin protein is expressed in the normal breast epithelium, but is downregulated in primary breast tumors (Stein et al., 2010). The reduction of reelin levels in breast tumors correlates with poor survival. The triple negative human breast cancer cell line MDA-MB-231 normally expresses low levels of reelin, and overexpression of reelin in these cells rendered them less migratory and reduced their invasiveness (Stein et al., 2010). Another study reported higher levels of reelin in HER2+ primary tumors and breast-to-brain metastases compared to triple negative primary and metastatic tumor samples. Moreover, HER2 protein can interact with reelin, but the significance of this interaction remains to be elucidated (Neman et al., 2014).

Reelin signaling in the mammary gland

The work presented in the following chapters describes the evidence for functions of the reelin signaling pathway in mammary gland development and breast cancer progression. In

Chapter 1, we show that reelin and its adaptor Dab1 are essential for timely development of the mammary gland, and that the disruption of reelin signaling results in delayed ductal elongation and disorganized mammary epithelium. In Chapter 2, we present evidence for the essential role of reelin in the tumor microenvironment, and its impact on mammary tumor growth and metastatic progression. Finally, in Chapter 3 we show that alternative splicing of Dab1 may regulate the cellular response to the reelin signal during mammary gland development. Taken together, our results define novel roles for reelin signaling in the development of the mammary gland and in breast cancer, further expanding the scope of this signaling pathway outside of the central nervous system development.

Cancer type:	Reference:	Downregulated (↓) or upregulated (↑):		Control:	Notes:
		RELN mRNA	Reelin protein (IHC)		
Breast cancer	Ma et al., 2009	↓	-	Normal breast stroma	In tumor-associated stroma
	Stein et al., 2010	↓	↓	Normal breast tissue	*RELN* is frequently methylated in breast cancer cell lines
Colorectal cancer	Vignot et al., 2015	↑	-	Primary tumors	In metastases of colorectal tumors
Esophageal carcinoma	Wang et al., 2002	↑	↑	Normal esophageal tissue	
Ewings sarcoma	Jahromi et al., 2012	↓	-	Primary tumors	In metastatic lesions
Gastric cancer	Yamashita et al., 2004	↑	-	Normal rat stomach tissue	In rats, MNNG-induced
	Dohi et al., 2010	↓	↓	Normal gastric tissue	*RELN* is frequently methylated in primary tumors and gastric cancer cell lines
Head and neck cancer	Schlecht et al., 2007	↓	-	HPV-negative tumors	In HPV16-positive head and neck squamous carcinomas, never-smokers
Hepatocellular carcinoma	Okamura et al., 2011	↓	-	Normal liver tissue	*RELN* is frequently methylated in hepatocellular carcinomas
	Lin et al., 2012	↓	-	Non-invasive congenic cell lines	In newly established invasive hepatocellular carcinoma cell lines
Lung cancer	Govindan et al., 2012				*RELN* is frequently mutated in non-small cell lung cancer
Melanoma	Berthier-Vergnes et al., 2011	↑	-	Non-invasive congenic cell line	In invasive melanoma cell line
Neuroblastoma	Becker et al., 2012	↓	↓	Stage 1 and 2 neuroblastoma tumors	In metastatic stages 3, 4, 4s
Pancreatic cancer	Sato et al., 2006	↓	↓	Normal pancreatic tissue	
	Hong et al., 2008	↓	-	Non-invasive pancreatic neoplasm	*RELN* methylation increases with histological grade of papillary mucinous neoplasms
Prostate cancer	Perrone et al., 2007	-	↑	Normal prostate tissue	In high grade prostate cancer samples
Retinoblastoma	Seigel et al., 2007	↑	-	Normal retinal tissue	
T-cell acute lymphoblastic leukemia	Zhang et al., 2012				*RELN* is frequently mutated in T-cell acute lymphoblastic leukemia

Table 1. Alterations of reelin expression in cancers.

References

Appleton, C.T., Pitelka, V., Henry, J., Beier, F. (2007). Global analyses of gene expression in early experimental osteoarthritis. *Arthritis. Rheum.* **56**:1854-1868.

Bailey, J.M., Singh, P.K., Hollingsworth, M.A. (2007). Cancer metastasis facilitated by developmental pathways: Sonic hedgehog, Notch, and bone morphogenic proteins. *J. Cell. Biochem.* **102**:829-839.

Bakalian, A., Kopmels, B., Messer, A., Fradelizi, D., Delhaye-Bouchaud, N., Wollman, E., Mariani, J. (1992). Peripheral macrophage abnormalities in mutant mice with spinocerebellar degeneration. *Res. Immunol.* **143**:129-139.

Barakat, M.T., Humke, E.W., Scott, M.P. (2010). Learning from Jekyll to control Hyde: Hedgehog signaling in development and cancer. *Trends Mol. Med.* **16**:337-348.

Barnholtz-Sloan, J.S., Shetty, P.B., Guan, X., Nyante, S.J., Luo, J., Brennan, D.J., Millikan, R.C. (2010). FGFR2 and other loci identified in genome-wide association studies are associated with breast cancer in African-American and younger women. *Carcinogenesis.* **31**:1417-1423.

Becker, J., Fröhlich, J., Perske, C., Pavlakovic, H., Wilting, J. (2012). Reelin signalling in neuroblastoma: migratory switch in metastatic stages. *Int. J. Oncol.* **41**:681-689.

Berthier-Vergnes, O., Kharbili, M.E., de la Fouchardière, A., Pointecouteau, T., Verrando, P., Wierinckx, A., Lachuer, J., Le Naour, F., Lamartine, J. (2011). Gene expression profiles of human melanoma cells with different invasive potential reveal TSPAN8 as a novel mediator of invasion. *Br. J. Cancer.* **104**:155-165.

Bleicher, F., Couble, M.L., Buchaille, R., Farges, J.C., Magloire, H. (2001). New genes involved in odontoblast differentiation. *Adv. Dent. Res.* **15**:30-33.

Bock, H.H., Herz, J. (2003). Reelin activates SRC family tyrosine kinases in neurons. *Curr. Biol.* **13**:18-26.

Botella-Lopez, A., de Madaria, E., Jover, R., Bataller, R., Sancho-Bru, P., Candela, A., Compañ, A., Pérez-Mateo, M., Martinez, S., Sáez-Valero, J. (2008). Reelin is overexpressed in the liver and plasma of bile duct ligated rats and its levels and glycosylation are altered in plasma of humans with cirrhosis. *Int. J. Biochem. Cell. Biol.* **40**:766-775.

Buchaille, R., Couble, M.L., Magloire, H., Bleicher, F. (2000). A substractive PCR-based cDNA library from human odontoblast cells: identification of novel genes expressed in tooth forming cells. *Matrix. Biol.* **19**:421-430.

Carotti, S., Amato, M.M., Perrone, G., Vespasiani-Gentilucci, U., Pellegrini, C., Picardi, A., Onetti-Muda, A., Morini, S. (2015). Reelin expression by hepatic stellate cells and ductular reaction in HCV related liver fibrosis. *Italian J. Anat. Emb.* **120**:94. doi:10.13128/IJAE-16955.

Cerri, R.L., Thompson, I.M., Kim, I.H., Ealy, A.D., Hansen, P.J., Staples, C.R., Li, J.L., Santos, J.E., Thatcher, W.W. (2012). Effects of lactation and pregnancy on gene expression of endometrium of Holstein cows at day 17 of the estrous cycle or pregnancy. *J. Dairy Sci.* **95**:5657-5675.

Chen, X., Guo, Z., Okoro, E.U., Zhang, H., Zhou, L., Lin, X., Rollins, A.T., Yang, H. (2012). Up-regulation of ATP binding cassette transporter A1 expression by very low density lipoprotein receptor and apolipoprotein E receptor 2. *J. Biol. Chem.* **287**:3751-3759.

Chu, H.C., Lee, H.Y., Huang, Y.S., Tseng, W.L., Yen, C.J., Cheng, J.C., Tseng, C.P. (2014). Erythroid differentiation is augmented in Reelin-deficient K562 cells and homozygous reeler mice. *FEBS Lett.* **588**:58-64.

D'Arcangelo, G., Miao, G.G., Chen, S.C., Soares, H.D., Morgan, J.I. and Curran, T. (1995). A protein related to extracellular matrix proteins deleted in the mouse mutant reeler. *Nature* **374**:719-723.

D'Arcangelo, G. (2014). Reelin in the years: controlling neuronal migration and maturation in the mammalian brain. *Advances in Neuroscience*. Article ID 597395, doi:10.1155/2014/597395.

Díaz-Mendoza, M.J., Lorda-Diez, C.I., Montero, J.A., García-Porrero, J.A., Hurlé, J.M. (2013). Interdigital cell death in the embryonic limb is associated with depletion of Reelin in the extracellular matrix. *Cell. Death. Dis.* **4**:e800, doi: 10.1038/cddis.2013.322.

Diaz-Mendoza, M.J., Lorda-Diez, C.I., Montero, J.A., Garcia-Porrero, J.A., Hurle, J.M. (2014). Reelin/DAB-1 signaling in the embryonic limb regulates the chondrogenic differentiation of digit mesodermal progenitors. *J. Cell. Physiol.* **229**:1397-1404.

Dohi, O., Takada, H., Wakabayashi, N., Yasui, K., Sakakura, C., Mitsufuji, S., Naito, Y., Taniwaki, M., Yoshikawa, T. (2010). Epigenetic silencing of RELN in gastric cancer. *Int. J. Oncol.* **36**:85-92.

Endo, Y., Zhang, M., Yamaji, S., Cang, Y. (2012). Genetic abolishment of hepatocyte proliferation activates hepatic stem cells. *PLOS One.* **7**:e31846. doi: 10.1371/journal.pone.0031846.

Eresheim, C., Leeb, C., Buchegger, P., Nimpf, J. (2014). Signaling by the extracellular matrix protein Reelin promotes granulosa cell proliferation in the chicken follicle. *J. Biol. Chem.* **289**:10182-10191.

Evangelisti, C., Florian, M.C., Massimi, I., Dominici, C., Giannini, G., Galardi, S., Buè, M.C., Massalini, S., McDowell, H.P., Messi, E., et al. (2009). MiR-128 up-regulation inhibits Reelin and DCX expression and reduces neuroblastoma cell motility and invasiveness. *FASEB J.* **23**:4276-4287.

Falconer, D. S. (1951). Two new mutants, 'trembler' and 'reeler', with neurological actions in the house mouse (Mus musculus L.). *J. Genet.* **50**:192-201.

Fayad, T., Lefebvre, R., Nimpf, J., Silversides, D.W., Lussier, J.G. (2007). Low-density lipoprotein receptor-related protein 8 (LRP8) is upregulated in granulosa cells of bovine

dominant follicle: molecular characterization and spatio-temporal expression studies. *Biol. Reprod.* **76**:466-475.

Fejerman, L., Stern, M.C., Ziv, E., John, E.M., Torres-Mejia, G., Hines, L.M., Wolff, R., Wang, W., Baumgartner, K.B., Giuliano, A.R., et al. (2013). Genetic ancestry modifies the association between genetic risk variants and breast cancer risk among Hispanic and non-Hispanic white women. *Carcinogenesis.* **34**:1787-1793.

García-Miranda, P., Peral, M.J., Ilundain, A.A. (2010). Rat small intestine expresses the reelin-Disabled-1 signalling pathway. *Exp. Physiol.* **95**:498-507.

García-Miranda, P., Vázquez-Carretero, M.D., Gutiérrez, G., Peral, M.J., Ilundáin, A.A. (2012). Lack of reelin modifies the gene expression in the small intestine of mice. *J. Physiol. Biochem.* **68**:205-218.

Govindan, R., Ding, L., Griffith, M., Subramanian, J., Dees, N.D., Kanchi, K.L., Maher, C.A., Fulton, R., Fulton, L., Wallis, J., et al. (2012). Genomic landscape of non-small cell lung cancer in smokers and never-smokers. *Cell.* **150**:1121-1134.

Green-Johnson, J.M., Zalcman, S., Vriend, C.Y., Nance, D.M., Greenberg, A.H. (1995). Suppressed T cell and macrophage function in the "reeler" (rl/rl) mutant, a murine strain with elevated cerebellar norepinephrine concentration. *Brain Behav. Immun.* **9**:47-60.

Herz, J., Chen, Y. (2006). Reelin, lipoprotein receptors and synaptic plasticity. *Nat. Rev. Neurosci.* **7**:850–859.

Heymann, R., Kallenbach, S., Alonso, S., Carroll, P., Mitsiadis, T.A. (2001). Dynamic expression patterns of the new protocadherin families CNRs and Pcdh-gamma during mouse odontogenesis: comparison with reelin expression. *Mech. Dev.* **106**:181-184.

Hirotsune, S., Takahara, T., Sasaki, N., Hirose, K., Yoshiki, A., Ohashi, T., Kusakabe, M., Murakami, Y., Muramatsu, M., Watanabe, S., et al. (1995). The reeler gene encodes a protein with an EGF-like motif expressed by pioneer neurons. *Nat. Genet.* **10**:77-83.

Honda, T., Kobayashi, K., Mikoshiba, K., Nakajima, K. (2011). Regulation of cortical neuron migration by the Reelin signaling pathway. *Neurochem. Res.* **36**:1270-1279.

Hong, S.M., Kelly, D., Griffith, M., Omura, N., Li, A., Li, C.P., Hruban, R.H., Goggins, M. (2008). Multiple genes are hypermethylated in intraductal papillary mucinous neoplasms of the pancreas. *Mod. Pathol.* **21**:1499-1507.

Hong, Y.K., Foreman, K., Shin, J.W., Hirakawa, S., Curry, C.L., Sage, D.R., Libermann, T., Dezube, B.J., Fingeroth, J.D., Detmar, M. (2004). Lymphatic reprogramming of blood vascular endothelium by Kaposi sarcoma-associated herpesvirus. *Nat. Genet.* **36**:683-685.

Ikeda, Y., Terashima, T. (1997). Expression of reelin, the gene responsible for the reeler mutation, in embryonic development and adulthood in the mouse. *Dev. Dyn.* **210**:157-172.

Izrailit, J., Reedijk, M. (2012). Developmental pathways in breast cancer and breast tumor-initiating cells: therapeutic implications. *Cancer Lett.* **317**:115-126.

Jacquel, A., Herrant, M., Legros, L., Belhacene, N., Luciano, F., Pages, G., Hofman, P., Auberger, P. (2003). Imatinib induces mitochondria-dependent apoptosis of the Bcr-Abl-positive K562 cell line and its differentiation toward the erythroid lineage. *FASEB J.* **17**:2160-2162.

Jahromi, M.S., Putnam, A.R., Druzgal, C., Wright, J., Spraker-Perlman, H., Kinsey, M., Zhou, H., Boucher, K.M., Randall, R.L., Jones, K.B., et al. (2012). Molecular inversion probe analysis detects novel copy number alterations in Ewing sarcoma. *Cancer Genet.* **205**:391-404.

Jossin, Y., Ignatova, N., Hiesberger, T., Herz, J., Lambert de Rouvroit, C., Goffinet, A.M. (2004). The central fragment of Reelin, generated by proteolytic processing in vivo, is critical to its function during cortical plate development. *J. Neurosci.* **24**:514-521.

Kobold, D., Grundmann, A., Piscaglia, F., Eisenbach, C., Neubauer, K., Steffgen, J., Ramadori, G., Knittel, T. (2002). Expression of reelin in hepatic stellate cells and during hepatic tissue repair: a novel marker for the differentiation of HSC from other liver myofibroblasts. *J. Hepatol.* **36**:607-613.

Kopmels, B., Wollman, E.E., Guastavino, J.M., Delhaye-Bouchaud, N., Fradelizi, D., Mariani, J. (1990). Interleukin-1 hyperproduction by in vitro activated peripheral macrophages from cerebellar mutant mice. *J. Neurochem.* **55**:1980-1985.

Kuo, G., Arnaud, L., Kronstad-O'Brien, P., Cooper, J.A. (2005). Absence of Fyn and Src causes a reeler-like phenotype. *J. Neurosci.* **25**:8578-8586.

Larue, L., Bellacosa, A. (2005). Epithelial-mesenchymal transition in development and cancer: role of phosphatidylinositol 3' kinase/AKT pathways. *Oncogene.* **24**:7443-7454.

Lee, G.H., Chhangawala, Z., von Daake, S., Savas, J.N., Yates, J.R. 3rd, Comoletti, D., D'Arcangelo, G. (2014). Reelin induces Erk1/2 signaling in cortical neurons through a non-canonical pathway. *J. Biol. Chem.* **289**:20307-20317.

Lin, Z.Y., Chuang, W.L. (2012). Genes responsible for the characteristics of primary cultured invasive phenotype hepatocellular carcinoma cells. *Biomed. Pharmacother.* **66**:454-458.

Lutter, S., Xie, S., Tatin, F., Makinen, T. (2012). Smooth muscle-endothelial cell communication activates Reelin signaling and regulates lymphatic vessel formation. *J. Cell. Biol.* **197**:837-849.

Ma, X.J., Dahiya, S., Richardson, E., Erlander, M., Sgroi, D.C. (2009). Gene expression profiling of the tumor microenvironment during breast cancer progression. *Breast Cancer Res.* **11**:R7. doi: 10.1186/bcr2222.

Ma, Y., Wu, X., Li, X., Fu, J., Shen, J., Li, X., Wang, H. (2012). Corticosterone regulates the expression of neuropeptide Y and reelin in MLO-Y4 cells. *Mol. Cells.* **33**:611-616.

Ma, Y., Li, X., Fu, J., Li, Y., Gao, L., Yang, L., Zhang, P., Shen, J., Wang, H. (2014). Acetylcholine affects osteocytic MLO-Y4 cells via acetylcholine receptors. *Mol. Cell. Endocrinol.* **384**:155-164.

Magloire. H., Couble, M.L., Thivichon-Prince, B., Maurin, J.C., Bleicher, F. (2009). Odontoblast: a mechano-sensory cell. *J. Exp. Zool. B. Mol. Dev. Evol.* **312B**:416-424.

Magnani, A., Pattacini, L., Boiardi, L., Casali, B., Salvarani, C. (2010). Reelin levels are increased in synovial fluid of patients with rheumatoid arthritis. *Clin. Exp. Rheumatol.* **28**:546-548.

Magness, S.T., Bataller, R., Yang, L., Brenner, D.A. (2004). A dual reporter gene transgenic mouse demonstrates heterogeneity in hepatic fibrogenic cell populations. *Hepatology.* **40**:1151-1159.

Mansy, S.S., Nosseir, M.M., Zoheiry, M.A., Hassanein, M.H., Guda, M.F., Othman, M.M., AbuTalab, H. (2014). Value of reelin for assessing hepatic fibrogenesis in a group of Egyptian HCV infected patients. *Clin. Chem. Lab. Method.* **52**:1319-1328.

Massagué, J. (2008). TGFbeta in Cancer. *Cell.* **134**:215-230.

Maurin, J.C., Couble, M.L., Didier-Bazes, M., Brisson, C., Magloire, H., Bleicher, F. (2004). Expression and localization of reelin in human odontoblasts. *Matrix. Biol.* **23**:277-285.

Neman, J., Termini, J., Wilczynski, S., Vaidehi, N., Choy, C., Kowolik, C.M., Li, H., Hambrecht, A.C., Roberts, E., Jandial, R. (2014). Human breast cancer metastases to the brain display GABAergic properties in the neural niche. *Proc. Natl. Acad. Sci. USA.* **111**:984-989.

Nivet, A.L., Vigneault, C., Blondin, P., Sirard, M.A. (2013). Changes in granulosa cells' gene expression associated with increased oocyte competence in bovine. *Reproduction.* **145**:555-565.

Norgall, S., Papoutsi, M., Rössler, J., Schweigerer, L., Wilting, J., Weich, H.A. (2007). Elevated expression of VEGFR-3 in lymphatic endothelial cells from lymphangiomas. *BMC Cancer.* **7**:105.

Okamura, Y., Nomoto, S., Kanda, M., Hayashi, M., Nishikawa, Y., Fujii, T., Sugimoto, H., Takeda, S., Nakao, A. (2011). Reduced expression of reelin (RELN) gene is associated with high recurrence rate of hepatocellular carcinoma. *Ann. Surg. Oncol.* **18**:572-579.

Okoro, E.U., Zhang, H., Guo, Z., Yang, F., Smith, C. Jr., Yang, H. (2015). A Subregion of Reelin Suppresses Lipoprotein-Induced Cholesterol Accumulation in Macrophages. *PLOS One.* **10**:e0136895. doi: 10.1371/journal.pone.0136895

Paic, F., Igwe, J.C., Nori, R., Kronenberg, M.S., Franceschetti, T., Harrington, P., Kuo, L., Shin, D.G., Rowe, D.W., Harris, S.E., et al. (2009). Identification of differentially expressed genes between osteoblasts and osteocytes. *Bone.* **45**:682-692.

Perrone, G., Vincenzi, B., Zagami, M., Santini, D., Panteri, R., Flammia, G., Verzì, A., Lepanto, D., Morini, S., Russo, A., et al. (2007). Reelin expression in human prostate cancer: a marker of tumor aggressiveness based on correlation with grade. *Mod. Pathol.* **20**:344-351.

Rawlinson, S.C., McKay, I.J., Ghuman, M., Wellmann, C., Ryan, P., Prajaneh, S., Zaman, G., Hughes, F.J., Kingsmill, V.J. (2009). Adult rat bones maintain distinct regionalized

expression of markers associated with their development. *PLOS One*. **4**:e8358. doi: 10.1371/journal.pone.0008358.

Rebustini, I.T., Hayashi, T., Reynolds, A.D., Dillard, M.L., Carpenter, E.M., Hoffman, M.P. (2012). miR-200c regulates FGFR-dependent epithelial proliferation via Vldlr during submandibular gland branching morphogenesis. *Development.* **139**:191-202.

Redmond, L.C., Dumur, C.I., Archer, K.J., Haar, J.L., Lloyd, J.A. (2008). Identification of erythroid-enriched gene expression in the mouse embryonic yolk sac using microdissected cells. *Dev. Dyn.* **237**:436-446.

Redmond, L.C., Dumur, C.I., Archer, K.J., Grayson, D.R., Haar, J.L., Lloyd, J.A. (2011). Krüppel-like factor 2 regulated gene expression in mouse embryonic yolk sac erythroid cells. *Blood Cells Mol. Dis.* **47**:1-11

Rice, D. S., Curran, T. (2001). Role of the reelin signaling pathway in central nervous system development. *Annu. Rev. Neurosci.* **24**:1005–1039.

Rivera-Baltanas, T., Romay-Tallon, R., Dopeso-Reyes, I.G., Caruncho, H.J. (2010). Serotonin transporter clustering in blood lymphocytes of reeler mice. *Cardiovasc. Psychiatry Neurol.* **2010**:396282. doi: 10.1155/2010/396282.

Samama, B., Boehm, N. (2005). Reelin immunoreactivity in lymphatics and liver during development and adult life. *Anat. Rec. A Discov. Mol. Cell. Evol. Biol.* **285**:595-599.

Sato, N., Fukushima, N., Chang, R., Matsubayashi, H., Goggins, M. (2006). Differential and epigenetic gene expression profiling identifies frequent disruption of the RELN pathway in pancreatic cancers. *Gastroenterology.* **130**:548-565.

Schlecht, N.F., Burk, R.D., Adrien, L., Dunne, A., Kawachi, N., Sarta, C., Chen, Q., Brandwein-Gensler, M., Prystowsky, M.B., Childs, G., et al. (2007). Gene expression profiles in HPV-infected head and neck cancer. *J. Pathol.* **213**:283-293.

Schrauwen, I., Ealy, M., Huentelman, M.J., Thys, M., Homer, N., Vanderstraeten, K., Fransen, E., Corneveaux, J.J., Craig, D.W., Claustres, M., et al. (2009). A genome-wide analysis identifies genetic variants in the RELN gene associated with otosclerosis. *Am. J. Hum. Genet.* **84**:328-338.

Seigel, G.M., Hackam, A.S., Ganguly, A., Mandell, L.M., Gonzalez-Fernandez, F. (2007). Human embryonic and neuronal stem cell markers in retinoblastoma. *Mol. Vis.* **13**:823-832.

Smalheiser, N.R., Costa, E., Guidotti, A., Impagnatiello, F., Auta, J., Lacor, P., Kriho, V., Pappas, G.D. (2000). Expression of reelin in adult mammalian blood, liver, pituitary pars intermedia, and adrenal chromaffin cells. *Proc. Natl. Acad. Sci. USA* **97**:1281-1286.

Stein, T., Cosimo, E., Yu, X., Smith, P.R., Simon, R., Cottrell, L., Pringle, M.A., Bell, A.K., Lattanzio, L., Sauter, G., et al. (2010). Loss of reelin expression in breast cancer is epigenetically controlled and associated with poor prognosis. *Am. J. Pathol.* **177**:2323-2333.

Thorpe, L.M., Yuzugullu, H., Zhao, J.J. (2015). PI3K in cancer: divergent roles of isoforms, modes of activation and therapeutic targeting. *Nat. Rev. Cancer.* **15**:7-24.

Tseng, W.L., Huang, C.L., Chong ,K.Y., Liao, C.H., Stern, A., Cheng, J.C., Tseng, C.P. (2010). Reelin is a platelet protein and functions as a positive regulator of platelet spreading on fibrinogen. Cell. *Mol. Life Sci.* **67**:641-653.

Tseng, W.L., Chen, T.H., Huang, C.C., Huang, Y.H., Yeh, C.F., Tsai, H.J., Lee, H.Y., Kao, C.Y., Lin, S.W., Liao, H.R., et al. (2014). Impaired thrombin generation in Reelin-deficient mice: a potential role of plasma Reelin in hemostasis. *J. Thromb. Haemost.* **12**:2054-2064.

Underhill, G.H., George, D., Bremer, E.G., Kansas, G.S. (2003). Gene expression profiling reveals a highly specialized genetic program of plasma cells. *Blood.* **101**:4013-4021.

Vázquez-Carretero, M.D., García-Miranda, P., Calonge, M.L., Peral, M.J., Ilundain, A.A. (2014). Dab1 and reelin participate in a common signal pathway that controls intestinal crypt/villus unit dynamics. *Biol. Cell.* **106**:83-96.

Vignot, S., Lefebvre, C., Frampton, G.M., Meurice, G., Yelensky, R., Palmer, G., Capron, F., Lazar, V., Hannoun, L., Miller, V.A., et al. (2015). Comparative analysis of primary tumour and matched metastases in colorectal cancer patients: evaluation of concordance between genomic and transcriptional profiles. *Eur. J. Cancer.* **51**:791-799.

Wang, Q., Lu, J., Yang, C., Wang, X., Cheng, L., Hu, G., Sun, Y., Zhang, X., Wu, M., Liu, Z. (2002). CASK and its target gene Reelin were co-upregulated in human esophageal carcinoma. *Cancer Lett.* **179**:71-77.

Yamashita, S., Nomoto, T., Abe, M., Tatematsu, M., Sugimura, T., Ushijima, T. (2004). Persistence of gene expression changes in stomach mucosae induced by short-term N-methyl-N'-nitro-N-nitrosoguanidine treatment and their presence in stomach cancers. *Mutat. Res.* **549**:185-193.

Yuan, Y., Chen, H., Ma, G., Cao, X., Liu, Z. (2012). Reelin is involved in transforming growth factor-β1-induced cell migration in esophageal carcinoma cells. *PLOS One.* **7**:e31802. doi: 10.1371/journal.pone.0031802.

Zhang, J., Ding, L., Holmfeldt, L., Wu, G., Heatley, S.L., Payne-Turner, D., Easton, J., Chen, X., Wang, J., Rusch, M., et al. (2012). The genetic basis of early T-cell precursor acute lymphoblastic leukaemia. *Nature.* **481**:157-163.

CHAPTER ONE: Disruption of reelin signaling alters mammary gland morphogenesis

Abstract

Reelin signaling is required for appropriate cell migration and ductal patterning during mammary gland morphogenesis. Dab1, an intracellular adaptor protein activated in response to reelin signaling, is expressed in the developing mammary bud and in luminal epithelial cells in the adult gland. Reelin protein is expressed in a complementary pattern, first in the epithelium overlying the mammary bud during embryogenesis and then in the myoepithelium and periductal stroma in the adult. Deletion in mouse of either reelin or Dab1 induced alterations in the development of the ductal network, including significant retardation in ductal elongation, decreased terminal branching, and thickening and disorganization of the luminal wall. At later stages, some mutant glands overcame these early delays, but went on to exhibit enlarged and chaotic ductal morphologies and decreased terminal branching: these phenotypes are suggestive of a role for reelin in spatial patterning or structural organization of the mammary epithelium. Isolated mammary epithelial cells exhibited decreased migration in response to exogenous reelin in vitro, a response that required Dab1. These observations highlight a role for reelin signaling in the directed migration of mammary epithelial cells driving ductal elongation into the mammary fat pad and provide the first evidence that reelin signaling may be crucial for regulating the migration and organization of non-neural tissues.

Introduction

Reelin signaling has been identified as a key factor in regulating cell migration and positioning throughout the central nervous system (Caviness and Sidman, 1973; Caviness, 1976; Goffinet, 1984; Yip et al., 2000; Phelps et al., 2002). Anatomical examination of the brain and spinal cord in *reeler* mice, which carry a naturally occurring deletion mutation in the *reelin* gene (D'Arcangelo et al., 1995), has revealed defects including a lack of foliation and reduction in the size of the cerebellum, disrupted lamination in the hippocampus, inverted cortical lamination and abnormal positioning of nuclei in the brain and spinal cord (reviewed by D'Arcangelo and Curran, 1998; Rice and Curran, 2001). Observations on cellular activities governed by reelin signaling have been largely restricted to the nervous system, but recent studies have suggested a number of non-neuronal activities for reelin signaling. The *reelin* gene is expressed in odontoblasts, where it may mediate terminal innervation of tooth pulp (Maurin et al., 2004). Reelin is also frequently silenced in pancreatic cancer, and knockdown of multiple components of the reelin signaling pathway leads to increased cell motility and invasiveness in pancreatic cancer cells (Sato et al., 2006). Several isoforms of Dab1 are expressed in non-neural tissues such as kidney, liver and limbs in mice and zebrafish (Costagli et al., 2006; Howell et al., 1997a) suggesting possible additional roles for reelin signaling in the development of these structures.

We have explored a role for reelin signaling in the development and morphogenesis of the mammary gland. Mammary glands are skin appendages that develop via extensive epithelial-mesenchymal interactions (reviewed by Mikkola and Millar, 2006; Robinson, 2007). During embryogenesis, epithelially derived mammary placodes invaginate into the underlying mesenchyme to produce mammary buds. These buds then proliferate and extend into the

mesenchyme to produce the mammary sprout. Once the sprout reaches the underlying stromal fat pad, it begins to branch and a lumen forms within the epithelium to generate a primary ductal tree. The ductal tree is quiescent until the onset of puberty, at which time the gland enters a period of extensive growth and branching to form a mature ductal network that completely fills the fat pad. During the process of ductal elongation and branching, the ducts are tipped with terminal end buds, club-shaped bilayered epithelial structures that are the site of rapid cell proliferation (Ball, 1998). Retraction of these buds occurs once ductal growth is complete and the mature branching pattern has been established.

Growth and extension of mammary ducts requires extensive communication between epithelial and mesenchymal components of the gland. Mammary mesenchyme induces the overlying epithelium to form the mammary buds, probably by inducing epithelial cell migration and changes in epithelial cell shape (reviewed by Cunha, 1994). Interactions between the epithelium and the stroma then dictate the terminal branching pattern of the ducts (Naylor and Ormandy, 2002). Cavitation of the ducts also involves epithelial-mesenchymal interactions, as epithelial cells in contact with the surrounding basal lamina become organized into the luminal epithelium, whereas those that lose contact undergo apoptosis to clear the center of the lumen (reviewed by Gjorevski and Nelson, 2009). Cell-matrix interactions are mediated by a variety of cell adhesion molecules and these interactions are crucial in establishing the specific expression of milk protein genes in the mammary gland (Streuli et al., 1995). Thus, epithelial-mesenchymal interactions are required for the development, shaping and maturation of the mammary gland.

In this study, we have identified a role for reelin, a large extracellular matrix glycoprotein, and the reelin signaling pathway in the morphogenesis of the mammary gland. In the nervous system, reelin signaling is initiated by the deposition of reelin into the extracellular matrix. Reelin then binds to multimeric complexes of two low-density lipoprotein receptors, ApoER2 and VLDLR (reviewed by Herz and Chen, 2006). Signal transduction is mediated through the Dab1

intracellular adaptor protein, which is phosphorylated in response to reelin signaling primarily by Src family kinases (Howell et al., 1999; Kuo et al., 2005). Phosphorylated Dab1 activates a cascade of events that ultimately inhibits tau phosphorylation and promotes microtubule stabilization in the cytoskeleton, thus triggering the cessation of migration. In the absence of reelin signaling, neurons mis-migrate, producing numerous errors in cell positioning and cell layering (e.g. Caviness and Sidman, 1973; Caviness, 1976; Goffinet et al., 1984; Yip et al., 2000; Phelps et al., 2002; Förster et al., 2006). In our current study, we have demonstrated that reelin signaling pathway components are expressed in and around the mammary bud, with Dab1 expressed in invaginating placodal cells and reelin expressed in the overlying epithelium. Expression continues postnatally, with reelin in the mesenchymally derived periductal stroma and myoepithelial cells, and Dab1 in the luminal mammary epithelial cells lining the developing ducts. *Reelin* and *Dab1* genes are both required for normal mammary gland morphogenesis, as disruptions in either of these genes produces delays in ductal extension and chaotic ductal morphology. We have also shown that migration of isolated mammary epithelial cells is inhibited by exogenous reelin. These studies demonstrate an important role for reelin signaling in mammary gland morphogenesis and provide the first evidence that reelin signaling has the capacity to regulate the migration and organization of non-neural tissue.

Materials and Methods

Mouse lines

Reeler mice (B6C3Fe-*a/a-Reln*^{rl}/J) were obtained from the Jackson Laboratory (Bar Harbor, ME, USA). Two types of *Dab1* mice were used. CBy.12954-*Dab1*^{tm1Cpr}/J mice, which carry a disruption of the protein interaction/protein binding domain of *Dab1* (Howell et al., 1997a; Howell et al., 1997b) were obtained from the Jackson Laboratory. *Dab1*^{exKIneo} mice, in which a *lacZ* reporter gene replaces exon 1 of *Dab1*, were kindly provided by Dr Brian Howell (Pramatarova et al., 2008). *Dab1* mutant mice were used interchangeably for anatomical analysis, as the mutant phenotypes are indistinguishable in the two lines. *lacZ* gene expression was analyzed exclusively in *Dab1*^{exKIneo} mice. *Reeler* and *Dab1*^{exKIneo} mice are maintained on a C57Bl/6 background, whereas *Dab1*^{tm1Cpr}/J mice are maintained on a Balb/C background. Homozygous mutant mice and wild- type controls were obtained by intercrossing heterozygous parents. Offspring from *reeler* and CBy.12954-*Dab1*^{tm1Cpr}/J intercrosses were genotyped by PCR as described (D'Arcangelo et al., 1995; Howell et al., 1997a). *Dab1*^{exKIneo} intercross offspring were genotyped using the following primers: Ngen04, 5'-TGATGCTATCCCTAGCAAGAC-3'; Exon3 Rev, 5'-GTGGCTTCGCTGCGATCCTGAC-3'; CKO R3, 5'-CTTGAAGACGAAAGGGCCT-3'.

X-Gal staining, immunohistochemistry and histology

lacZ gene expression was visualized in formalin-fixed whole embryos, and 20-40 µm tissue sections, following overnight incubation in a bromo-chloro-indolyl-galactopyranoside (X-Gal) reaction buffer composed of 1 mg/ml X-Gal in 5 mM $K_3Fe(CN)_6$, 5 mM $K_4Fe(CN)_6$-$3H_2O$, 1 mM $MgCl_2$, 0.01% deoxycholic acid (DOC) and 0.02% Igepal (Sigma, USA). For

immunohistochemistry, tissue sections were reacted to reveal X-Gal as above, post-fixed briefly with 4% paraformaldehyde, then incubated overnight with primary antibodies diluted in 1X PBS + 10% dry milk powder. Horseradish peroxidase (HRP)-conjugated secondary antibodies (Jackson ImmunoResearch, West Grove, PA, USA) were diluted 1:250 in PBS+10% dry milk powder and incubated for 2-4 hours at room temperature. HRP was visualized using diaminobenzidine. Paraffin sections were dewaxed and rehydrated through graded ethanols. Antigen retrieval was performed by boiling for 10 minutes in Tris-HCl buffer, then sections were incubated for 60 minutes with primary antibodies diluted in 1% bovine serum albumin in Tris-buffered saline. Streptavidin-conjugated secondary antibody incubation and HRP visualization were performed following the manufacturer's instructions (Dako NA, Carpinteria, CA, USA). Primary antibody dilutions were as follows: anti-reelin (Millipore, Billerica, MA USA) 1:500; anti-Dab1 (Millipore) 1:500, anti-K14 (Covance, Princeton, NJ, USA) 1:1000; anti-K8/18 (ProGen, Germany) 1:300; anti-NKCC1 (gift of Dr Jim Turner, National Institute of Craniofacial and Dental Research, NIH, Bethesda, MD, USA) 1:1000; anti-Ki67 (Vector Laboratories, Burlingame, CA, USA), 1:1000. For histology, 7 μm paraffin sections were stained using hematoxylin and eosin.

RT-PCR

Mammary buds were dissected from abdominal walls of embryonic day 13.5 (E13.5) embryos and were flash-frozen. Buds collected from three embryos of the same genotype were pooled and total RNA was extracted using RNA Wiz as described (Anderson et al., 2002), reverse transcribed using Superscript II (Invitrogen, Carlsbad, CA, USA), then amplified using the following primers: ApoER2 forward, 5'-AGCGTTTGTACTGGGTGGAC-3'; ApoER2 reverse, 5'-GCTGGAGATTTGAGGAGCAG-3'; VLDLR forward, 5'-ACGGCCAGTGTGTTCCTAAC-3'; VLDLR reverse, 5'-CCATCGTCACAGTCATCCTG-3'.

Carmine Red staining and branch analysis

Whole mammary glands were collected and stained as previously described (Li et al., 2002). The extent of fat pad colonization was determined by measuring the length and width of the stromal fat pad, and the length and width of the ductal tree at its widest extent. Areas for both fat pad and ductal tree were calculated and the ratio of ductal tree:fat pad was determined. Terminal end buds and terminal branches were counted from photomicrographs of the entire gland.

Mammary gland transplantation

Mammary glands from six 3-week-old Balb/C host females were cleared of endogenous epithelium as described (DeOme et al., 1959). Donor mammary glands were collected from adult wild-type and *Dab1*^{tm1Cpr}/J mutants and dissected into small fragments. Wild-type and *Dab1*^{tm1Cpr}/J mutant mammary fragments were transplanted into the cleared fat pads, with each host mouse receiving a wild-type transplant and a contralateral *Dab1*^{tm1Cpr}/J mutant transplant. After 6 weeks, host mammary glands were removed and processed for whole-mount Carmine Red staining as described above.

MEC isolation and culture

Primary mammary epithelial cells (MECs) were isolated from freshly dissected mammary glands obtained from females at 13 days of gestation. Minced tissues were incubated in a digestion buffer containing collagenase and hyaluronidase for 6 hours, then digested with Dispase, filtered through 100 μm mesh tissue strainers and grown in MEC media as described (Hu et al., 2005). To ensure that isolated cells were primarily MECs, primary cultures were initially plated for 1 hour to allow fibroblasts to adhere to the culture flask. Suspended MECs were then transferred to a fresh flask and allowed to adhere. After 4 days in primary culture, MECs were serum-starved for 24 hours, then 10^5 MECs were plated into the top well of a transwell chamber. For live-cell assays, the bottom chamber contained live cells, either reelin-

secreting pCrl cells (D'Arcangelo et al., 1999) (kindly provided by Dr Tom Curran, University of Pennsylvania, Philadelphia, PA, USA) or control mock-transfected 293T cells. For conditioned media cultures, media was collected from pCrl or 293T cells after 3 days of culture.

Results

Reelin signaling pathway components are expressed in the mammary gland

To determine if reelin signaling might be involved in mammary gland development, we first examined the expression of reelin signaling pathway components in the embryonic mammary gland. Using a *Dab1*^{lacZ} reporter mouse [*Dab1*^{exKIneo} (Pramatarova et al., 2008)], we found that Dab1 was expressed in mammary buds in mouse embryos (Figure 1.1A-D), with expression evident as early as E12.5. Reporter gene expression was limited to the mammary bud itself, with no expression in the surrounding epithelial or mesodermal tissues (Figure 1.1F). Immunohistochemical labeling with anti-Dab1 antibodies also labeled the mammary buds (Figure 1.1G), confirming the fidelity of reporter gene expression. Reelin expression appeared at low levels in the condensing mesenchyme surrounding the mammary bud, as well as at higher levels in the overlying epithelium. Reelin expression was specific to the epithelium of the abdominal wall, and was excluded from adjacent limb bud epithelium (Figure 1.1H). ApoER2 and VLDLR were also expressed in the developing mammary bud (Figure 1.1E). These observations suggest that many key elements of the reelin signaling pathway, including reelin itself, Dab1, ApoER2 and VLDLR are expressed during embryonic mammary gland development.

Next, we investigated whether reelin signaling might be active during postnatal mammary gland morphogenesis. We found that in adults, Dab1 was expressed in the adult luminal epithelium (Figure 1.2A, G), where it colocalized with K8/18, a luminal cell marker (Figure 1.2E). Reelin was expressed in the periductal stroma (Figure 1.2B, H), complementary to where Dab1 was expressed and overlapping the expression of K14, a basal cell marker (Figure 1.2F). The *lacZ* reporter gene was also expressed in adult tissue sections, and double

labeling for β-galactosidase and anti-reelin expression illustrated the complementary expression patterns (Figure 1.2C, D). This localization suggests a continued role for reelin signaling during postnatal mammary gland morphogenesis.

Loss of reelin signaling disrupts ductal tree formation

To determine if loss of reelin signaling affects mammary gland development, we examined *reeler* mutant mice and *Dab1* knockout mice for possible effects on mammary gland morphogenesis. Sections taken through *reeler* and *Dab1* embryos suggested that the initial stages of mammary gland development, i.e. mammary bud formation and invagination, were normal (data not shown); therefore we focused on postnatal mammary glands. At 6 weeks of age, wild-type glands contained an extensive ductal network, extending from the nipple well past the inguinal lymph node into the distal fat pad (Figure 1.3A). Many distal branches were tipped with terminal end buds (TEBs), suggesting that active ductal growth was in progress. By contrast, both *reeler* and *Dab1* mutant glands had very small ductal trees that rarely extended even as far as the lymph node (Figure 1.3B, C). TEBs were observed at the ends of some branches (Figure 1.3C), but branches without TEBs were also observed. By 2 months of age, wild-type glands were fully colonized, with profusely branched ducts extending to the distal end of the fat pad, and most TEBs had regressed, indicating that ductal branching and extension was nearly complete (Figure 1.3D). By comparison, at the same age, many mutant glands had small, underdeveloped ductal trees (Figure 1.3E, F). As seen at 6 weeks, some distal branches were tipped with TEBs, but others were not. At 3 months of age, wild-type gland ductal branching patterns were not qualitatively different from those seen at 2 months of age (Figure 1.3G). However, no TEBs were observed in wild-type glands at this age, indicating that the glands are fully mature. Mutant animals at 3 months of age showed a variety of phenotypes. Some mutant glands had fat pads that were fully colonized by a ductal network (Figure 1.3H, I), whereas others had only rudimentary ductal trees (Figue 1.3H', I'). However, even in mutants with fully colonized ducts, the distal branching patterns were qualitatively different from those

seen in wild-type mice. These differences were not due to differences in estrous cycle phase. Ductal arborization appeared to be less extensive than that in wild-type glands, distal branches appeared sparser (insets, Figure 1.3H, I) and occasionally there were multiple branches extending from the same location (Figure 1.3H, inset). TEBs were usually not present in mutant animals at this age. These observations suggest that initial ductal extension is delayed in all mutant animals. In some cases, the early delays were apparently overcome and the animals were able to develop more extensive ductal trees, whereas in others, rudimentary ductal trees were retained well into adulthood. The absence of TEBs in mutants at later ages suggests that despite the apparent failure in ductal extension, the glands have reached maturity.

To quantify the differences in ductal development, we first determined whether mammary glands had rudimentary ducts, immature ducts, or mature ductal trees. Rudimentary ducts had few branches, and no ductal extension past the level of the lymph node (e.g. Figure 1.3H', I'), immature ducts showed sparse branching patterns and occasional TEBs (e.g. Figure 1.3E), whereas mature ductal trees had profuse branches and no evidence of TEBs (e.g. Figure 1.3G). At 6 weeks of age, about 65% of control wild-type glands had immature ductal patterns, whereas the remainder exhibited mature ductal trees (Figure 1.4A). By contrast, rudimentary ducts were seen in almost all *reeler* and *Dab1* mutants. At 2 and 3 months of age, all of the control glands had mature ductal trees, whereas a substantial fraction of mutant animals exhibited either rudimentary or immature ductal trees (Figure 1.4A). Even at 3 months of age, rudimentary and immature ductal trees were still observed in mutant animals.

Second, we quantified the area of the fat pad occupied by the ductal network. At 6 weeks of age, mammary ducts filled an average of 76% of the wild-type fat pad, whereas *reeler* and *Dab1* mutant mammary fat pads were on average 12.94 and 9.83% colonized, respectively (Figure 1.4B). By 2 months of age, wild-type glands were fully colonized with ducts. Although some mutant glands were also fully colonized, five of seven *reeler* mutant glands were only partially colonized, with the extent of colonization ranging from 21.23 to 87.92%, and two of five

Dab1 mutant glands were minimally colonized, with colonization ranging from 5.00 to 10.04%. At three months of age, a number of mutant glands continued to show only partial ductal colonization (three of nine *reeler* glands, 1.53–66.67% of area colonized; four of seven *Dab1* mutant glands, 4.49–56.73% of area colonized), whereas all wild-type glands were fully colonized. These observations suggest that persistent changes in mammary gland colonization occur in the absence of reelin signaling.

Loss of reelin signaling disrupts gland maturation and ductal branching

During mammary gland morphogenesis, ductal growth is heralded by the formation of TEBs, enlarged bilaminar structures at the distal tips of growing ducts (Ball, 1998). TEBs are present during active ductal growth and are resorbed once the ducts have completed their growth (Sternlicht et al., 2006). At 6 weeks of age, five of seven wild-type glands had visible TEBs (Figure 1.5A). The remaining two glands were those glands that were 100% colonized by ducts, and had no visible TEBs. We interpret this to mean that ductal development in these glands was complete and that the TEBs had been resorbed. At the same age, all mutant glands examined had visible TEBs. Comparison of the number of TEBs in each type of gland showed that mutants had significantly fewer TEBs than wild-type animals (Figure 1.5A). At 2 months of age, only three of 12 wild-type glands had TEBs, with an average of 6.7 TEBs per animal. In comparison, six of seven *reeler* mutant glands and two of four *Dab1* mutant glands had visible TEBs (Figure 1.3E), with an average of 5.9 TEBs per gland. TEBs were also examined in histological sections to determine if there were alterations in morphology in mutant animals. At two months of age, both *reeler* $^{-/-}$ and *Dab1* $^{-/-}$ glands had terminal end buds resembling those seen in 6-week-old wild-type animals (Figure 1.5C-E). TEBs were tipped with a thin cap cell layer, which transitioned to a thicker myoepithelial layer at the collar of the TEB. The TEB distribution suggests two possibilities: either that at 2 months of age, both wild-type and mutant ductal tree development is nearly complete, with only a few residual TEBs remaining; or that,

because mutant glands have fewer terminal branches (see below), active growth is continuing, albeit with fewer ducts being extended. The normal TEB morphology seen in mutant glands supports the latter possibility. By 3 months of age, TEBs were not seen in *reeler* mutant glands, whereas four of eight *Dab1* mutant glands still had discernible TEBs, with an average of 8.3 TEBs per gland. This observation suggests that ductal growth may be complete in *reeler* mutants at this age, whereas development continues in *Dab1* mutants.

To establish an estimate of the stage of maturity of the glands, we determined the average ratio of TEBs to total terminal branches (Table 1.1). At 6 weeks of age, wild-type glands had an average ratio of 0.337 (n=7), decreasing to 0.028 at 2 months and 0.000 at 3 months, reflecting the maturity of the glands. In comparison, *reeler* mutant glands at 6 weeks of age had a ratio of 0.667 (n=7), which decreased to 0.289 (n=7) at 2 months of age and to 0.000 (n=8) at 3 months of age. *Dab1* mutants showed a similar decrease in TEB/branch ratio from 0.401 (n=5) at 6 weeks and 0.125 (n=4) at 2 months, but four of eight glands still had visible terminal end buds at 3 months of age, producing a TEB/branch ratio of 0.200 (n=8). These ratios suggest that *reeler* and *Dab1* mutant glands are still undergoing ductal elongation at 2 months of age. By 3 months of age, TEBs were not present in any *reeler* glands, even in those with rudimentary or immature ductal trees. However, some *Dab1* mutant glands with rudimentary or immature ductal networks still had visible TEBs. These data suggest that gland maturation is complete in *reeler* mutants by 3 months of age, despite the lack of complete ductal trees. However, *Dab1* mutants might retain the capacity for continued development.

We also counted the number of terminal branches, which were defined as distal ductal segments exceeding 100 μm in length, present in each gland. At 6 weeks of age, all branches were counted, whereas at 2 and 3 months of age, only those branches distal to the inguinal lymph node were counted. At all ages, there were on average fewer branches in both *reeler* and *Dab1* mutants compared with controls (Figure 1.5B). However, the range of branches was variable in mutant animals, with some animals having near normal numbers of branches,

whereas others showed significantly reduced branch numbers. This is evidenced by the large standard deviations seen in the *reeler* and *Dab1* mutant samples.

Alterations in ductal morphogenesis are not due to maternal hormonal status

Reeler and *Dab1* mutant mice display altered nervous system anatomy along with somewhat stunted growth at younger ages. However, despite grossly abnormal morphology, many local and long-distance neural circuits are established correctly (Simmons and Pearlman, 1983; Yip et al., 2003). The brain abnormalities and the reduced body size suggest that hormonal functions governed by the brain might be adversely affected in mutant animals. To test this, we performed mammary gland transplantation to introduce mutant mammary gland tissue into a wild-type environment. We found that in five out of six glands, wild-type transplanted tissue generally formed a robust ductal network. By contrast, in five out of six *Dab1* mutant transplants, transplanted tissue was visible, but mutant tissue either failed to generate a ductal network, or, at best, formed a few rudimentary ducts (Figure 1.6). The failure of *Dab1* $^{-/-}$ epithelium to generate a ductal network, either *in situ* or following transplantation into a wild-type environment, suggests that ductal development is intrinsically impaired in the absence of a functional reelin signaling pathway, and that global changes in hormonal levels are not responsible for the observed phenotypes.

Loss of reelin signaling alters ductal wall morphology

At 6 weeks of age, wild-type glands had a significant number of ducts visible within the mammary stroma in histological sections (Figure 1.7). Ductal profiles were rounded or oval, with even wall thickness and regularly arranged cell bodies in the walls of the ducts (Figure 1.7A). By contrast, *reeler* and *Dab1* mutant animals had few visible ducts, and sections through these ducts revealed abnormally thick and disarrayed ductal walls (Figure 1.7B). Many ducts also appeared to be occluded (Figure 1.7B''), suggesting a delay or defect in cavitation. At 2 months

of age, control glands were colonized with regularly spaced ducts that had smooth, even walls (Figure 1.7C). Sections through the ducts revealed well-defined lumens, even at their most distal extent. Luminal cell bodies were arranged in a compact single layer with rounded cellular profiles (Figure 1.7C''). By contrast, *reeler* and *Dab1* mutant mice had thickened ductal walls and irregular lumens. Luminal cells appeared to be piled on top of each other, creating a luminal wall that was several cell diameters thick (Figure 1.7D''). Also, as seen in 6-week-old animals, the distal ends of some ducts did not have discernible lumens. By 3 months of age, control glands had large numbers of ductal profiles. Most ducts had narrow lumens with smooth, even ductal walls and tightly juxtaposed cellular profiles (Figure 1.7E, G). By contrast, *reeler* and *Dab1* mutant glands exhibited a variety of abnormal phenotypes. Some glands had very few ducts, with thicker walls and occluded lumens, similar to those seen at 2 months of age, whereas others had a large number of ducts with swollen, severely distended lumens (Figure 1.7F). Ducts with swollen lumens had luminal walls that appeared thinner and lacked the compact arrangement of epithelial cells seen in control animals. Instead, luminal cells had elongate nuclei arranged parallel to the lumen (Figure 1.7F'). In addition, these ducts appeared to have thinner layers of smooth muscle surrounding the duct. Distal profiles were irregular in shape and many lacked clearly defined lumens (Figure 1.7F'', H'').

Ducts from both wild-type and *Dab1* mutant animals at 2 months of age expressed markers for basal cells (K14) and for luminal epithelial cells (K8/18 and NKCC1). K14 labeling was present in the basal cell layer surrounding the luminal epithelial cells in both wild-type and mutant ducts, although labeling appeared somewhat denser in *Dab1* mutant animals, suggesting there may be more basal cells in these mutants (Figure 1.7I). K8/18 and NKCC1 were both expressed in luminal epithelial cells (Figure 1.7J, K); several layers of cells appeared to express these antigens in mutant animals, whereas a single layer of cells showed expression in wild- type animals. Thus, our results demonstrate that all expected components of the ductal

wall are present and identifiable in mutant animals, but that the organization and placement of cells differs in mutants.

Ductal cell proliferation is altered in the absence of reelin signaling

To determine if ductal wall thickening and hypertrophy of the ducts stemmed from changes in the proliferation of ductal cells, we performed Ki67 labeling. As expected, examination of the sectioned profiles in both *reeler* and *Dab1* mutants showed thickened ductal walls and frequent occluded tubules. Ki67-positive cells were prevalent in both thickened tubule walls and in occluded ducts in *Dab1* mutants (Figure 1.8F, H), suggesting a relatively high rate of cell proliferation in both of these types of structures. This suggests that the increased thickness of the tubule walls may stem from increased cell proliferation in the mammary epithelium. By contrast, *reeler* mice had few Ki67-positive cells in either type of profile (Figure 1.8E, G). In these animals, cell proliferation may have occurred at earlier ages, producing the thickened ductal walls and occluded tubules that are present in these mutants. We then quantified the percentage of Ki67-positive cells in wild-type and mutant animals (Table 1.2). As a baseline measure of proliferation, we counted the number of Ki67-positive profiles in sections through the lymph nodes. Baseline proliferation rates appeared somewhat lower in mutant animals than in wild-type animals (Figure 1.8), so we determined the ratio of proliferating cells in the mammary ducts vs proliferation in the lymph nodes for further comparisons. In wild-type mammary ducts, an average of 8.75% of the total number of cells was labeled with Ki67, compared with an average of 16.76% of cells in the lymph node, producing a ratio of 0.522. This rate of proliferation probably reflects the normal turnover of cells in the mature mammary epithelium. In *reeler* mutants, only 1.7% of cells in the mammary ducts were labeled with Ki67, compared with 9.7% in the lymph node (ratio=0.175). By contrast, in *Dab1* mutant mice, 14.5% of cells in the mammary ducts were labeled, along with 13.9% of cells in the lymph node

(ratio=1.043). These results suggest a very low level of cell proliferation in *reeler* mutants, but an increased rate of proliferation in *Dab1* mutants.

MEC migration is inhibited in the absence of reelin signaling

Because reelin signaling is known to be instrumental in regulating neuronal migration, we wondered whether it might have a similar function in regulating the migration of MECs. Therefore, we isolated wild-type MECs and examined their migration in transwell assays in the presence or absence of soluble reelin. MECs showed significantly reduced migration in the presence of reelin-secreting pCrl cells or pCrl-conditioned media (Figure 1.9). We noted a more prominent reduction in MEC migration in the presence of pCrl-conditioned medium (Figure 1.9) that may be due to a higher concentration of reelin in conditioned media than in live cell culture.

We performed similar experiments using MECs isolated from *reeler* mutants (Figure 1.9). In this experiment, we expected that *reeler* mutant MECs would behave like wild-type cells, as the cellular machinery permitting a response to reelin signaling should be intact in these cells. As shown in Figure 1.9, *reeler* mutant MECs behaved similarly to wild-type MECs, with reduced migration in the presence of pCrl cells or conditioned medium. Again, a greater reduction in migration was observed with conditioned medium than with live cell cultures.

We also performed the same experiment using MECs isolated from *Dab1* mutants. We expected that *Dab1* mutant cells would not respond to the presence of reelin in the transwells, as disruption of the *Dab1* gene ablates the canonical reelin signaling pathway cell autonomously. *Dab1* mutant MEC migration was not impeded either by the presence of pCrl cells or by pCrl-conditioned media. The migration rate of *Dab1* mutant cells even appeared to increase slightly in the presence of pCrl cells or conditioned media, although these increases were not statistically significant. These observations support the hypothesis that reelin may act

directly on MECs to limit their migration, and that disrupting the reelin signaling pathway abrogates the effect of reelin on MEC migration.

Discussion

Several lines of evidence support a role for reelin signaling in mammary gland morphogenesis. First, disruption of the reelin signaling pathway in both *reeler* and *Dab1* mutants alters ductal development and arborization. Second, transplantation studies demonstrate a requirement for intact reelin signaling in promoting ductal outgrowth. Third, reelin has direct and demonstrable effects on the migration of mammary epithelial cells. Taken together, these observations suggest a pivotal role for reelin signaling in regulating mammary ductal development.

The molecular mechanisms of reelin signaling have been widely studied in the central nervous system. Extracellular reelin binds to ApoER2 and VLDLR receptors, triggering the phosphorylation of Dab1 and initiating a cascade of events leading to microtubule stabilization (reviewed by Herz and Chen, 2006). The expression of reelin, ApoER2, VLDLR and Dab1 in and around the mammary bud and in the luminal epithelial and periductal stroma of the mature gland suggests that an identical chain of events is utilized in the mammary gland. The early distribution of Dab1 and reelin suggests that reelin expressed in the epithelium may regulate the migration or positioning of Dab1-expressing cells in the invaginating mammary bud; however, loss of *reelin* or *Dab1* does not disrupt early mammary bud development.

In the maturing gland, reelin was expressed in the periductal stroma and myoepithelial layers surrounding the luminal epithelium, whereas Dab1 was expressed in a complementary pattern in the luminal epithelium. This arrangement suggests that reelin from the stromal and myoepithelial layers might provide a signal to the Dab1- expressing cells in the luminal

epithelium. Reelin is a large extracellular matrix glycoprotein (D'Arcangelo et al., 1995); therefore, one possibility is that reelin is a component of the mammary gland extracellular matrix (ECM). Interactions between luminal epithelial cells and the surrounding ECM are crucial for directing epithelial organization and cavitation, as well as for establishing the position of ductal branch points (reviewed by Gjorevski and Nelson, 2009). During cavitation, luminal cells that maintained contact with the basal lamina persisted, whereas detachment from the basal lamina led to apoptosis, leaving an organized epithelium surrounding a hollow central lumen. In the absence of reelin signaling, mammary ducts developed thick, multilayered walls and often remained occluded. These phenotypes suggest disruption of interactions between the luminal epithelial cells and the ECM, such that the signals necessary to induce apoptosis are not properly transmitted, leading to the presence of occluded ducts. In contrast to the thickened walls and lack of cavitation, some ducts appeared distended, with thin epithelial walls. Bloating of these ducts may be caused by a lack of structural integrity in the epithelial walls also as a result of disrupted matrix interactions; the epithelial walls then become distended due to pressure from the lumen.

Thickened ductal walls and occluded tubules suggest that additional cells are present in the mutant ducts. The additional cells could reflect a failure in cell death, as might be produced by disruptions in the interactions with the ECM, or might reflect increased cell proliferation. Ki67 labeling suggests an increased rate of cell proliferation in *Dab1* mutant glands, lending some credence to the second hypothesis. However, this increased cell proliferation might also indicate an earlier phase of ductal development, suggesting that *Dab1* mutant ducts are less mature than comparably aged *reeler* or wild-type ducts. If this is the case, then one might expect that rates of cell proliferation would decrease in older glands, and this remains to be tested. Alternatively, if high rates of cell proliferation are retained at later ages, then these cells might represent carcinoma *in situ*. Loss of reelin signaling has been linked to increased motility and invasiveness in pancreatic cancer (Sato et al., 2006); similar activities might occur in the

mammary gland. Owing to the limited survival of older mutant animals, it remains to be seen if mammary tumors develop at a higher rate in *reeler* or *Dab1* mutants.

One possible explanation for the observed mammary gland phenotypes might be a global delay in development. *Reeler* and *Dab1* mutant mice are generally smaller than wild-type mice and have abnormal brain structures that could result in disruptions in hormone production and/or secretion, altering mammary gland development (Hennighausen and Robinson, 2005). Whereas these processes could be contributing factors, particularly to the early delays in ductal morphogenesis observed in virtually all mutant mice, our transplantation studies suggested that the probable cause of later phenotypes, including decreased branching and ductal wall abnormalities, is the intrinsic disruption of reelin signaling. The retraction of TEBs in mutants, even in the absence of complete ductal elongation, suggested that maturation of the gland had occurred and that limited ductal arborization was a persistent and permanent phenotype. TEBs depend on signals from a variety of growth factors, including IGF-1, growth hormone and sex steroids (Kleinberg and Ruan, 2008), and these signals may also be disrupted in *reeler* and *Dab1* mutants.

The isolation of mammary stem cells (MaSCs) (Shackleton et al., 2006) illustrates a key player in the expansion of the ductal network during puberty and pregnancy. MaSC expansion is normally restricted by Notch signaling (Bouras et al., 2008). Recent findings in the CNS suggest that Notch is a downstream mediator of reelin signaling (Hashimoto-Torii et al., 2008). In the mammary gland, loss of reelin signaling and a concomitant decrease in Notch expression might lead to the expansion of the MaSC population; this might be reflected in the increased K14 expression evident in *reeler* and *Dab1* mutants. However, this might also predict an increase in ductal growth and expansion, which is clearly not seen in these mutants, suggesting that additional signals might be required to stimulate stem cell proliferation and contribution to ductal growth. However, an expanded stem cell population might also predispose mutant ducts to increased tumorigenesis, which remains to be seen.

Our finding that MEC migration was slowed in the presence of reelin suggests a direct effect of reelin signaling on the cellular machinery of MECs. In neurons, reelin signaling initiates a cascade of events, ultimately inhibiting the phosphorylation of tau protein and stabilizing the cytoskeleton (reviewed by Herz and Chen, 2006). Knocking down expression of reelin pathway components increases the migration of pancreatic cancer cells (Sato et al., 2006), and our results showed similar effects on the migration of mammary epithelial cells. Thus, reelin in the extracellular matrix surrounding the developing ducts might serve to inhibit the migration of mammary epithelial cells, constraining these cells to remain within the luminal epithelium. In the absence of reelin signaling, enhanced cell migration could contribute to the abnormal ductal morphology, particularly to the increased thickness of the ductal walls. This phenotype may reflect an effort by mammary epithelial cells to continue migrating, even in the presence of a stabilizing extracellular matrix. This might lead to changes in cell layering, similar to changes seen in the developing brain and evidenced as thickened ductal walls or possibly at later stages to carcinoma *in situ*.

In summary, we have found a novel, independent role for reelin signaling in mammary gland morphogenesis. Reelin signaling is required for the extension and elaboration of the mammary ductal network, as well as for the organization of the luminal epithelial wall. Loss of reelin signaling results in increased proliferation and migration of luminal mammary epithelial cells; these changes may stem from disrupted interactions with the extracellular matrix. These studies demonstrate an important role for reelin signaling in shaping the mammary gland and provide the first evidence that reelin signaling may be crucial for regulating the migration and organization of non-neural tissues.

Acknowledgements

We thank J. Colicelli and P. Phelps for helpful discussions and critical reading of the manuscript; D. Anthony, J. Philipps and K. Bui for assistance with cell counting; E. Kirkbride for assistance with RT-PCR; J. Han, J. Stevens and J. Huang for assistance with immunohistochemistry; and D. Crandall for assistance with figure preparation. This research was supported by the UCLA Stein/Oppenheimer Endowment and by grants from the NIH (HD061815) and the California Breast Cancer Research Program (161B-0110) to E.M.C.

Figures

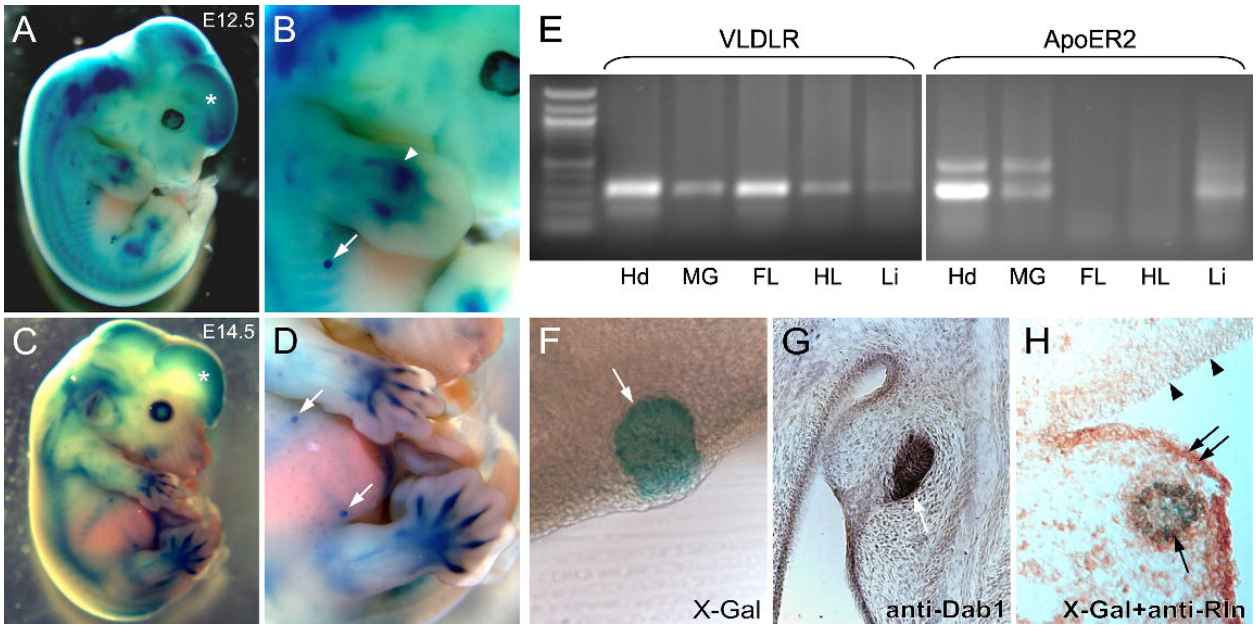

Figure 1.1. Expression of reelin signaling pathway components in the embryonic mammary gland.
(A-D) *Dab1* reporter gene expression in whole embryos at E12.5 (A, B) and E14.5 (C, D). Reporter gene expression is evident in the forebrain (A, C, asterisks), in the developing limb (B, arrowhead) and in the mammary placodes (B, D, arrows). B and D are higher magnification lateral views of the embryos in A and C, respectively. (E) RT-PCR detection of VLDLR and ApoER2 in wild-type E13.5 embryonic tissues. (F, G) Mammary buds at E14.5 visualized for *lacZ* reporter gene expression (F, arrow) and anti-Dab1 immunohistochemistry (G, arrow). (H) Double labeling for the $Dab1^{lacZ}$ reporter gene (blue, arrow) and anti-reelin (brown, double arrows). Reelin is expressed in the abdominal epithelium but is excluded from the adjacent limb epithelium (arrowheads). FL, forelimb; Hd, head; HL, hindlimb; Li, liver; MG, mammary gland.

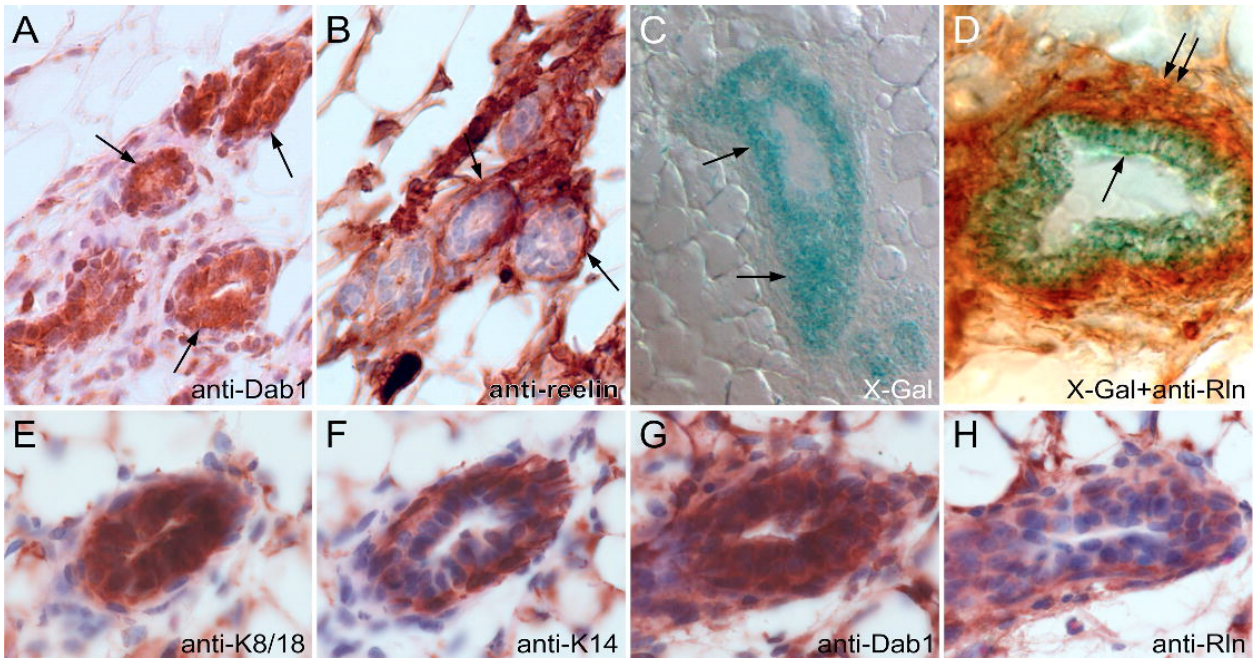

Figure 1.2. Reelin and Dab1 expression in the adult mammary gland.
(A-D) Dab1 is expressed in the luminal epithelium of adult females (A, C, D arrows). Reelin (B, D) is expressed in a complementary pattern in the periductal stroma (B, arrow; D, double arrow). (E-H) Serial sections through the same duct labeled for K8/18 (E), K14 (F), Dab1 (G) and reelin (H) confirm that Dab1 is expressed in the luminal cells and reelin is expressed in the periductal stroma.

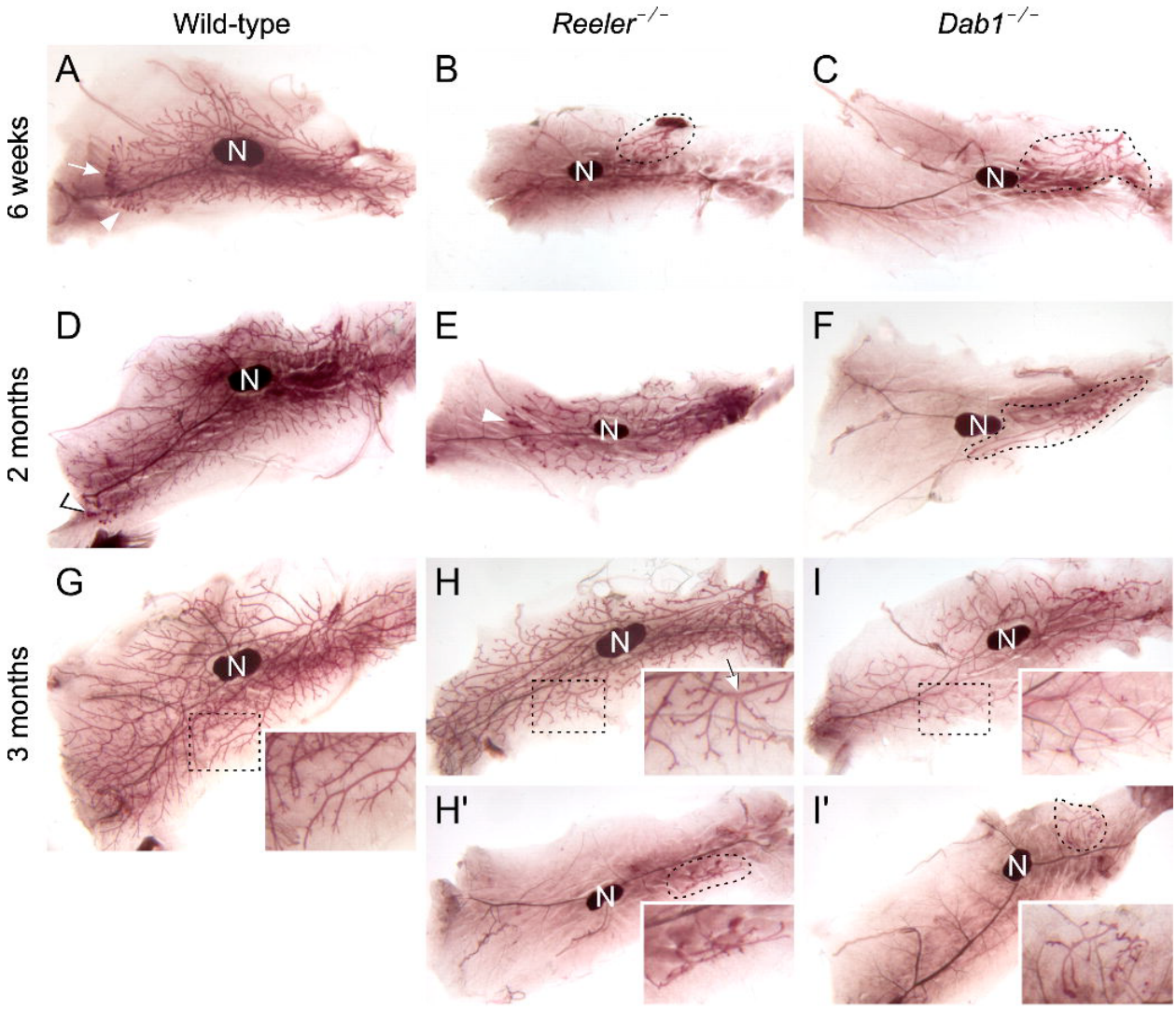

Figure 1.3. Loss of *reelin* and *Dab1* expression delays and disrupts ductal tree formation. (A) Wild-type mammary gland with immature ductal arborization. Arrowheads indicate TEBs. (B, C) *Reeler* and *Dab1* mutant mammary glands with rudimentary ductal arborization. Mammary ducts are indicated with the dotted outlines. (D) Wild-type mammary gland with mature arborization. The arrowhead indicates a distal TEB. (E) *Reeler* mutant mammary gland with immature arborization. The arrowhead indicates a TEB. (F) *Dab1* mutant mammary gland with rudimentary ductal arborization. Mammary ducts are indicated by the dotted outline. (G) Wild-

type mammary gland with mature arborization. The inset shows higher magnification of the terminal branches in the outlined area. (H, H') *Reeler* mutant mammary glands with mature (H) and rudimentary (H') ductal arborization. Insets show terminal branching (H) or the complete ductal network (H'). An abnormal branch point is indicated by the arrow in the H inset. (I, I') *Dab1* mutant mammary glands with mature (I) and rudimentary (I') arborization. Insets show terminal branching (I) or the complete ductal network (I'). All panels show the #4 inguinal mammary gland, oriented with the nipple to the right. N, inguinal lymph node.

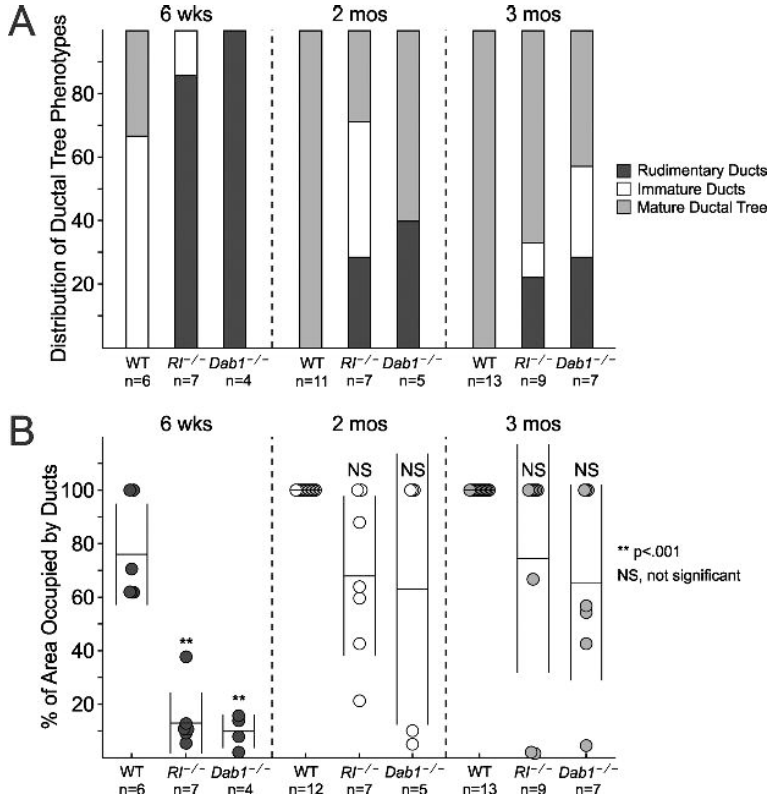

Figure 1.4. Mutant animals have rudimentary or immature ducts and show decreased fat pad colonization.

(A) Distribution of rudimentary, immature and mature ductal branching phenotypes in wild-type, *reeler* (*Rl*$^{-/-}$) and *Dab1*$^{-/-}$ mice at 6 weeks, 2 months and 3 months of age. (B) Quantification of the fat pad area occupied by ductal branches in wild-type, *Rl*$^{-/-}$, and *Dab1*$^{-/-}$ mammary glands at 6 weeks, 2 months and 3 months of age. Horizontal bars across each group of points designate the average area occupied, with the standard deviation indicated by vertical bars flanking each group of points. Significance was determined using t-test comparisons between wild-type and mutant groups assuming unequal variance. WT, wild type.

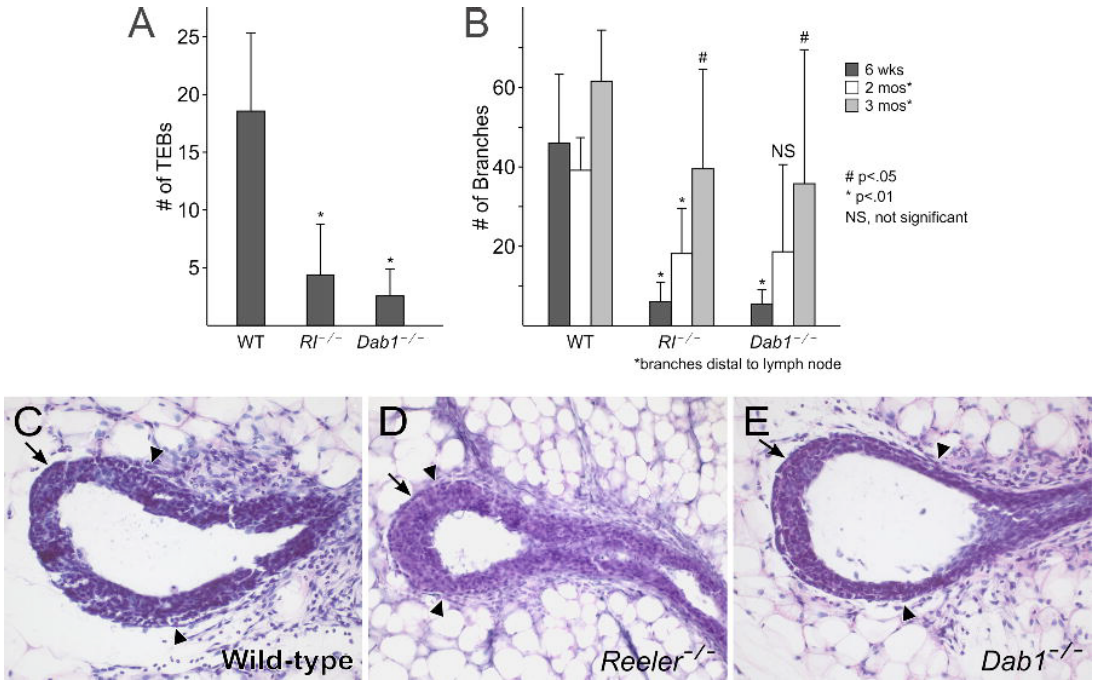

Figure 1.5. TEB distribution and morphology.
(A, B) TEBs were counted in 6-week-old mammary glands (A), whereas terminal branches were counted at 6 weeks, 2 months and 3 months of age (B). For 2- and 3-month-old glands, only those terminal branches extending past the level of the inguinal lymph node were counted. WT: n=7 (6 weeks), n=12 (2 months), n=7 (3 months); *Rl*$^{-/-}$: n=7 (6 weeks), n=7 (2 months), n=8 (3 months); *Dab1*$^{-/-}$ n=5 (6 weeks), n=4 (2 months), n=8 (3 months). Statistical significance was determined using t-test comparisons assuming unequal variance. Error bars indicate s.d. (C-E) Sections through TEBs in a wild-type gland at 6 weeks of age (C), and through *reeler* (D), and *Dab1* (E) mutant glands at 2 months of age. Cap cells (arrows) are seen at the distal tip of all three TEBs and the transition point from cap cells to myoepithelial cells is marked with arrowheads. WT, wild type.

TEB/Branch Ratio			
	WT	*Rl*$^{-/-}$	*Dab1*$^{-/-}$
6 weeks	0.337, n=7	0.677, n=7	0.401, n=5
2 months	0.028, n=9	0.289, n=7	0.125, n=4
3 months	0.000, n=6	0.000, n=8	0.200, n=8

Table 1.1. The average ratio of TEBs to total terminal branches.

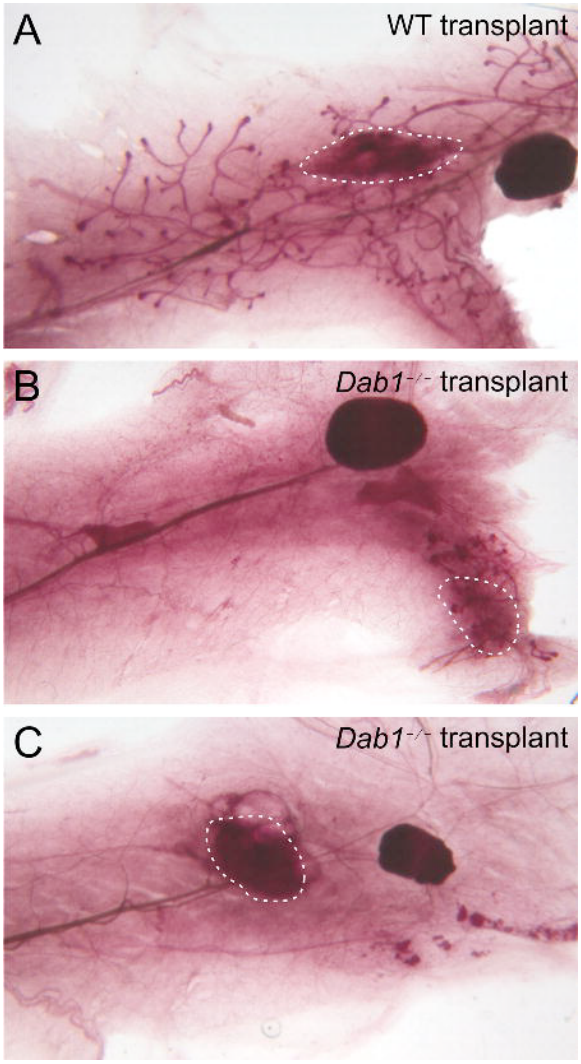

Figure 1.6. Mutant tissue transplanted into wild-type hosts fails to elaborate a ductal network.
(A) Mammary ducts extend from a fragment of a wild-type gland (outlined) in the cleared fat pad of a wild-type host. (B, C) Transplanted *Dab1* mutant gland fragments (outlined) fail to extend ducts (C) or extend only rudimentary ducts (B).

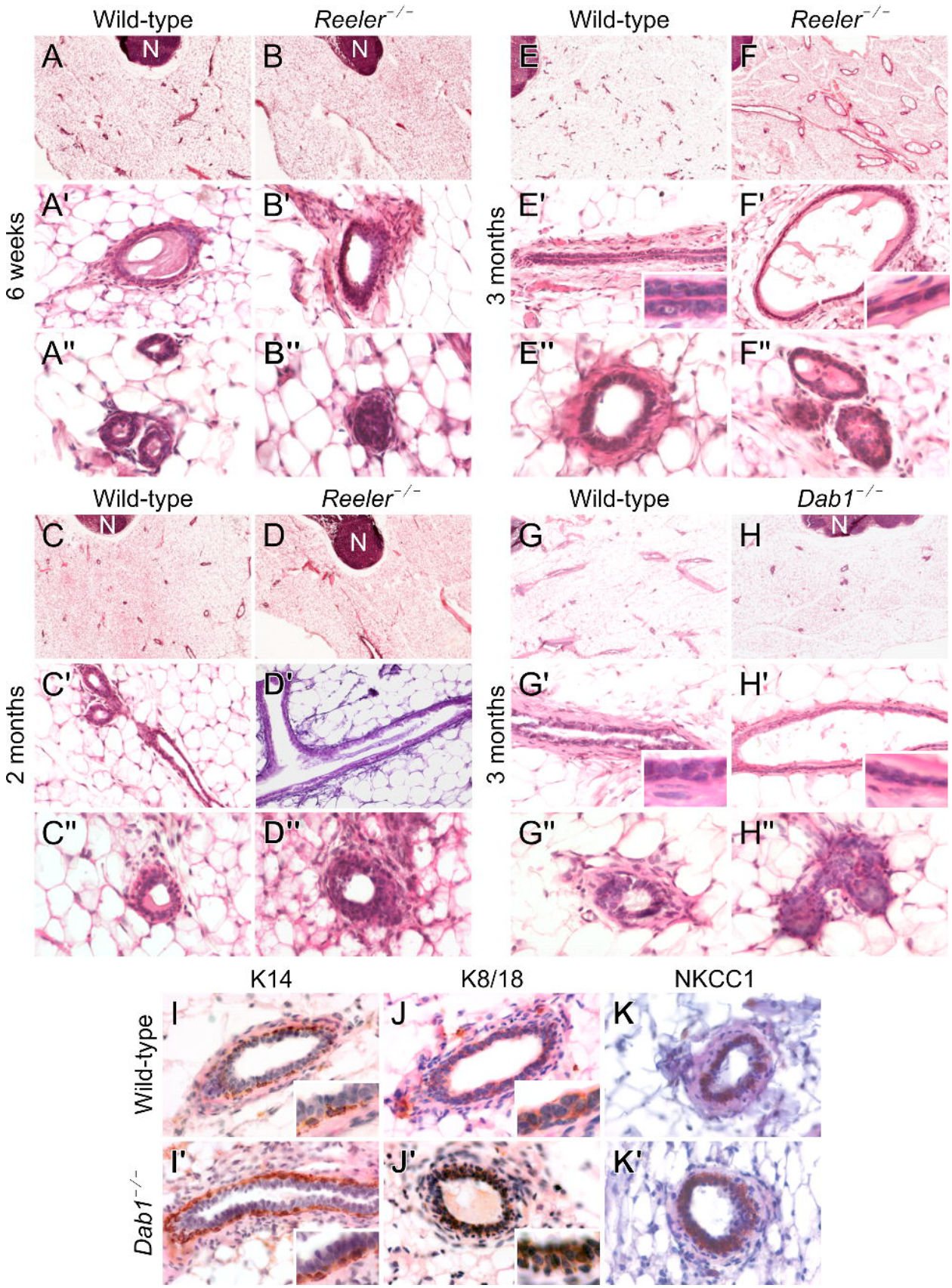
Wild-type
Reeler−/−
Wild-type
Reeler−/−
6 weeks
3 months
A
B
E
F
A'
B'
E'
F'
A''
B''
E''
F''
N
Wild-type
Reeler−/−
Wild-type
Dab1−/−
2 months
3 months
C
D
G
H
C'
D'
G'
H'
C''
D''
G''
H''
K14
K8/18
NKCC1
Wild-type
Dab1−/−
I
J
K
I'
J'
K'

Figure 1.7. Mutant mammary ducts have altered morphology.
(A-H) Low magnification views of hematoxylin and eosin-stained sections taken from inguinal mammary gland #4. (A'-H', A''-H'') Higher magnification views of selected ductal profiles from the corresponding section. The inguinal lymph node (N) is included at the top or top left of all low magnification sections for orientation. (I, I') K14 expression in wild-type and *Dab1* mutant ducts. (J, J') K8/18 expression in wild-type and *Dab1* mutant ducts. (K, K') NKCC1 expression in wild-type and *Dab1* mutant ducts. Insets show higher magnification views of the associated panels.

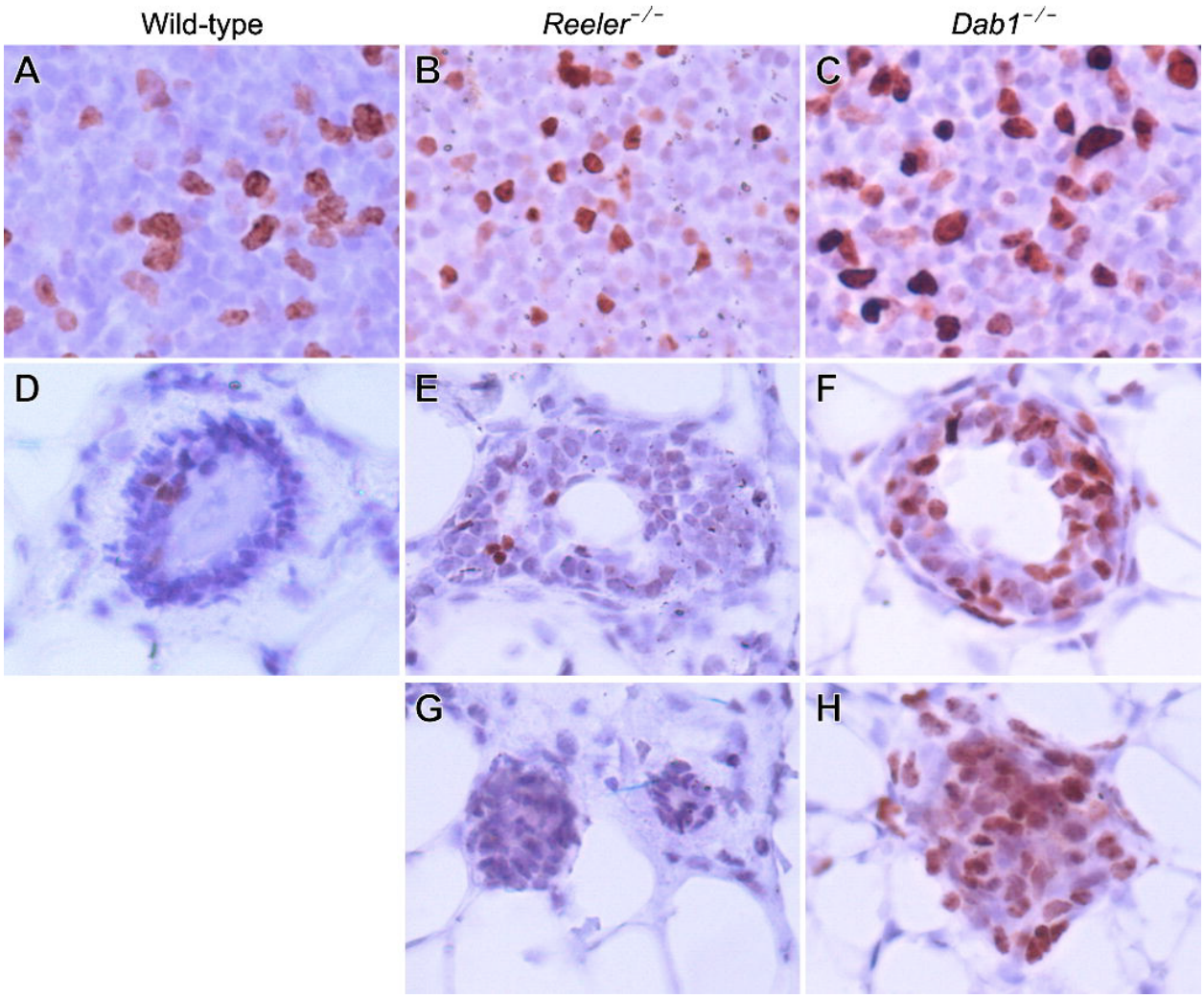

Figure 1.8. Ki67 labeling shows altered proliferation in mutant ducts.
(A, D) Wild-type inguinal lymph node (A) and mammary duct (D) labeled for Ki67 expression (brown label). (B, E, G) Ki67 labeling of lymph node (B) and mammary ducts (E, G) in *reeler* mutant. (C, F, H) Ki67 labeling of lymph node (C) and mammary ducts (F, H) in *Dab1* mutant. Occluded ducts were seen in both *reeler* (G) and *Dab1* (H) mutants. All sections are from animals at 3 months of age.

Percentage of Ki67-labeled cells			
	Lymph Node	Mammary Ducts	Ratio
WT	16.76, n=8	8.75, n=19	0.522
Reeler$^{-/-}$	9.7, n=4	1.7, n=9	0.175
Dab1$^{-/-}$	13.9, n=4	14.5, n=19	1.043

Table 1.2. The percentage of Ki67-positive cells in wild-type and mutant mice.

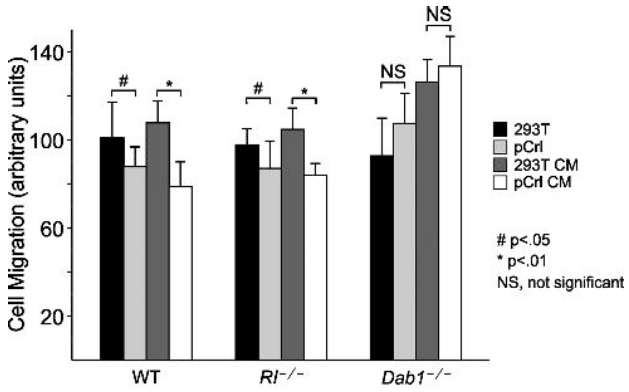

Figure 1.9. Exogenous reelin inhibits MEC migration.
Migration of primary MECs in transwell assays. Wild-type, *Rl*$^{-/-}$ or *Dab1*$^{-/-}$ MECs were introduced into transwells in the presence of control cells, control conditioned medium, reelin-secreting cells or reelin-secreting cell conditioned medium. Mean cell migration rate was calculated as a percentage of the migration rate observed in the presence of DMEM+FBS alone; error bars indicate s.d. Statistical significance was determined using two-sample t-test comparisons assuming equal variance. 293T, control cells; 293T CM, control conditioned medium; pCrl, reelin-secreting cells; pCrl CM, reelin-secreting cell conditioned medium.

References

Anderson, T.R., Hedlund, E., Carpenter, E.M. (2002). Differential Pax6 promoter activity and transcript expression during forebrain development. *Mech. Dev.* **114**:171-175.

Ball, S. (1998). The development of the terminal end bud in the prepubertal-pubertal mouse mammary gland. *Anat. Rec.* **250**:459-464.

Bouras, R., Pal, B., Vaillani, F., Harburg, G., Asselin-Labat, M.-L., Oakes, S.R., Lindeman, G.J., Visvader, J.E. (2008). Notch signaling regulates mammary stem cell function and luminal cell-fate commitment. *Cell Stem Cell.* **3**:429-441.

Caviness, V.S. (1976). Patterns of cell and fiber distribution in the neocortex of the reeler mutant mouse. *J. Comp. Neurol.* **170**:435-447.

Caviness, V.S., Sidman, R.L. (1973). Retrohippocampal, hippocampal and related structures of the forebrain in the reeler mutant mouse. *J. Comp. Neurol.* **147**:235-254.

Costagli, A., Felice, B., Guffanti, A., Wilson, S.W., Mione, M. (2006). Identification of alternatively spliced dab1 isoforms in zebrafish. *Dev. Genes Evol.* **216**:291-299.

Cunha, G.R. (1994). Role of mesenchymal-epithelial interactions in normal and abnormal development of the mammary gland and prostate. *Cancer.* **74**:1030-1044.

D'Arcangelo, G., Curran, T. (1998). Reeler: new tales on an old mouse mutant. *BioEssays*. **20**:235-244.

D'Arcangelo, G., Miao, G.G., Chen, S.C., Soares, H.D., Morgan, J.I., Curran, T. (1995). A protein related to extracellular matrix proteins deleted in the mouse mutant reeler. *Nature.* **374**:719-723.

D'Arcangelo, G., Homayouni, R., Keshvara, L., Rice, D.S., Sheldon, M., Curran, T. (1999). Reelin is a ligand for lipoprotein receptors. *Neuron.* **24**:471- 479.

DeOme, K.B., Faulkin, L.J. Jr, Bern, H.A., Blair, P.B. (1959). Development of mammary tumors from hyperplastic alveolar nodules transplanted into gland-free mammary fat pads of female C3H mice. *Cancer Res.* **19**:515-520.

Förster, E., Jossin, Y., Zhao, S., Chai, X., Frotscher, M., Goffinet, A.M. (2006). Recent progress in understanding the role of Reelin in radial neuronal migration, with specific emphasis on the dentate gyrus. *Eur. J. Neurosci.* **23**:901-909.

Gjorevski, N., Nelson, C.M. (2009). Bidirectional extracellular matrix signaling during tissue morphogenesis. *Cytokine Growth Factor Rev.* **20**:459-465.

Goffinet, A.M. (1984). Events governing organization of postmigratory neurons: studies on brain development in normal and reeler mice. *Brain Res.* **319**:261-296.

Goffinet, A.M., So, K.F., Yamamoto, M., Edwards, M., Caviness, V.S. (1984). Architectonic and hodological organization of the cerebellum in reeler mutant mice. *Brain Res.* **318**:263-276.

Hashimoto-Torii, K., Torii, M., Sarkisian, M.R., Bartley, C.M., Shen, J., Radtke, F., Gridley, T., Sestan, N., Rakic, P. (2008). Interaction between reelin and notch signaling regulates neuronal migration in the cerebral cortex. *Neuron.* **60**:273-284.

Hennighausen, L., Robinson, G.W. (2005). Information networks in the mammary gland. *Nat. Rev. Mol. Cell. Biol.* **6**:715-725.

Herz, J., Chen, Y. (2006). Reelin, lipoprotein receptors and synaptic plasticity. *Nat. Rev. Neurosci.* **7**:850-859.

Howell, B.W., Gertler, F.B., Cooper, J.A. (1997a). Mouse disabled (mDab1): a Src binding protein implicated in neuronal development. *EMBO J.* **16**:121-132.

Howell, B.W., Hawkes, R., Soriano, P., Cooper, J.A. (1997b). Neuronal position in the developing brain is regulated by mouse disabled-1. *Nature.* **389**:733-737.

Howell, B.W., Herrick, T.M., Cooper, J.A. (1999). Reelin-induced tyrosine phosphorylation of Disabled 1 during neuronal positioning. *Genes Dev.* **13**:643-648.

Hu, H., Bliss, J.M., Wang, Y., Colicelli, J. (2005). RIN1 is an ABL tyrosine kinase activator and a regulator of epithelial-cell adhesion and migration. *Curr. Biol.* **15**:815-823.

Kleinberg, D.L., Ruan, W. (2008). IGF-1, GH, and sex steroid effects in normal mammary gland development. *J. Mammary Gland Biol. Neoplasia*. **13**:353-360.

Kuo, G., Arnaud, L., Kronstad-O'Brien, P., Cooper, J.A. (2005). Absence of Fyn and Src causes a reeler-like phenotype. *J. Neurosci.* **25**:8578-8586.

Li, G., Robinson, G.W., Lesche, R., Martinez-Diaz, H., Jiang, Z., Rozengurt, N., Wagner, K.-U., Wu, D.-C., Lane, T.F., Liu, X., et al. (2002). Conditional loss of PTEN leads to precocious development and neoplasia in the mammary gland. *Development* **129**:4159-4170.

Maurin, J.C., Couble, M.L., Didier-Bazes, M., Brisson, C., Magloire, H., Bleicher, F. (2004). Expression and localization of reelin in human odontoblasts. *Matrix Biol.* **23**:277-285.

Mikkola, M.L., Millar, S.E. (2006). The mammary bud as a skin appendage: unique and shared aspects of development. *J. Mammary Gland Biol. Neoplasia* **11**:187-203.

Naylor, M.J., Ormandy, C.J. (2002). Mouse strain-specific patterns of mammary epithelial ductal side branching are elicited by stromal factors. *Dev. Dyn.* **225**:100-105.

Phelps, P.E., Rich, R., Dupuy-Davis, S., Rios, Y., Wong, T. (2002). Evidence for a cell-specific action of Reelin in the spinal cord. *Dev. Biol.* **244**:180-198.

Pramatarova, A., Chen, K., Howell, B.W. (2008). A genetic interaction between the APP and Dab1 genes influences brain development. *Mol. Cell. Neurosci.* **37**:178-186.

Rice, D.S., Curran, T. (2001). Role of the Reelin signaling pathway in central nervous system development. *Annu. Rev. Neurosci.* **24**:1005-1039.

Robinson, G.W. (2007). Cooperation of signaling pathways in embryonic mammary gland development. *Nat. Rev. Genet.* **8**:963-972.

Sato, N., Fukushima, N., Chang, R., Matsubayashi, H., Goggins, M. (2006). Differential and epigenetic gene expression profiling identifies frequent disruption of the RELN pathway in pancreatic cancers. *Gastroenterology.* **130**:548-565.

Shackleton, M., Vaillant, F., Simpson, K.J., Stingl, J., Smyth, G.K., Asselin-Labal, M.-L., Lindeman, G.J., Visvader, J.E. (2006). Generation of a functional mammary gland from a single stem cell. *Nature*. **439**:84-88.

Simmons, P.A., Pearlman, A.L. (1983). Receptive-field properties of transcallosal visual cortical neurons in the normal and reeler mouse. *J. Neurophysiol.* **50**:838-848.

Sternlicht, M.D., Kouros-Mehr, H., Lu, P., Werb, Z. (2006). Hormonal and local control of mammary branching morphogenesis. *Differentiation.* **74**:365-381.

Streuli, C.H., Schmidhauser, C., Bailey, N., Yurchenco, P., Skubitz, A.P., Roskelley, C., Bissell, M.J. (1995). Laminin mediates tissue-specific gene expression in mammary epithelia. *J. Cell Biol.* **129**:591-603.

Yip, J.W., Yip, Y.P., Nakajima, K., Capriotti, C. (2000). Reelin controls position of autonomic neurons in the spinal cord. *Proc. Natl. Acad. Sci. USA.* **97**:8612-8616.

Yip, Y.P., Rinaman, L., Capriotti, C., Yip, J.W. (2003). Ectopic sympathetic preganglionic neurons maintain proper connectivity in the reeler mutant mouse. *Neuroscience.* **118**:439-450.

CHAPTER TWO: Reelin deficiency delays mammary tumor growth and metastatic progression

Abstract

Reelin is a regulator of cell migration in the nervous system, and has other functions in the development of a number of non-neuronal tissues. In addition, alterations in reelin expression levels have been reported in breast, pancreatic, liver, gastric, and other cancers. Reelin is normally expressed in mammary gland stromal cells, but whether stromal reelin contributes to breast cancer progression is unknown. Herein, we used a syngeneic mouse mammary tumor transplantation model to examine the impact of host-derived reelin on breast cancer progression. We found that transplanted syngeneic tumors grew more slowly in reelin-deficient ($rl^{Orl-/-}$) mice and had delayed metastatic colonization of the lungs. Immunohistochemistry of primary tumors revealed that tumors grown in $rl^{Orl\ -/-}$ animals had fewer blood vessels and increased macrophage infiltration. Gene expression studies from tumor tissues indicate that loss of host derived reelin alters the balance of M1- and M2-associated macrophage markers, suggesting that reelin may influence the polarization of these cells. Consistent with this, $rl^{Orl\ -/-}$ M1-polarized bone marrow-derived macrophages have heightened levels of the M1-associated cytokines *iNOS* and *IL-6*. Based on these observations, we propose a novel function for the reelin protein in breast cancer progression.

Introduction

The reelin signaling pathway is widely recognized as an important regulator of cell migration in the developing central nervous system (Fatemi, 2008; Honda et al., 2011; Abadesco et al., 2014; D'Arcangelo, 2014). Reelin is a glycoprotein secreted into the extracellular matrix, and canonically signals by binding to low-density lipoprotein receptors Apo E receptor 2 (ApoER2) and very low-density lipoprotein receptor (VLDLR) located on the surface of reelin-responsive cells (Herz and Chen, 2006). Binding of reelin to its receptors recruits the intracellular adaptor protein Disabled-1 (Dab1), which is phosphorylated by Src family kinases on tyrosine residues (Bock and Herz, 2003; Kuo et al., 2005). Phosphorylated Dab1 activates multiple downstream effectors, including phosphatidylinositol-3-kinase (PI3K)/Akt and C3G/Rap1 (Honda et al., 2011). This cascade of signaling events leads to changes in cytoskeleton stabilization, allowing reelin to orchestrate cell migration in the central nervous system. Although the primary mode of reelin signaling involves binding to lipoprotein receptors and activation of Dab1, a growing body of evidence suggests that reelin is also able to signal via non-canonical pathways that may involve other receptors and downstream effectors. For example, activation of extracellular-signal-regulated kinase 1/2 (Erk1/2) by reelin does not involve ApoER2 or VLDLR, and seems to be independent of Dab1 (Lee et al., 2014). However, the exact mechanisms of non-canonical reelin signaling remain poorly understood.

Recent studies have identified a number of non-neuronal functions for reelin (Botella-López et al., 2008; Lutter et al., 2012; Diaz-Mendoza et al., 2014; Tseng et al., 2014; Vázquez-Carretero et al., 2014). For example, reelin signaling was found to regulate the homeostasis of the intestinal crypt-villus unit, formation of thrombin clots, and to be important for establishment of the lymphatic vasculature (Lutter et al., 2012; Tseng et al., 2014; Vázquez-Carretero et al., 2014). Our laboratory found that canonical reelin signaling is essential for proper mammary gland development (Khialeeva et al., 2011). Reelin is normally expressed in the myoepithelial layer and the stroma of the developing and mature mammary ducts, while Dab1 is expressed in

the luminal epithelium. Reelin and Dab1 coordinate ductal extension and refine the morphology of the mammary ducts. Absence of canonical reelin signaling results in ductal growth delays, abnormal branching patterns and disorganized cellular layers within the mammary ducts (Khialeeva et al., 2011). Alterations in reelin signaling have been reported in pancreatic, gastric, prostate, and esophageal cancers (Wang et al., 2002; Perrone et al., 2007; Hong et al., 2008; Dohi et al., 2010). Interestingly, reelin expression is lost in many human breast tumors, and the loss of reelin protein correlates with poor survival (Stein et al., 2010), but the mechanisms by which reelin may affect breast cancer progression *in vivo* remain to be determined.

To better understand the relationship between reelin signaling and breast cancer, we monitored mammary tumor growth and metastatic progression following transplantation of 4T1 mouse mammary tumor cells into mice that lack functional reelin protein ($rl^{Orl\ -/-}$) or canonical reelin signaling ($Dab1^{-/-}$). We chose the 4T1 mammary tumor transplantation model for two reasons. First, 4T1 cells mimic stage IV human breast cancer, and rapidly form primary tumors and spontaneous lung metastases when orthotopically injected into Balb/C mice (Pulaski and Ostrand-Rosenberg, 2001). Second, the 4T1 model allows us to study tumor progression in immunocompetent mice carrying the rl^{Orl} mutation, and provides us with the ability to address the contribution of the host immune response to the growth of primary tumors and metastasis.

We report that the absence of reelin from the host environment delays primary tumor growth and metastatic spread of mammary carcinoma cells, possibly via alterations in the cytokine expression profile of tumor-associated macrophages (TAMs). Loss of reelin does not directly affect tumor cells, but may modulate the activation of macrophages in the tumor microenvironment, diminishing their tumor-promoting properties. Furthermore, these effects of reelin likely do not stem from canonical reelin signaling, as tumor growth and metastasis are not affected in $Dab1^{-/-}$ mice. Our results indicate a novel function for the reelin protein in mammary tumor progression, and suggest possible roles for reelin in macrophage activation.

Materials and Methods

Mouse lines

All animal studies were conducted in accordance with the UCLA Office of Animal Research Oversight and Institutional Animal Care and Use Committee protocols. *Reeler Orleans* (*rl*$^{Orl\ -/-}$) mice were obtained from a breeding colony maintained at UCLA. These mice carry a naturally occurring mutation, in which a transposon insertion leads to exon skipping and a 220 bp deletion in the *reelin* mRNA (Takahara et al., 1996). The resulting reelin protein is truncated and is not secreted (De Bergeyck et al., 1997). CBy.129S4-*Dab1*^{tm1cpr}/J (*Dab1* $^{-/-}$) mice were purchased from the Jackson Laboratory, and carry a targeted disruption of the protein-interacting (PI/PTB) domain of *Dab1* (Howell et al., 1997). *Dab1* $^{-/-}$ mice were maintained on the Balb/C background by the Jackson Laboratory at the time of purchase. *Rl*^{Orl} mice were initially on a mixed, 70-75% Balb/C and 20-25% 129/Sv background, and were backcrossed to the Balb/C strain for three generations to obtain ≥95% Balb/C offspring. The genetic background of *Dab1* and *rl*^{Orl} lines was confirmed by single nucleotide polymorphism (SNP) scanning (The Jackson Laboratory). The use of a Balb/C background is necessary for histocompatibility, as 4T1 cells are derived from Balb/C mice (Pulaski and Ostrand-Rosenberg, 2001). Homozygous mutant and wild type control female offspring were obtained from intercrosses of heterozygous *rl*$^{Orl\ +/-}$ or *Dab1*$^{+/-}$ animals. *Rl*^{Orl} and *Dab1* mice were genotyped by PCR as described (Takahara et al., 1996; Howell et al., 1997).

Cell lines

The 4T1 cell line was purchased from American Type Culture Collection, and maintained according to ATCC guidelines. Cells were cultured in RPMI-1640 medium (Life Technologies) supplemented with 10% fetal bovine serum (FBS, Omega) and 100 u/mL penicillin/streptomycin (Life Technologies). Sub-confluent cultures were treated with 0.25% trypsin-EDTA (Life

Technologies) and passaged, or counted using a hemocytometer and used for *in vitro* or *in vivo* experiments.

The reelin-secreting HEK293T cell line (stably transfected with a full-length reelin clone) was kindly provided by Dr. Tom Curran, Children's Hospital of Philadelphia, PA, USA (D'Arcangelo et al., 1999). The control HEK293T cell line was kindly provided by Dr. Harley Kornblum, University of California Los Angeles, CA, USA. Both cell lines were cultured in DMEM (Life Technologies) supplemented with 10% FBS and 100 u/mL penicillin/streptomycin. Conditioned media was collected from confluent cells after 48 hours of culture, centrifuged at 600 g for 10 min, and the supernatant was collected and used immediately for treatment of 4T1 cells and migration assays.

Mammary epithelial cell (MEC) purification

MECs were purified as previously described (Ewald, 2013). Briefly, pairs of #3 thoracic and #4 inguinal mammary glands were dissected from 8-10 week-old female mice, minced and incubated in DMEM/F12 (Corning) containing 5% FBS, 100 u/mL penicillin/streptomycin, 2 mg/mL collagenase IV (Sigma), 2 mg/mL trypsin (Sigma), and 5 µg/mL insulin (Life Technologies) on an orbital shaker at 100 RPM, 37°C, for 1 hr. Digested tissue was treated with 4 u/mL DNAse (Sigma), and organoids containing MECs were purified by repeated pulse centrifugation.

Transwell migration assay

10^5 4T1 cells in serum-free DMEM were seeded on top of Boyden transwells fitted with membranes containing 8 µm pores, and allowed to migrate overnight in response to conditioned media from reelin-secreting HEK293T cells or control HEK293T cells with 10% FBS. Cell nuclei were stained with DAPI, and membranes were imaged on a Zeiss Axioskop with a cooled CCD camera. Four evenly spaced 100X fields per membrane were photographed and used to count

the number of cells that migrated through the membrane. Cell counts were used to determine the average number of migrating cells for each membrane.

Tumor challenge

10^5 4T1 cells in HBSS were injected into the left #4 mammary fat pad of homozygous mutant and control wild type rl^{Orl} or *Dab1* 8-10 week-old female mice. The tumor diameters were measured every 3-4 days beginning on day 11 after transplantation using electronic calipers. The tumor volume was calculated using the formula $L \times W^2 \times 0.52$, where L = longest diameter, and W = perpendicular diameter (Kim et al., 2011). All mice were sacrificed before the primary tumor diameter reached 1.5 cm or when the animals became moribund.

Micrometastasis assay

Lungs from tumor-bearing mutant and wild type rl^{Orl} or *Dab1* mice were dissected in sterile conditions, and lung tissue was processed as described (Pulaski and Ostrand-Rosenberg, 2001). Briefly, lungs were minced and incubated in digestion buffer containing collagenase I (Sigma) for 1 hour at 37°C. Digested tissue was sieved through 70 µm cell strainers, and red blood cells were lysed in RBC lysis buffer (StemCell Technologies). The resulting cell suspension was serially diluted into 6-well plates in RPMI-1640 medium supplemented with FBS and penicillin/streptomycin. The next day, medium was replaced with complete RPMI-1640 containing 60 µM 6-thioguanine. After 10 days of incubation, resistant 4T1 colonies were stained with methylene blue and counted. The number of 4T1 colonies was equated to the number of 4T1 cells in the seeded cell suspension, normalized to the number of cells plated, and the resulting percentage was reported as the metastatic burden.

Immunohistochemistry and histology

For paraffin-embedded samples, dissected tumor slices were fixed overnight in Bouin's fixative, washed, dehydrated, and embedded in paraffin. For frozen samples, tumor slices were fixed in 4% paraformaldehyde for 4 hours, cryoprotected in 30% sucrose and embedded in Optimal Cutting Temperature compound (Sakura).

For Ki-67 and CD31 labeling, paraffin-embedded samples were sectioned at 10 μm. The sections were rehydrated through graded ethanols and boiled in 10 mM sodium citrate buffer to retrieve antigens. After blocking endogenous peroxidases, as well as avidin and biotin, sections were incubated with primary, and then biotinylated secondary antibodies. The antibodies used were rabbit anti-Ki-67 (1:500, Vector Labs), rat anti-CD31 (1:200, Dianova), biotinylated goat anti-rabbit (1:500, Jackson Immunoresearch), biotinylated donkey anti-rat (1:500, Jackson Immunoresearch). The antibodies were visualized using an ABC Elite Kit (Vector Labs) and diaminobenzidine (DAB) staining. Cell nuclei were counterstained with hematoxylin.

For F4/80 labeling, 10 μm frozen sections were treated with 1% Triton X-100 (Sigma), blocked with donkey serum, and incubated with primary antibody, then AlexaFluor 594-conjugated secondary antibody. Cell nuclei were counterstained with DAPI. The antibodies used were rat anti-F4/80 (1:1000, Abbiotec), Alexa Fluor 594 donkey anti-rat (1:500, Life Technologies).

For histological evaluation of tumor sections, 10 μm paraffin sections were rehydrated through graded ethanols and stained with hematoxylin and eosin.

For Ki-67 labeling analysis, Ki-67-positive and Ki-67-negative cell nuclei were counted in 4 random fields per sample using the ObjectJ plugin in ImageJ (NIH), and the average percentage of Ki-67-positive nuclei was calculated for each sample. Each analyzed field contained at least 500 total cells. For CD31 and F4/80 labeling analysis, 6 random 200X fields per sample were imaged, DAB signal (for CD31) or AlexaFluor 594 signal (for F4/80) was

thresholded in ImageJ, and the average percentage of CD31-positive or F4/80-positive area was calculated for each sample.

Quantitative PCR (qPCR)

RNA from tumor tissues or cells was extracted using TRI reagent (Sigma), and the cDNA was generated using an iScript cDNA Synthesis kit (Bio-Rad). qPCR was carried out using the KAPA SYBR FAST master mix (KAPA Biosystems) on a Light Cycler 480 (Roche). Expression values were normalized to the housekeeping gene *36b4/RPLP0*. Primer sequences are listed in Table 2-1.

Western blotting

Tumor tissue was homogenized in radioimmunoprecipitation (RIPA) buffer containing phosphatase inhibitor cocktail (Zmtech scientific). Protein samples (35 µg) were separated on 4-12% Bis-Tris SDS-PAGE gels (Life Technologies), and transferred onto Immuno-Blot PVDF membranes (Bio-Rad). Membranes were blocked in PBS with 5% skim milk and 0.1% Tween-20 for 1 hour, and incubated with primary antibodies overnight at 4°C, then with secondary antibodies for 30 min at room temperature. Protein bands were detected using the ECL Western blotting detection reagent (GE Amersham). Band intensities were quantified using ImageJ and relative protein levels were normalized to β-actin levels. The following antibodies were used: mouse anti-arginase-1 (1:4000, BD Biosciences), mouse anti-β-actin (1:10,000, Sigma), mouse anti-reelin (1:500, Millipore), peroxidase conjugated goat anti-mouse (1:3000, Cell Signaling).

Bone marrow-derived macrophage (BMDM) culture

Femurs and tibias were collected from 6-8 week old female mutant and wild type rl^{Orl} and *Dab1* mice. BMDM cultures were prepared as described (York et al., 2015). Briefly, the bone marrow was flushed and passed through 26G needles to generate a single cell suspension and

the red blood cells were lysed in RBC lysis buffer. The remaining cells were counted, and equal numbers were plated into 6-well plates. Macrophages were differentiated over the course of 7 days in DMEM with addition of 20% FBS, 100 u/mL penicillin/streptomycin, 2 mM L-glutamine (Life Technologies), 0.5 mM sodium pyruvate (Life Technologies), and 5% conditioned media from CMG 14-12 cells, which contains macrophage colony-stimulating factor (M-CSF). To generate M1 polarized macrophages, BMDM were treated with 50 ng/mL IFN-γ (Life Technologies) and 100 ng/mL LPS (InvivoGen) overnight.

Results

Reelin influences mammary tumor growth and metastasis in vivo

Loss of reelin expression in breast tumors correlates with poor patient prognosis and survival (Stein et al., 2010). In order to better understand the impact of reelin on the progression of breast cancer, we examined growth of 4T1-derived mouse mammary tumors in syngeneic reelin-deficient mice ($rl^{Orl\ -/-}$). Tumor development was initiated by injecting the mammary fat pads of female $rl^{Orl\ -/-}$ mice or wild type $rl^{Orl\ +/+}$ controls with 10^5 4T1 cells. Primary tumors grew more slowly in $rl^{Orl\ -/-}$ mice (Figure 2.1A), and weighed significantly less than tumors from wild type control mice 25 days after the 4T1 cell injection (Figure 2.1B). Mice with mutations in the *reelin* gene are usually smaller in size than their wild type and heterozygous littermates, and the $rl^{Orl\ -/-}$ mice used in our study also weighed significantly less than the $rl^{Orl\ +/+}$ controls (Figure 2.1C) (Falconer, 1951). However, tumor growth had no impact on the overall weight of tumor-bearing animals, as the body weight of $rl^{Orl\ -/-}$ and $rl^{Orl\ +/+}$ mice did not change significantly from day 1 to day 25 (Figure 2.1C). The metastatic spread of 4T1 cells to the lungs was assessed by a micrometastasis assay. In $rl^{Orl\ +/+}$ mice, the tumor cells on average comprised 0.36% of all cells in lung suspensions (Figure 2.1D). The rate of lung metastasis in $rl^{Orl\ +/+}$ mice was similar to that in Balb/C mice co-injected with 10^5 4T1 cells in the same experiment, and resembled previously published results from other groups (Figure 2.1E) (Thomas and Fraser, 2003; DuPré et al., 2007; Chen et al., 2010). We observed a significant reduction of the metastatic burden in the lungs of $rl^{Orl\ -/-}$ mice (Figure 2.1D, E). These results indicated that the absence of reelin from the host environment impedes growth of primary 4T1-derived tumors and metastatic progression *in vivo*.

Reelin does not directly affect migration or growth of 4T1 cells

Next, we asked whether reelin could impact tumor growth via direct effects on 4T1 cells. Previous studies showed that primary mammary epithelial cells (MECs) normally express reelin,

Dab1, and the reelin receptors ApoER2 and VLDLR (Khialeeva et al., 2011). We assessed the expression of the reelin pathway components in 4T1 cells by qPCR, and found that both *reelin* and *Dab1* were significantly downregulated in comparison to normal MECs (Figure 2.2A). 4T1 cells expressed higher levels of *ApoER2*, while expression levels of *Vldlr* were similar to those in primary MECs (Figure 2.2A). Primary MECs respond to reelin by slowing their migration rate, and we hypothesized that this effect would be abolished in 4T1 cells because they lacked Dab1 (Khialeeva et al., 2011). As we expected, addition of reelin to culture medium had no effect on migration of 4T1 cells in transwell assays (Figure 2.2B). The proliferation of 4T1 cells was also unaltered in the presence of reelin (Figure 2.2C). Full-length reelin (400 kD), as well as two smaller reelin fragments (300 kD, 180 kD) resulting from protein processing were all present in the conditioned medium from reelin-expressing HEK293T cells (Figure 2.2D), suggesting that these results were not due to lack of available reelin. Thus, despite the expression of canonical reelin receptors in 4T1 cells, reelin does not appear to directly modulate the growth or migration of 4T1 cells.

Primary tumors grown in $rl^{Orl\ -/-}$ mice display alterations in blood vessel formation

Histological analysis of the primary tumors from $rl^{Orl\ -/-}$ mice did not reveal gross morphological differences from $rl^{Orl\ +/+}$ controls. In both cohorts, layers of tumor cells and infiltrating immune cells surrounded the necrotic tumor core (Figure 2.3A, B). Cell proliferation, as assessed by Ki67 staining, was also not significantly different in $rl^{Orl\ -/-}$ animals (Figure 2.3C, D). Tumor angiogenesis was impeded, as significantly fewer CD31-positive blood vessels were observed in primary tumors from $rl^{Orl\ -/-}$ mice (Figure 2.3E, F). However, analysis of angiogenic gene expression in primary tumors by qPCR showed no differences in levels of vascular endothelial growth factors A, B, and C (*Vegfa*, *Vegfb*, *Vegfc*), or transforming growth factor β (*Tgfb*) (Figure 2.4). Additionally, levels of the anti-angiogenic factor chemokine (C-X-C motif) ligand 10 (*Cxcl10*) were not significantly different (Figure 2.4).

TAMs are altered in the absence of reelin

Progression of 4T1 tumors is marked by the expansion of the myeloid cell compartment, with subsequent infiltration by immune cells, such as tumor associated macrophages (TAMs), into the primary tumor microenvironment (DuPré et al., 2007). TAMs are recognized as major contributors to tumor angiogenesis (Cho et al., 2012). Mice with the *reeler* mutation were previously reported to have deficits in the function of macrophages and T cells (Green-Johnson et al., 1995). We hypothesized that the $rl^{Orl\ -/-}$ environment may lead to alterations in the number or function of TAMs, which could contribute to the reduction in tumor angiogenesis. Consistent with this hypothesis, we saw increased levels of the chemokine *Cxcl5* and the metalloproteinase 9 (*Mmp-9*) mRNA in tumors from $rl^{Orl\ -/-}$ mice (Figure 2.4). CXCL5 and MMP-9 are factors secreted by TAMs, and we reasoned that their augmented expression may be indicative of elevated numbers of TAMs in the primary tumors from $rl^{Orl\ -/-}$ animals (Murdoch et al., 2008). Labeling of primary tumor sections with α-F4/80 antibody, a marker of TAMs, showed an increase in the area occupied by F4/80-positive cells in tumors from $rl^{Orl\ -/-}$ mice (Figure 2.5A, B, C) (DuPré et al., 2007). Thus, the elevated levels of CXCL5 and MMP-9 in the tumors from mice that lack reelin are likely due to an increase in TAM infiltration.

The activation state of TAMs determines their effect on cancer progression. M2-activated macrophages promote tumor angiogenesis and provide a variety of factors to elicit a sustained tumor-promoting Type 2 immune response. In contrast, abundance of M1-activated TAMs impedes angiogenesis and tumor growth, and results in a tumoricidal Type 1 immune response (Ma et al., 2010; Mills, 2012). To test whether reelin influenced the M1/M2 balance in TAMs, we examined the expression levels of several cytokines associated with M1 and M2 macrophages in the primary tumors from $rl^{Orl\ -/-}$ mice and wild type controls (Figure 2.5D). Absence of reelin from the host environment resulted in altered levels of these genes. Specifically, we observed increased levels of a hallmark M1 cytokine inducible nitric oxide synthase (*iNOS*), while the levels of *arginase 1 (Arg1)* and mannose receptor, C Type 1 (*Mrc1*)

mRNA, two genes expressed by M2-activated macrophages, were downregulated in primary tumors from *rl*$^{Orl\ -/-}$ mice (Figure 2.5D) (Mantovani et al., 2002; Mills, 2012). Western blotting confirmed the reduction in Arg1 levels (Figure 2.5E, F). Additionally, we observed higher levels of interleukin-10 (*IL-10*) in tumors from *rl*$^{Orl\ -/-}$ mice (Figure 2.5D). IL-10 is a broadly expressed cytokine with anti-inflammatory properties, and is produced in response to factors that promote a Type 1 immune response (Trinchieri, 2007; Saraiva and O'Garra, 2010). Our results indicate that in the absence of reelin, TAMs may shift to an M1-like state and elicit a tumor-restrictive Type 1 immune response.

Reelin influences mammary tumor progression independently of Dab1

In order to elucidate whether the absence of reelin impedes 4T1 tumor progression via canonical, Dab1-dependent mechanisms, we injected the mammary tumor cells into female *Dab1*$^{-/-}$ mice and wild type *Dab1*$^{+/+}$ controls. 4T1-derived primary tumors grew and metastasized slower in the *Dab1* line compared to the *rl*^{Orl} line. 4T1 cells are derived from Balb/C mice, and background compatibility with the host is necessary for the expected course of tumor progression. In order to rule out possible effects of background differences between the *rl*^{Orl} and the *Dab1* mouse lines, we confirmed the Balb/C background through single nucleotide polymorphism (SNP) scanning of 4 mice from each line. The *rl*^{Orl} mice contained on average 96.5% (SD = 1) Balb/C-specific SNPs, while mice from the *Dab1* line contained on average 94.9% (SD = 0.48) Balb/C-specific SNPs. Therefore, we cannot conclusively exclude the possibility that the small difference in the background contributed to our results.

In order to maximize the metastatic potential of 4T1 cells in *Dab1*$^{+/+}$ and *Dab1*$^{-/-}$ mice, we extended the duration of primary tumor growth to 32 days. Intriguingly, we saw no differences in the rate of 4T1 tumor growth between *Dab1*$^{+/+}$ and *Dab1*$^{-/-}$ mice (Figure 2.6A). Tumor wet weight and the metastatic burden in the lungs were also unaffected (Figure 2.6B, C). Similar to *rl*$^{Orl\ -/-}$ animals, *Dab1*$^{-/-}$ mice were smaller than their wild type littermates (Figure 2.6D). Examination of

Ki-67, CD31, and F4/80 labeling, as well as Arg1 levels, revealed no differences in proliferation, angiogenesis, or TAM infiltration in primary tumors from *Dab1*$^{-/-}$ mice (Figure 2.7A-E). These results confirm that the effects observed in *rl*$^{Orl\ -/-}$ animals are specific to reelin, and suggest that the delays in tumor growth are independent of the animal's size. In addition, our observations imply that reelin in the tumor environment functions through non-canonical mechanisms, independently of Dab1.

Absence of reelin skews the M1 activation state of bone marrow-derived macrophages

To test if macrophage activation was altered in the absence of reelin, we differentiated bone marrow-derived macrophages (BMDM) from *rl*$^{Orl\ -/-}$ mice and wild type controls and polarized them to an M1 state with interferon-γ (IFNγ) and lipopolysaccharide (LPS) (Pineda-Torra et al., 2015). IFNγ and LPS treatment robustly induced the expression of M1-associated genes *IL-1β, IL-6*, *IL-12*, tumor necrosis factor-α (*Tnfa*), and *iNOS* (Figure 2.8A). Unstimulated *rl*$^{Orl\ -/-}$ BMDM expressed higher levels of *IL-1β* compared to unstimulated wild type control BMDM, while the expression of other M1 genes was not altered (Figure 2.9A). M1-polarized *rl*$^{Orl\ -/-}$ macrophages expressed significantly higher levels of *IL-6* and *iNOS* compared to wild type control M1 macrophages (Figure 2.9B). In addition, levels of *IL-10* were 3-fold higher in M1 macrophages from *rl*$^{Orl\ -/-}$ mice compared to control M1 macrophages. In this model of M1 macrophage activation, IFNγ primes the macrophages for a rapid response to LPS, which triggers toll-like receptor (TLR) signaling and production of cytokines associated with the Type 1 immune response (Schroder et al., 2004). TLR signaling induces IL-10 expression in macrophages in order to negatively regulate the inflammatory response (Boonstra et al., 2006; Saraiva and O'Garra, 2010; Martinez and Gordon, 2014). Our results suggest that the upregulation of IL-10 in *rl*$^{Orl\ -/-}$ mice may be a part of a similar negative feedback mechanism. Thus, BMDM display a higher propensity towards M1 activation in the absence of reelin.

Next, we tested the induction of M1-specific cytokines in BMDM from *Dab1*$^{-/-}$ mice and wild type controls. Interestingly, unstimulated *Dab1*$^{-/-}$ BMDM expressed lower levels of *IL-1β* and *Tnfa* compared to unstimulated wild type control BMDM (Figure 2.9C). In addition, *Dab1*$^{-/-}$ macrophages treated with IFNγ and LPS expressed lower levels of *Tnfa* and *IL-10*, and marginally higher levels of *IL6* compared to wild type control M1 macrophages (Figure 2.8B, Figure 2.9D). Our results suggest that the effects of reelin on macrophage activation are independent of Dab1.

Discussion

The goal of the studies presented here was to better understand the role of reelin signaling in breast cancer growth and metastatic progression. We found that reelin deficiency delays primary tumor growth and lung metastasis, likely via Dab1-independent mechanisms. Because the size of the primary 4T1 tumor correlates with the extent of the metastatic burden, and 4T1 cells metastasize primarily via blood vessels, the reduction in lung metastases in $rl^{Orl\ -/-}$ mice is likely due to the smaller size and poor vascularization of the primary tumors (Aslakson and Miller, 1992; Pulaski and Ostrand-Rosenberg, 1998; Thomas and Fraser, 2003).

Although reelin did not directly affect proliferation or migration of 4T1 cells, we cannot rule out the possibility that reelin affects 4T1 cells via alternative mechanisms. For example, absence of reelin may lead to alterations in the gene expression profile of 4T1 cells, resulting in a tumor-restrictive microenvironment. The reduction in CD31-positive labeling of primary tumors from $rl^{Orl\ -/-}$ mice suggested a deficit in tumor angiogenesis. Surprisingly, we observed increased levels of the *Mmp-9* transcript in primary tumors from $rl^{Orl\ -/-}$ mice. MMP-9 activity is provided by myeloid cells in the tumor microenvironment and is required for tumor vasculogenesis (Kessenbrock et al., 2010). However, the pro-angiogenic effects of MMP-9 are contingent on its activation via a proteolytic cascade (Kessenbrock et al., 2010). The absence of reelin could affect the activation of MMP-9, but we cannot make definitive conclusions based on the available data. Alternatively, the deficit in vascularization of tumors in the absence of reelin could be due to alterations in endothelial cells, but past studies did not find a role for reelin in angiogenesis, and the vascular network of *reeler* mice is normal (Stubbs et al., 2009; Lutter et al., 2012; Guy et al., 2015).

The increased levels of M1-specific iNOS and decreased levels of M2-specific Arg1 in primary tumors from $rl^{Orl\ -/-}$ mice indicate the predominance of M1-activated TAMs that may impede tumor growth and angiogenesis. In addition, macrophages from $rl^{Orl\ -/-}$ mice display increased propensity for M1 activation, while $Dab1^{-/-}$ macrophages do not. These results further

support our hypothesis that the absence of reelin affects macrophage activation and progression of breast cancer via Dab1-independent mechanisms.

The influence of reelin signaling on the development and function of the immune system has not been studied extensively. However, one study found functional deficits in macrophages and T cells from *reeler* $^{-/-}$ animals on a C57/B6 background (Green-Johnson et al., 1995). These *reeler* mutants differ from our model because they completely lack reelin. In addition, peritoneal macrophages from these mice showed elevated production of IL1β when activated by LPS *in vitro* (Kopmels et al., 1990; Bakalian et al., 1992). Another group proposed a role for reelin in clustering of the serotonin transporter (SERT) in blood lymphocytes, as peripheral lymphocytes from *reeler* $^{-/-}$ mice displayed spreading of the SERT clusters (Rivera-Baltanas et al., 2010).

Interestingly, dysregulation of the immune system shows co-morbidity with mental illnesses such as schizophrenia and autism, and alterations in reelin levels are frequently found in patients with these disorders (Muller and Schwartz, 2000; Fatemi et al., 2005; Grayson et al., 2005; Michel et al., 2012; Onore et al., 2012; Folsom and Fatemi, 2013). Moreover, maternal immune challenge is thought to contribute to neurodevelopmental pathologies, and often results in decreased reelin levels in the offspring (Fatemi et al., 1999; Brown et al., 2000; Meyer et al., 2006; Ghiani et al., 2011; Patterson, 2011). A functional link between reelin and the immune system likely exists, but the mechanisms by which reelin may regulate the immune response remain unknown.

Our results indicate that the phenotype of TAMs observed in the absence of reelin is independent of the canonical intracellular adaptor Dab1. Although mice with *reelin* or *Dab1* mutations have very similar phenotypes in the central nervous system, several recent studies provided evidence for the existence of Dab1-independent functions of reelin. Reelin is thought to recruit smooth muscle cells to the lymphatic endothelium by upregulation of monocyte chemotactic protein 1 (MCP1) expression in lymphatic endothelial cells, and this activity does not rely on Dab1 (Lutter et al., 2012). In the nervous system, reelin induced Erk1/2

phosphorylation in cortical neurons independently of Dab1 or the lipoprotein receptors (Lee et al., 2014). In addition, induction of Dab1 phosphorylation by anti-ApoER2 or anti-VLDLR receptor antibodies did not correct the *reeler* $^{-/-}$ phenotype in embryonic telencephalon slice cultures, while treatment with reelin rescued the formation of neuronal layers, implying that additional, Dab1-independent roles for reelin exist during the development of the central nervous system (Jossin et al., 2004). The alternative receptors for reelin and its downstream effectors have yet to be identified.

Previous studies on reelin signaling in the context of tumor progression focused mainly on the expression of reelin pathway components in the primary tumor tissue, or in cancer cell lines (Hong et al., 2008; Resende et al., 2010; Stein et al., 2010; Berthier-Vergnes et al., 2011; Zhang et al., 2012). For instance, downregulation of reelin was observed in primary breast tumors, and loss of reelin expression correlated with poor survival. In addition, reelin expression was epigenetically silenced in breast cancer cell lines (Stein et al., 2010). It is therefore interesting that in our model, loss of functional reelin protein in the host environment delayed the growth of normally aggressive 4T1 tumors. However, our finding that the 4T1 cell line does not express reelin correlates with previously published results. The human triple-negative breast cancer cell line MDA-MB-231 was reported to have a low baseline expression of reelin (Stein et al., 2010). Transfection of this cell line with the full-length reelin construct decreased the migratory and invasive potential of MDA-MB-231 cells (Stein et al., 2010). Because reelin impedes the migration of epithelial cells, the results of previous studies imply that cancer cells may downregulate reelin expression in order to become more migratory and invasive. On the other hand, our studies demonstrate that reelin may be necessary for tumor-promoting responses of host immune cells, and therefore may play a dual role in cancer progression.

In summary, our findings provide evidence for additional non-neuronal functions of reelin accomplished via Dab1-independent mechanisms. Our observations offer insight into the

importance of stromal reelin in breast cancer progression, and suggest a potential role for reelin signaling in the development and function of the innate immune system.

Acknowledgments

We thank Dr. Patricia Phelps, Dr. Cristina Ghiani, Dr. Catalina Abad Rabat and Dr. Diana Moughon for kindly providing reagents and for thoughtful discussion. We are thankful to Donna Crandall for assistance with figure preparation and Joseph Argus for assistance with manuscript editing.

Figures

Gene	Forward Primer (5' - 3')	Reverse Primer (5' - 3')
ApoER2	CGGACAGCGACTTCACCT	CTTCTCGGCAGGACACTCTT
Arg1	GCAGAGGTCCAGAAGAATGG	AGCATCCACCCAAATGACAC
Cxcl2	AATCATCCAAAAGATACTGAACAAAG	TTCTCTTTGGTTCTTCCGTTG
Cxcl5	TGCGTTGTGTTTGCTTAACCG	CTTCCACCGTAGGGCACTG
Cxcl10	CCAAGTGCTGCCGTCATTTTC	GGCTCGCAGGGATGATTTCAA
Dab1	GATGAAGTGTCCGCAGCTC	GTGTTCTCCCTTGGAACGTG
IL-1b	GCCCATCCTCTGTGACTCAT	AGGCCACAGGTATTTTGTCG
IL-6	AGTTGCCTTCTTGGGACTGA	TCCACGATTTCCCAGAGAAC
IL-10	GCTCTTACTGACTGGCATGAG	CGCAGCTCTAGGAGCATGTG
IL-12	CCATCAGCAGATCATTCTAGACAA	CGCCATTATGATTCAGAGACTG
iNOS	CACCTTGGAGTTCACCCAGT	ACCACTCGTACTTGGGATGC
Mmp-9	GGACCCGAAGCGGACATTG	CGTCGTCGAAATGGGCATCT
Mrc1	ATTGTGGAGCAGATGGAAGG	TGAATGGAAATGCACAGACG
Reln	GTCACGGTCTACCTGCCACT	TCAATAGCCCAGGAATCTGC
Tgfb	TTGCTTCAGCTCCACAGAGA	TGGTTGTAGAGGGCAAGGAC
Tnfa	TGCCTATGTCTCAGCCTCTTC	GAGGCCATTTGGGAACTTCT
Vegfa	GGAGAGCAGAAGTCCCATGA	GGGGTACTCCTGGAAGATGTC
Vegfb	TCTGAGCATGGAACTCATGG	TCTGCATTCACATTGGCTGT
Vegfc	CAAGGCTTTTGAAGGCAAAG	TGCTGAGGTAACCTGTGCTG
Vldlr	TACCCTAGACGGAGCCAAGA	GTAAACAAAGCCCGACAACG

Table 2.1. Primers used for qPCR gene expression analysis.

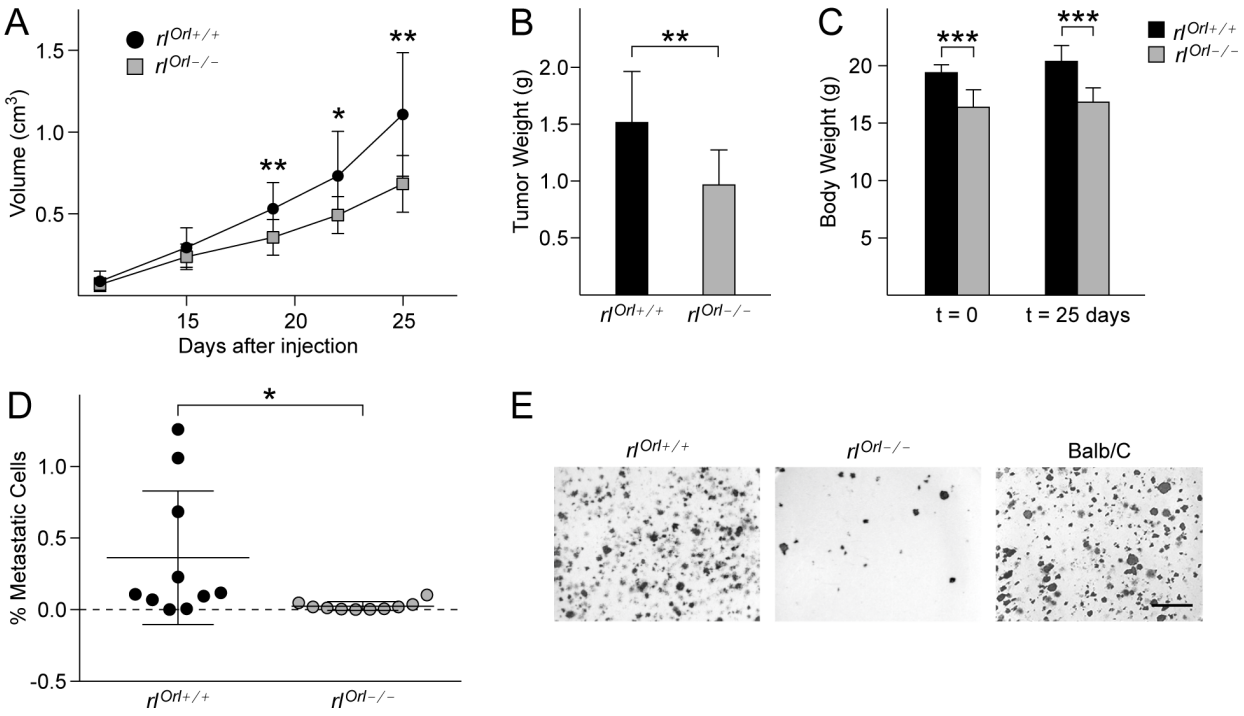

Figure 2.1. 4T1 mammary tumor growth and lung metastasis in *rl*$^{Orl\ -/-}$ mice.
(A) Growth of primary tumors in *rl*$^{Orl\ -/-}$ (n=10) and *rl*$^{Orl\ +/+}$ (n=10) control mice. (B) Wet weight of primary tumors collected 25 days after 4T1 cell injection. (C) Total body weight of animals on the day of 4T1 injections (t = 0) and the day of sacrifice (t = 25 days). (D) Quantification of metastatic burden in the lungs. (E) Representative images of 4T1-derived metastatic colonies from the lungs of *rl*$^{Orl\ +/+}$ and *rl*$^{Orl\ -/-}$ mice used for quantification in (D), and from Balb/C controls. Bar = 5 mm. *P < 0.05, **P < 0.01, ***P < 0.001. Statistical significance determined using two-tailed, unpaired Student's t-test.

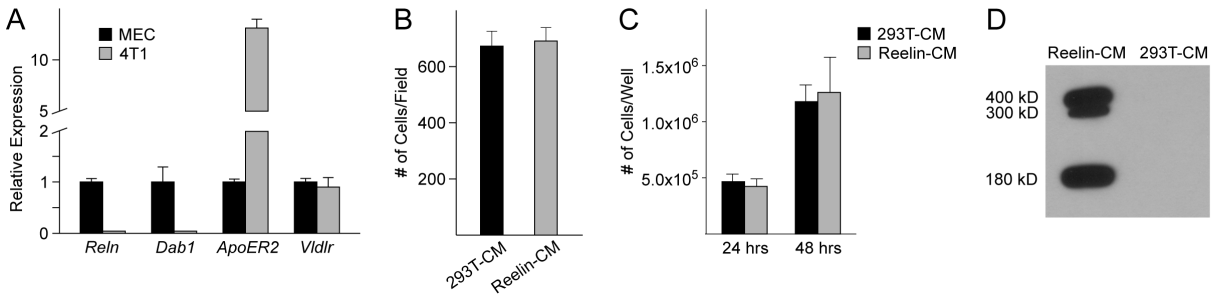

Figure 2.2. Expression of reelin signaling pathway components and the effect of reelin on growth and migration of 4T1 cells.
(A) qPCR analysis of relative expression levels of reelin signaling pathway components in 4T1 cells. Gene expression levels are normalized to those in wild type mammary epithelial cells (MEC). (B) Transwell migration assay of 4T1 cells in the presence of reelin conditioned media (Reelin-CM) or controlled conditioned media (293T-CM). (C) Number of 4T1 cells grown in the presence or absence of reelin for 24 or 48 hours. (D) Western blot of reelin expression in conditioned media from reelin expressing HEK293T cells (Reelin-CM) or conditioned media from control cells (293-CM). 20 μg of total protein were loaded into each lane.

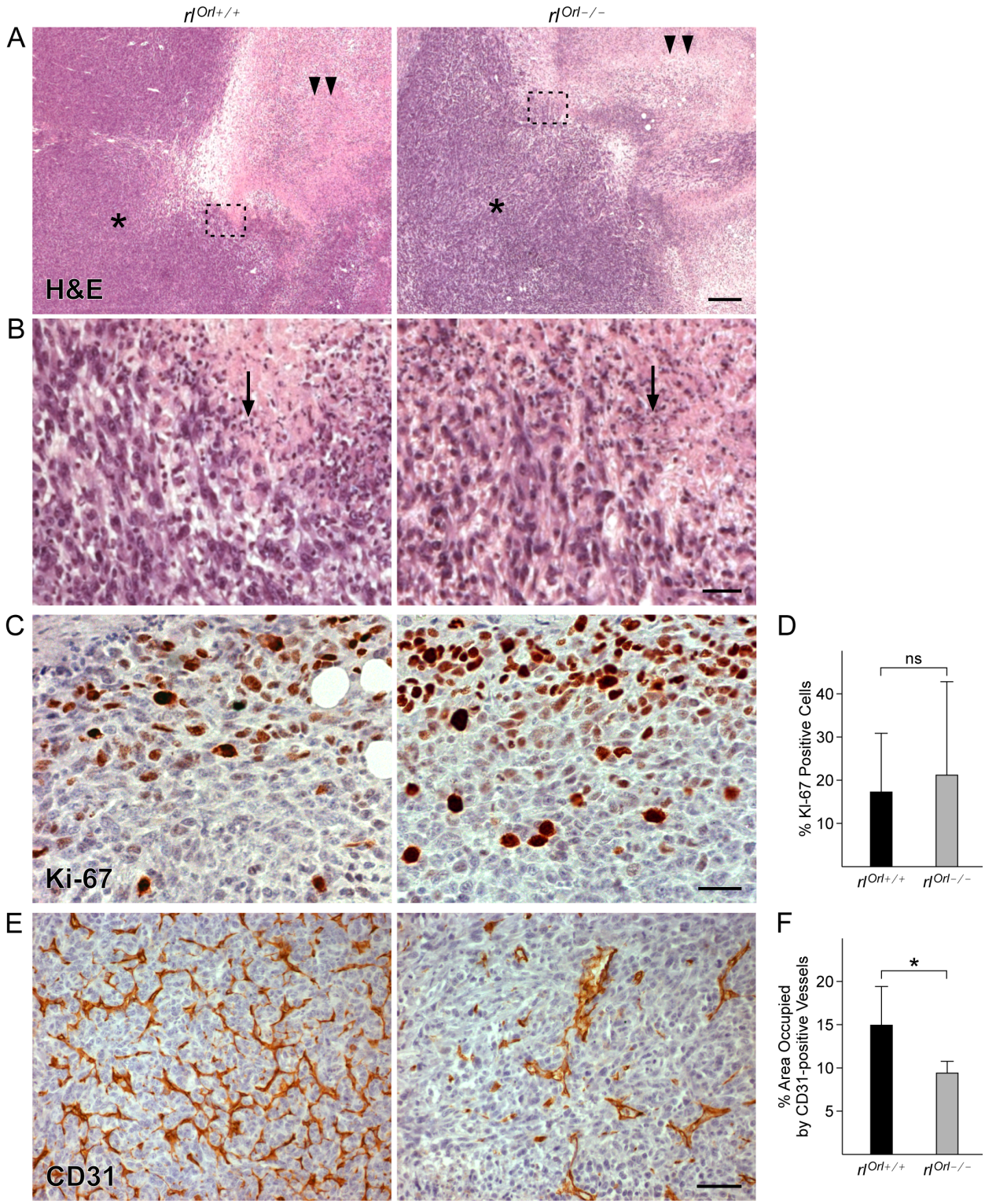

Figure 2.3. Characterization of proliferation and angiogenesis in primary tumors from *rlOrl*$^{-/-}$ mice.

(A) H&E staining of primary tumors from *rl*$^{Orl\ -/-}$ and *rl*$^{Orl\ +/+}$ control mice. Asterisk – tumor cells, double arrowheads – necrotic core. Bar = 200 μm. (B) High magnification view of the areas

outlined in (A). Arrow – infiltrating immune cells. Bar = 30 μm. (C) Ki-67 labeling of primary tumors from $rl^{Orl\ -/-}$ and $rl^{Orl\ +/+}$ mice. Bar = 30 μm. (D) Quantification of (C), $rl^{Orl\ +/+}$: n=7, $rl^{Orl\ -/-}$: n=7. (E) CD31 labeling of primary tumors from $rl^{Orl\ -/-}$ and $rl^{Orl\ +/+}$ mice. Bar = 50 μm. (F) Quantification of (E), $rl^{Orl\ +/+}$: n=7, $rl^{Orl\ -/-}$: n=6. ns – not significant, *P < 0.05. Statistical significance determined using two-tailed, unpaired Student's t-test.

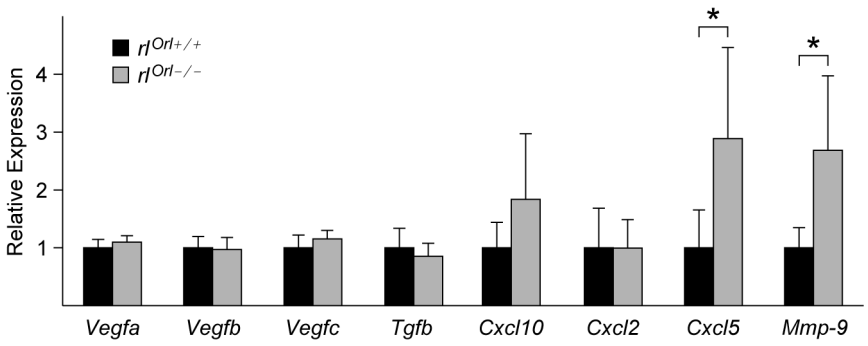

Figure 2.4. Gene expression analysis of primary tumors from *rl*$^{Orl\ -/-}$ mice.
qPCR analysis of angiogenic genes (*Vegfa*, *Vegfb*, *Vegfc*, *Tgfb*), chemokines (*Cxcl10*, *Cxcl2*, *Cxcl5*), and metalloproteinase *Mmp-9* in primary tumors from *rl*$^{Orl\ -/-}$ mice. Gene expression levels are relative to those in tumors from *rl*$^{Orl\ +/+}$ controls. *P < 0.05. Statistical significance determined using two-tailed, unpaired Student's t-test.

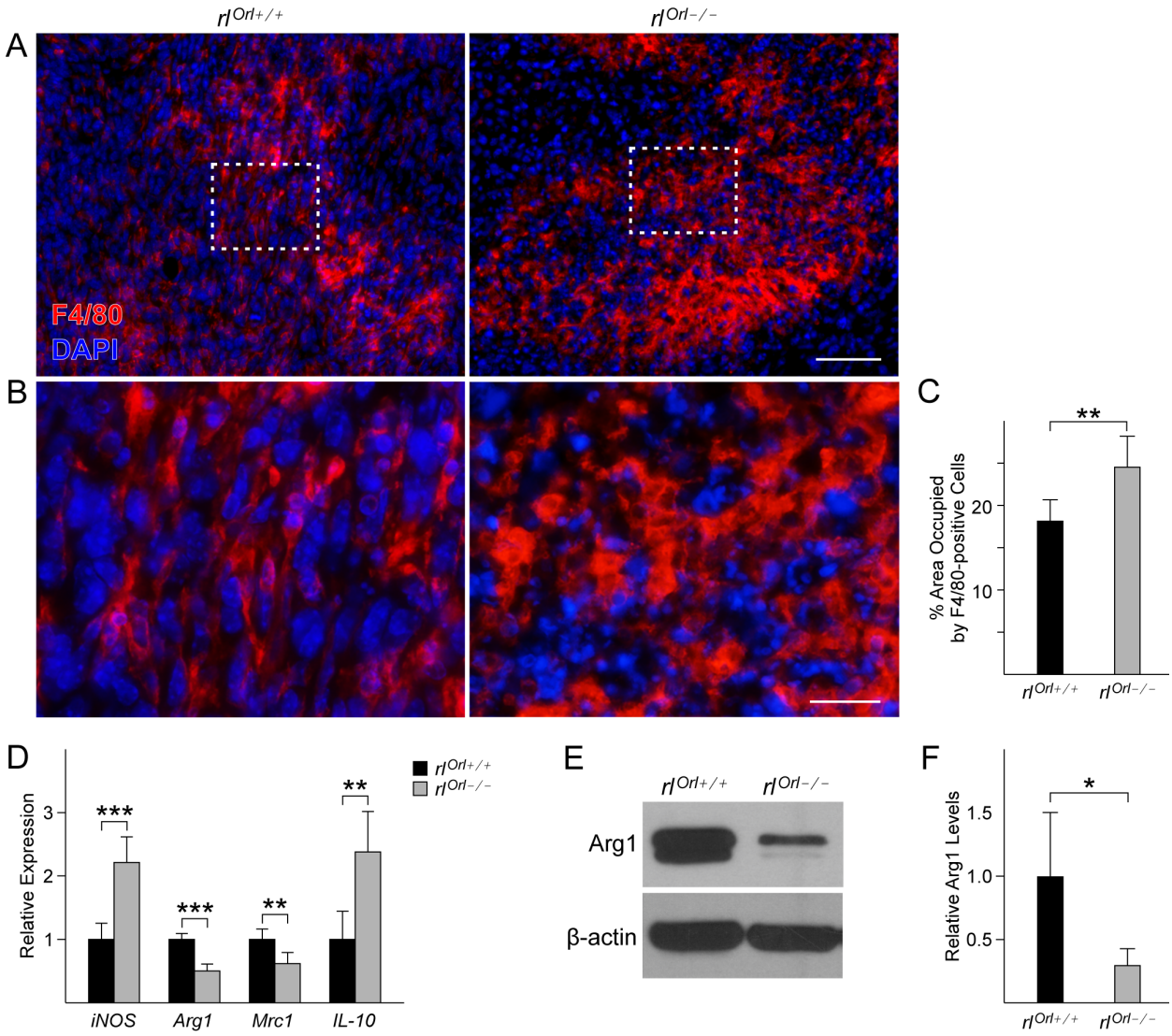

Figure 2.5. Analysis of tumor associated macrophages in primary tumors from *rl*$^{Orl\ -/-}$ mice.

(A) F4/80 labeling of primary tumors from *rl*$^{Orl\ -/-}$ and *rl*$^{Orl\ +/+}$ mice. Bar = 50 μm. (B) High magnification view of the areas outlined in (A). Bar = 20 μm. (C) Quantification of the area occupied by F4/80-positive cells, *rl*$^{Orl\ +/+}$: n=6, *rl*$^{Orl\ -/-}$: n=6. (D) qPCR analysis of *iNOS* (M1), *Arg1* (M2), *Mrc1 (M2)*, and *IL-10* gene expression in primary tumors from *rl*$^{Orl\ -/-}$ mice, gene expression levels are relative to those in tumors from *rl*$^{Orl\ +/+}$ controls. (E) Western blot of Arg1 and β-actin expression in primary tumors from *rl*$^{Orl\ -/-}$ and *rl*$^{Orl\ +/+}$ mice. (F) Quantification of band intensities in (D). *P < 0.05, **P < 0.01, ***P < 0.001. Statistical significance determined using two-tailed, unpaired Student's t-test.

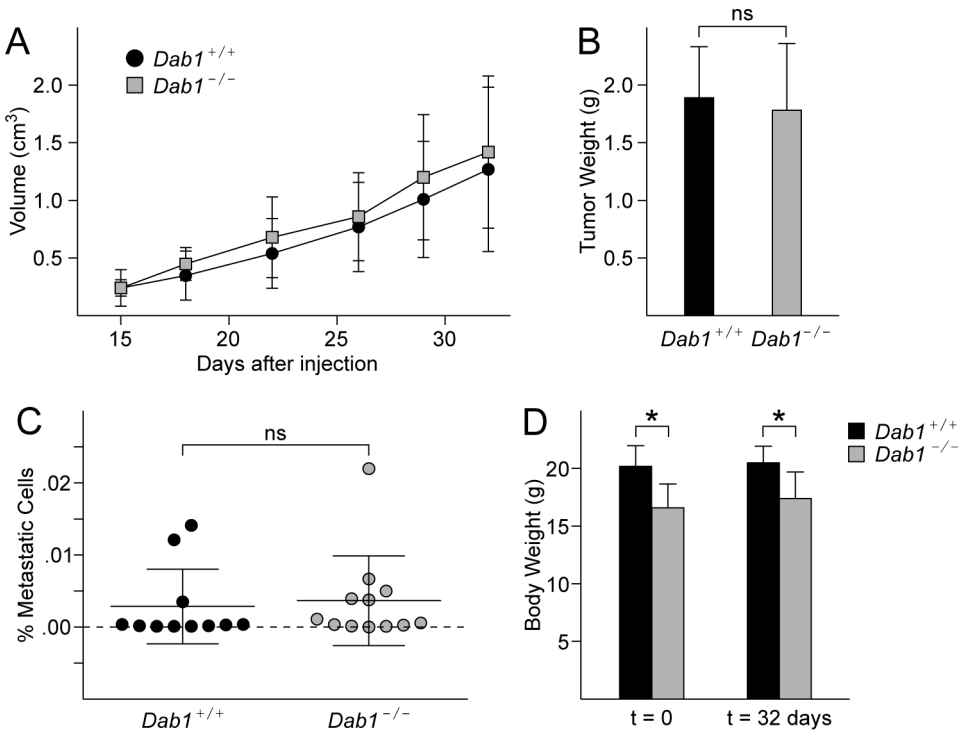

Figure 2.6. 4T1 mammary tumor growth and lung metastasis in *Dab1*$^{-/-}$ mice.
(A) Growth of primary tumors in *Dab1*$^{-/-}$ (n=11) and *Dab1*$^{+/+}$ (n=11) control mice. (B) Wet weight of primary tumors collected from *Dab1*$^{-/-}$ or *Dab1*$^{+/+}$ mice. (C) Quantification of metastatic burden in the lungs. (D) Total body weight of animals on the day of 4T1 injections (t = 0) and 32 days after the injections (t = 32 days). ns – not significant, *P < 0.05. Statistical significance determined using two-tailed, unpaired Student's t-test.

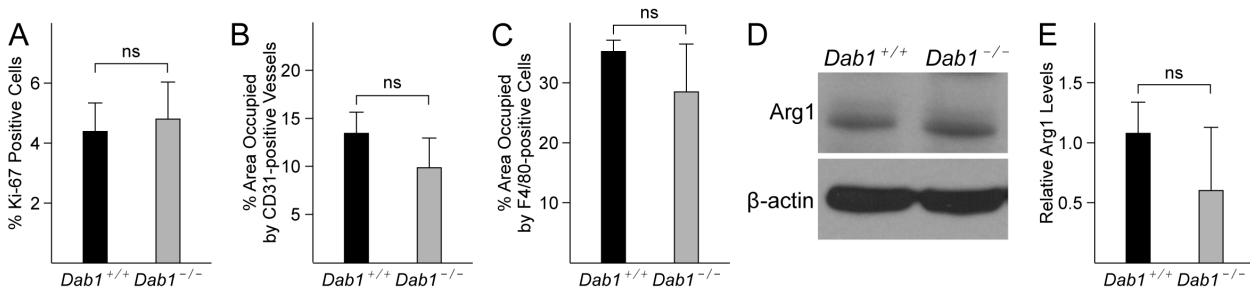

Figure 2.7. Analysis of proliferation, angiogenesis, and tumor associated macrophages in primary tumors from *Dab1*$^{-/-}$ mice.

(A – C) Quantification of (A) Ki-67, (B) CD31, and (C) F4/80 labeling of primary tumors from *Dab1*$^{-/-}$ and *Dab1*$^{+/+}$ control mice. (D) Western blot, Arg1 and β-actin expression in primary tumors from *Dab1*$^{-/-}$ and *Dab1*$^{+/+}$ mice. (E) Quantification of band intensities in (D). ns – not significant. Statistical significance determined using two-tailed, unpaired Student's t-test.

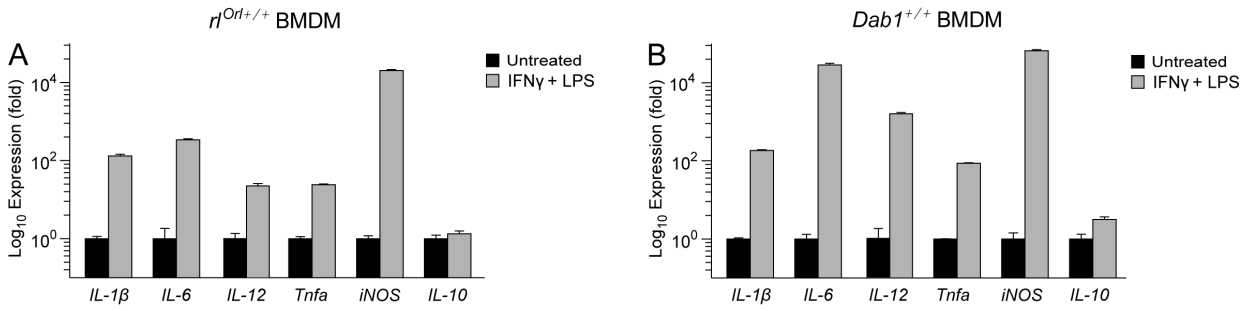

Figure 2.8. Cytokine expression levels in wild type BMDM treated with IFNγ and LPS.
(A, B) Cytokine expression levels in wild type (A) *rl*$^{Orl\ +/+}$ and (B) *Dab1*$^{+/+}$ BMDM treated with IFNγ and LPS. Gene expression levels are relative to those in the respective unstimulated *rl*$^{Orl\ +/+}$ or *Dab1*$^{+/+}$ BMDM controls.

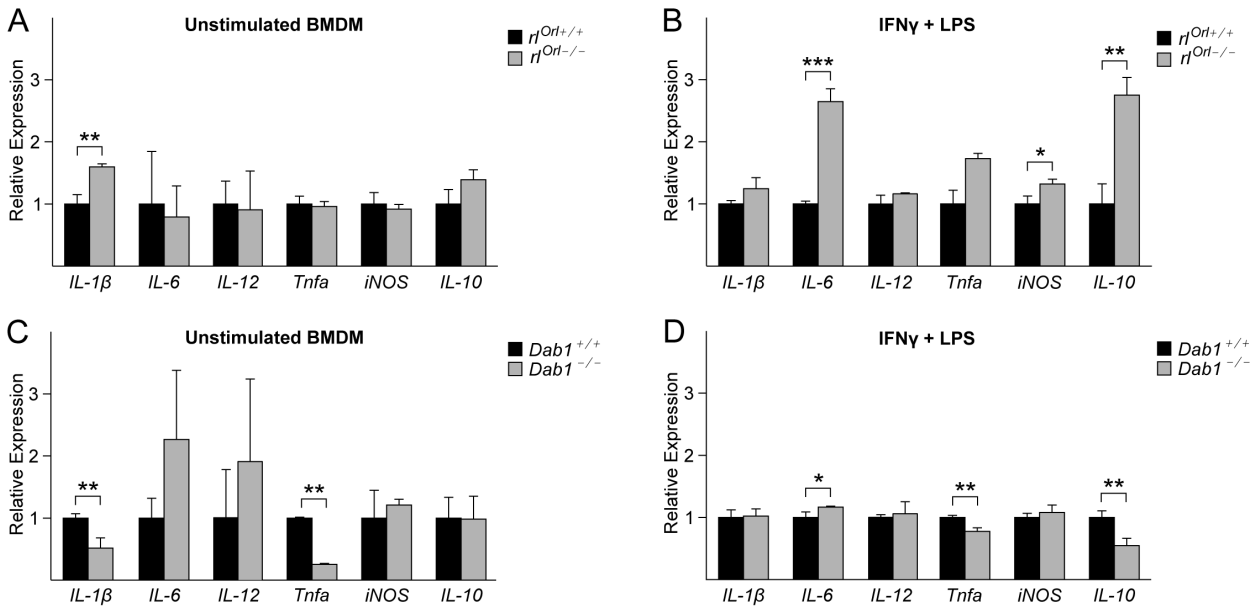

Figure 2.9. Cytokine expression levels in baseline and M1-polarized BMDM from *rl*$^{Orl\ -/-}$ and *Dab1*$^{-/-}$ mice.

(A, B) *IL-1β* (M1)*, IL-6* (M1)*, IL-12* (M1), *Tnfa* (M1)*, iNOS* (M1), and *IL-10* cytokine expression levels in (A) unstimulated BMDM and (B) M1-polarized BMDM from *rl*$^{Orl\ -/-}$ mice, analyzed by qPCR. Gene expression levels are relative to those in the respective *rl*$^{Orl\ +/+}$ BMDM controls. (C, D) M1-associated gene expression levels in (C) unstimulated BMDM and (D) M1-polarized BMDM from *Dab1*$^{-/-}$ mice. Gene expression levels are relative to those in the respective *Dab1*$^{+/+}$ BMDM controls. *P < 0.05, **P < 0.01, ***P < 0.001. Statistical significance determined using two-tailed, unpaired Student's t-test.

References

Abadesco, A.D., Cilluffo, M., Yvone, G.M., Carpenter, E.M., Howell, B.W., Phelps, P.E. (2014). Novel Disabled-1-expressing neurons identified in adult brain and spinal cord. *Eur. J. Neurosci.* **39**:579-592.

Aslakson, C.J., Miller, F.R. (1992). Selective events in the metastatic process defined by analysis of the sequential dissemination of subpopulations of a mouse mammary tumor. *Cancer Res.* **52**:1399–1405.

Bakalian, A., Kopmels, B., Messer, A., Fradelizi, D., Delhaye-Bouchaud, N., Wollman, E., Mariani, J. (1992). Peripheral macrophage abnormalities in mutant mice with spinocerebellar degeneration. *Res. Immunol.* **143**:129-139.

Berthier-Vergnes, O., Kharbili, M.E., de la Fouchardière, A., Pointecouteau, T., Verrando, P., Wierinckx, A., Lachuer, J., Le Naour, F., Lamartine, J. (2011). Gene expression profiles of human melanoma cells with different invasive potential reveal TSPAN8 as a novel mediator of invasion. *Br. J. Cancer.* **104**:155-165.

Bock, H.H., Herz, J. (2003). Reelin activates SRC family tyrosine kinases in neurons. *Curr. Biol.* **13**:18-26.

Boonstra, A., Rajsbaum, R., Holman, M., Marques, R., Asselin-Paturel, C., Pereira, J.P., Bates, E.E., Akira, S., Vieira, P., Liu, Y.J., et al. (2006). Macrophages and myeloid dendritic cells, but not plasmacytoid dendritic cells, produce IL-10 in response to MyD88- and TRIF-dependent TLR signals, and TLR-independent signals. *J. Immunol.* **177**:7551–7558.

Botella-Lopez, A., de Madaria, E., Jover, R., Bataller, R., Sancho-Bru, P., Candela, A., Compañ, A., Pérez-Mateo, M., Martinez, S., Sáez-Valero, J. (2008). Reelin is overexpressed in the liver and plasma of bile duct ligated rats and its levels and glycosylation are altered in plasma of humans with cirrhosis. *Int. J. Biochem. Cell. Biol.* **40**:766-775.

Brown, A.S., Schaefer, C.A., Wyatt, R.J., Goetz, R., Begg, M.D., Gorman, J.M., Susser, E.S. (2000). Maternal exposure to respiratory infections and adult schizophrenia spectrum disorders: a prospective birth cohort study. *Schizophr. Bull.* **26**:287–95.

Chen, L., Yang, S., Jakoncic, J., Zhang, J.J., Huang, X.Y. (2010). Migrastatin analogues target fascin to block tumour metastasis. *Nature.* **464**:1062-1066.

Cho, H.J., Jung, J.I., Lim, D.Y., Kwon, G.T., Her, S., Park, J.H., Park J.H. (2012) Bone marrow-derived, alternatively-activated macrophages enhance solid tumor growth and lung metastasis of mammary carcinoma cells in a Balb/C mouse orthotopic model. *Breast Cancer Res.* **14**:R81. doi:10.1186/bcr3195

D'Arcangelo, G., Homayouni, R., Keshvara, L., Rice, D.S., Sheldon, M., Curran, T. (1999). Reelin is a ligand for lipoprotein receptors. *Neuron.* **24**:471–479.

D'Arcangelo, G. (2014). Reelin in the years: controlling neuronal migration and maturation in the mammalian brain. *Advances in Neuroscience*. Article ID 597395, doi:10.1155/2014/597395.

De Bergeyck, V., Nakajima, K., Lambert de Rouvrait, C., Naerhuyzen, B., Goffinet, A.M., Miyata, T., Ogawa, M., Mikoshiba, K. (1997). A truncated Reelin protein is produced but not secreted in the “Orleans” reeler mutation (Reln(rl-Orl)). *Brain Res. Mol. Brain Res.* **50**:85–90.

Diaz-Mendoza, M.J., Lorda-Diez, C.I., Montero, J.A., Garcia-Porrero, J.A., Hurle, J.M. (2014). Reelin/DAB-1 signaling in the embryonic limb regulates the chondrogenic differentiation of digit mesodermal progenitors. *J. Cell. Physiol.* **229**:1397-1404.

Dohi, O., Takada, H., Wakabayashi, N., Yasui, K., Sakakura, C., Mitsufuji, S., Naito, Y., Taniwaki, M., Yoshikawa, T. (2010). Epigenetic silencing of RELN in gastric cancer. *Int. J. Oncol.* **36**:85-92.

DuPré, S.A., Redelman, D., Hunter, K.W. (2007). The mouse mammary carcinoma 4T1: characterization of the cellular landscape of primary tumours and metastatic tumour foci. *Int. J. Exp. Pathol.* **88**:351–60.

Ewald, A.J. (2013). Isolation of mouse mammary organoids for long-term time-lapse imaging. *Cold Spring Harb. Protoc.* **2**:130-133.

Falconer, D. S. (1951). Two new mutants, 'trembler' and 'reeler', with neurological actions in the house mouse (Mus musculus L.). *J. Genet.* **50**:192-201.

Fatemi, S.H., Emamian, E.S., Kist, D., Sidwell, R.W., Nakajima, K., Akhter, P., Shier, A., Sheikh, S., Bailey, K. (1999). Defective corticogenesis and reduction in Reelin immunoreactivity in cortex and hippocampus of prenatally infected neonatal mice. *Mol. Psychiatry.* **4**:145-154.

Fatemi, S.H., Snow, A.V., Stary, J.M., Araghi-Niknam, M., Reutiman, T.J., Lee, S., Brooks, A.I., Pearce, D.A. (2005). Reelin signaling is impaired in autism. *Biol. Psychiatry.* **57**:777-787.

Fatemi, S.H. (2008). Reelin glycoprotein: structure, biology, and roles in health and disease. New York, NY: Springer.

Folsom, T.D., Fatemi, S.H. (2013). The involvement of Reelin in neurodevelopmental disorders. *Neuropharmacology.* **68**:122-135.

Ghiani, C.A., Mattan, N.S., Nobuta, H., Malvar, J.S., Boles, J., Ross, M.G., Waschek, J.A., Carpenter, E.M., Fisher, R.S., de Vellis, J. (2011). Early effects of lipopolysaccharide-induced inflammation on foetal brain development in rat. *ASN Neuro.* **3**:233–45.

Grayson, D.R., Jia, X., Chen, Y., Sharma, R.P., Mitchell, C.P., Guidotti, A., Costa, E. (2005). Reelin promoter hypermethylation in schizophrenia. *Proc. Natl. Acad. Sci. USA*. **102**:9341-9346.

Green-Johnson, J.M., Zalcman, S., Vriend, C.Y., Nance, D.M., Greenberg, A.H. (1995). Suppressed T cell and macrophage function in the "reeler" (rl/rl) mutant, a murine strain with elevated cerebellar norepinephrine concentration. *Brain Behav. Immun.* **9**:47-60.

Guy, J., Wagener, R.J., Möck, M., Staiger, J.F. (2015). Persistence of functional sensory maps in the absence of cortical layers in the somsatosensory cortex of reeler mice. *Cereb. Cortex.* **25**:2517-2528.

Herz, J., Chen, Y. (2006). Reelin, lipoprotein receptors and synaptic plasticity. *Nat. Rev. Neurosci.* **7**:850–859.

Honda, T., Kobayashi, K., Mikoshiba, K., Nakajima, K. (2011). Regulation of cortical neuron migration by the reelin signaling pathway. *Neurochem. Res.* **36**:1270–1279.

Hong, S.M., Kelly, D., Griffith, M., Omura, N., Li, A., Li, C.P., Hruban, R.H., Goggins, M. (2008). Multiple genes are hypermethylated in intraductal papillary mucinous neoplasms of the pancreas. *Mod. Pathol.* **21**:1499-1507.

Howell, B.W., Hawkes, R., Soriano, P., Cooper, J.A. (1997). Neuronal position in the developing brain is regulated by mouse disabled-1. *Nature.* **389**:733–737.

Jossin, Y., Ignatova, N., Hiesberger, T., Herz, J., Lambert de Rouvroit, C., Goffinet, A.M. (2004). The central fragment of Reelin, generated by proteolytic processing in vivo, is critical to its function during cortical plate development. *J. Neurosci.* **24**:514-521.

Kessenbrock, K., Plaks, V., Werb, Z. (2010). Matrix metalloproteinases: regulators of the tumor microenvironment. *Cell.* **141**:52–67.

Khialeeva, E, Lane, T.F., Carpenter, E.M. (2011). Disruption of reelin signaling alters mammary gland morphogenesis. *Development.* **138**:767–776.

Kim, E.J., Choi, M.R., Park, H., Kim, M., Hong, J.E., Lee, J.Y., Chun, H.S., Lee, K.W., Yoon Park, J.H. (2011). Dietary fat increases solid tumor growth and metastasis of 4T1 murine mammary carcinoma cells and mortality in obesity-resistant BALB/c mice. *Breast Cancer Res.* **13**:R78. doi: 10.1186/bcr2927.

Kopmels, B., Wollman, E.E., Guastavino, J.M., Delhaye-Bouchaud, N., Fradelizi, D., Mariani, J. (1990). Interleukin-1 hyperproduction by in vitro activated peripheral macrophages from cerebellar mutant mice. *J. Neurochem.* **55**:1980-1985.

Kuo, G., Arnaud, L., Kronstad-O'Brien, P., Cooper, J.A. (2005). Absence of Fyn and Src causes a reeler-like phenotype. *J. Neurosci.* **25**:8578-8586.

Lee, G.H., Chhangawala, Z., von Daake, S., Savas, J.N., Yates, J.R. 3rd, Comoletti, D., D'Arcangelo, G. (2014). Reelin induces Erk1/2 signaling in cortical neurons through a non-canonical pathway. *J. Biol. Chem.* **289**:20307-20317.

Lutter, S., Xie, S., Tatin, F., Makinen, T. (2012). Smooth muscle-endothelial cell communication activates Reelin signaling and regulates lymphatic vessel formation. *J. Cell. Biol.* **197**:837-849.

Ma, J., Liu, L., Che, G., Yu, N., Dai, F., You, Z. (2010). The M1 form of tumor-associated macrophages in non-small cell lung cancer is positively associated with survival time. *BMC Cancer.* **10**:112. doi:10.1186/1471-2407-10-112.

Mantovani, A., Sozzani, S., Locati, M., Allavena, P., Sica, A. (2002). Macrophage polarization: tumor-associated macrophages as a paradigm for polarized M2 mononuclear phagocytes. *Trends Immunol.* **23**:549–555.

Martinez, F.O., Gordon, S. (2014) The M1 and M2 paradigm of macrophage activation: time for reassessment. *F1000Prime Rep.* **3**:1–13.

Meyer, U., Nyffeler, M., Engler, A., Urwyler, A., Schedlowski, M., Knuesel, I., Yee, B.K., Feldon, J. (2006). The time of prenatal immune challenge determines the specificity of inflammation-mediated brain and behavioral pathology. *J. Neurosci.* **26**:4752-4762.

Michel, M., Schmidt, M.J., Mirnics, K. (2012). Immune system gene dysregulation in autism and schizophrenia. *Dev. Neurobiol.* **72**:1277–87.

Mills, C.D. (2012). M1 and M2 macrophages: oracles of health and disease. *Crit. Rev. Immunol.* **32**:463–488.

Muller, N., Schwarz, M.J. (2000). Immune system and schizophrenia: an integrative view. *Ann. N. Y. Acad. Sci.* **917**:456-467.

Murdoch, C., Muthana, M., Coffelt, S.B., Lewis, C.E. (2008). The role of myeloid cells in the promotion of tumour angiogenesis. *Nat. Rev. Cancer.* **8**:618–631.

Onore, C., Careaga, M., Ashwood, P. (2012). The role of immune dysfunction in the pathophysiology of autism. *Brain Behav. Immun.* **26**:383–92.
Patterson, P.H. (2011). Maternal infection and immune involvement in autism. *Trends Mol. Med.* **17**:389-394.

Perrone, G., Vincenzi, B., Zagami, M., Santini, D., Panteri, R., Flammia, G., Verzì, A., Lepanto, D., Morini, S., Russo, A., et al. (2007). Reelin expression in human prostate cancer: a marker of tumor aggressiveness based on correlation with grade. *Mod. Pathol.* **20**:344-351.

Pineda-Torra, I., Gage, M., de Juan, A., Pello, O.M. (2015). Isolation, culture and polarization of murine bone marrow-derived and peritoneal macrophages. *Methods Mol. Biol.* **1339**:101–109.

Pulaski, B.A., Ostrand-Rosenberg, S. (1998). Reduction of established spontaneous mammary carcinoma metastases following immunotherapy with major histocompatibility complex class II and B7.1 cell-based tumor vaccines. *Cancer Res.* **58**:1486–1493.

Pulaski, B.A., Ostrand-Rosenberg, S. (2001). Mouse 4T1 breast tumor model. *Curr. Protoc. Immunol.* Chapter 20:Unit 20.2.

Resende, C., Ristimäki, A., Machado, J.C. (2010). Genetic and epigenetic alteration in gastric carcinogenesis. *Helicobacter.* **15**:34-39.

Rivera-Baltanas, T., Romay-Tallon, R., Dopeso-Reyes, I.G., Caruncho, H.J. (2010). Serotonin transporter clustering in blood lymphocytes of reeler mice. *Cardiovasc. Psychiatry Neurol.* **2010**:396282. doi: 10.1155/2010/396282.

Saraiva, M., O'Garra, A. (2010). The regulation of IL-10 production by immune cells. *Nat. Rev. Immunol.* **10**:170–181.

Schroder, K., Hertzog, P.J., Ravasi, T., Hume, D.A. (2004). Interferon-gamma: an overview of signals, mechanisms and functions. *J. Leukoc. Biol.* **75**:163-189.

Stein, T., Cosimo, E., Yu, X., Smith, P.R., Simon, R., Cottrell, L., Pringle, M.A., Bell, A.K., Lattanzio, L., Sauter, G., et al. (2010). Loss of reelin expression in breast cancer is epigenetically controlled and associated with poor prognosis. *Am. J. Pathol.* **177**:2323-2333.

Stubbs, D., DeProto, J., Nie, K., Englund, C., Mahmud, I., Hevner, R., Molnár, Z. (2009). Neurovascular congruence during cerebral cortical development. *Cereb. Cortex.* **19**:i32–41.

Takahara, T., Ohsumi, T., Kuromitsu, J., Shibata, K., Sasaki, N., Okazaki, Y., Shibata, H., Sato, S., Yoshiki, A., Kusakabe, M., et al. (1996). Dysfunction of the Orleans reeler gene arising from exon skipping due to transposition of a full-length copy of an active L1 sequence into the skipped exon. *Hum. Mol. Genet.* **5**:989–993.

Thomas, D.L., Fraser, N.W. (2003). HSV-1 therapy of primary tumors reduces the number of metastases in an immune-competent model of metastatic breast cancer. *Mol. Ther.* **8**:543-551.

Trinchieri, G. (2007). Interleukin-10 production by effector T cells: Th1 cells show self control. *J. Exp. Med.* **204**:239-243.

Tseng, W.L., Chen, T.H., Huang, C.C., Huang, Y.H., Yeh, C.F., Tsai, H.J., Lee, H.Y., Kao, C.Y., Lin, S.W., Liao, H.R., et al. (2014). Impaired thrombin generation in Reelin-deficient mice: a potential role of plasma Reelin in hemostasis. *J. Thromb. Haemost.* **12**:2054-2064.

Vázquez-Carretero, M.D., García-Miranda, P., Calonge, M.L., Peral, M.J., Ilundain, A.A. (2014). Dab1 and reelin participate in a common signal pathway that controls intestinal crypt/villus unit dynamics. *Biol. Cell.* **106**:83-96.

Wang, Q., Lu, J., Yang, C., Wang, X., Cheng, L., Hu, G., Sun, Y., Zhang, X., Wu, M., Liu, Z. (2002). CASK and its target gene Reelin were co-upregulated in human esophageal carcinoma. *Cancer Lett.* **179**:71-77.

York, A.G., Williams, K.J., Argus, J.P., Zhou, Q.D., Brar, G., Vergnes, L., Gray, E.E., Zhen, A., Wu, N.C., Yamada, D.H., et al. (2015). Limiting cholesterol biosynthetic flux spontaneously engages Type I IFN signaling. *Cell.* **163**:1716–1729.

Zhang, J., Ding, L., Holmfeldt, L., Wu, G., Heatley, S.L., Payne-Turner, D., Easton, J., Chen, X., Wang, J., Rusch, M., et al. (2012). The genetic basis of early T-cell precursor acute lymphoblastic leukaemia. *Nature.* **481**:157-163.

CHAPTER THREE: Alternative splicing of Disabled-1 during mammary gland development

Abstract

Disabled-1 (Dab1) is a crucial adaptor in the reelin signaling pathway. Alternative splicing of Dab1 has been proposed as a mechanism for regulation of the cellular response to the reelin signal in the brain and the retina. The reelin signaling pathway plays an important role in regulation of mammary gland development. Reelin and Dab1 are expressed in mammary epithelial cells during mammary gland morphogenesis and in adult mammary glands, but it is not known whether Dab1 is alternatively spliced in the mammary gland. Using RT-PCR and sequencing, we showed that several splice variants of Dab1 are expressed in the developing and mature mammary glands. In the developing mammary gland, Dab1 is differentially spliced in the proximal and distal regions, which contain established and developing ducts, respectively. We also showed that the predominant Dab1 splice variants change during pregnancy and lactation. Taken together, our results suggest that alternative splicing of Dab1 is spatially and temporally regulated in the mammary gland during puberty, pregnancy, and lactation.

Results

Disabled-1 (Dab1) is an essential intracellular adaptor in the reelin signaling pathway (Rice and Curran, 2001; Herz and Chen, 2006). Loss-of-function mutations in *Dab1* result in a *reeler*-like phenotype in mice, with severe abnormalities in neuronal layering throughout the central nervous system (Sheldon et al., 1997; Rice et al., 1998; Howell et al., 2000). In response to the reelin signal, Dab1 binds to the NPXY motifs of reelin receptors ApoER2 and VLDLR via its N-terminal protein interaction/protein-binding (PI/PTB) domain (Howell et al., 1999). Dab1 also contains a tyrosine-rich domain with five conserved tyrosine residues, four of which correspond to two Src family kinase (SFK) and two Abl family kinase (AFK) recognition sites YQXI and YXVP, respectively (Gao et al., 2012). Tyrosine phosphorylation on all four sites is necessary for functional reelin signaling, because the phenotype of mice with mutated tyrosine residues mimics the phenotype of *Dab1* null mice (Howell et al., 2000).

The *Dab1* gene contains 16 coding exons, which are highly conserved between humans and mice (Bar et al., 2003). Several alternative splice variants of Dab1 have been identified in the retinas and brains of chick, mice, and humans (Katyal et al., 2004; Katyal et al., 2011; Gao et al., 2012). These splice variants are generated by inclusion or exclusion of exons 7, 8, 9b, and 9c (Figure 3.1A). Exons 7 and 8 contain three of the four tyrosine residues critical for Dab1 phosphorylation. Exclusion of exon 7 or exon 8 results in the deletion of one SFK recognition site, while exclusion of both exons removes two SFK recognition sites, reducing activation of Src (Gao et al., 2012). Alternative splicing of Dab1 may therefore provide a mechanism by which the cellular response to reelin can be fine-tuned during development. Additional Dab1 splice isoforms are generated by inclusion of exons 9b and 9c. In the mouse brain, the Dab1 variants lacking exons 7/8 and containing exons 9b/9c are observed earlier in development, through embryonic day 11.5. Later born neurons express different isoforms of Dab1, which include exons 7/8 and lack exons 9b/9c (Gao et al., 2012). The exclusion of exons 9b/9c is

important for correct positioning of later-born neurons, indicating that the expression of Dab1 splice variants must be temporally controlled (Yano et al., 2010).

Mammary gland development is marked by several rounds of cellular proliferation and differentiation during puberty, pregnancy, and lactation (Hennighausen and Robinson, 2005). We showed that reelin and Dab1 are expressed in the mammary gland, and that the reelin signaling pathway is required for proper development of the mammary ducts (Khialeeva et al., 2011). It is currently not known whether the cellular response to the reelin signal in the mammary gland is modulated via alternative splicing of Dab1. To determine if alternatively spliced variants of Dab1 are present in mammary glands, we amplified the regions of Dab1 mRNA corresponding to exons 2-7, 2-8, and 2-9 from mammary epithelial cells (MECs) of adult virgin female mice. We successfully amplified the regions spanning exons 2-7 and exons 2-9 from MEC cDNA, but the amplification of the region spanning exons 2-8 was not as efficient. This amplicon appeared as a faint band that was nearly undetectable (Figure 3.1B). The band corresponding to exons 2-9 in adult MECs was approximately 100 bp shorter than the equivalent product of amplification from embryonic day 13.5 (E13.5) brain cDNA (Figure 3.1B). Sequencing of these fragments confirmed the absence of exons 7 and 8 in Dab1 from MECs (Figure 3.2). However, the successful amplification of the fragment corresponding to exons 2-7 in MECs suggests that Dab1 isoforms containing exon 7 must be present in the mammary gland in addition to the variants lacking exons 7/8. These results suggest that several splice variants of Dab1 may exist in the mammary gland.

Next, we addressed the possibility of spatial variation in expression of Dab1 isoforms in the developing mammary gland. Colonization of the mouse mammary fat pad by the ductal branches begins from the rudimentary ductal tree located underneath the nipple, and proceeds distally past the lymph node. At 6 weeks of age, the development of proximal branches is complete, while the distal tips of the mammary ducts contain highly proliferative terminal end buds (Morris et al., 2006). To detect alternative splicing of exons 7, 8, 9b, and 9c in the

developing mammary gland, we carried out RT-PCR analysis of MECs isolated from proximal and distal portions of #4 mammary glands of 6 week-old virgin mice using primers that spanned exons 5-11 of Dab1. We found that the predominant Dab1 isoform in more stable, proximally located MECs was similar to the predominant Dab1 isoform expressed in the E13.5 brain, likely containing exons 7 and 8, but not exons 9b and 9c (Figure 3.3A). However, MECs located more distally contained at least 3 other Dab1 splice variants (Figure 3.3A). The Dab1 variants likely to be present in MECs are listed in Table 3-1. Notably, the band of strongest intensity in distal MECs is the Dab1 variant which is absent from the E13.5 brain and lacks exons 7, 8, 9b, and 9c (Figure 3.3A). These results indicate that Dab1 is differentially spliced in the proximal and distal regions of the developing mammary gland.

Next, we wanted to determine if the switch in alternative splice variants of Dab1 accompanies proliferation and differentiation of MECs during pregnancy and lactation. To address this question, we isolated MECs from mammary glands of adult virgin, pregnant, and lactating mice, and analyzed the expression of the Dab1 region corresponding to exons 5-11 by RT-PCR. Dab1 variants similar to those observed in the distal mammary gland of 6 week-old mice were present in the virgin, pregnant, and lactating mice (Figure 3.3A). It appears that the prevalent Dab1 variants change as MECs undergo proliferation and differentiation. Amplification of exons 5-11 in virgin MECs resulted in several bands of similar intensities. However, MECs from pregnant mice contained a predominant band at approximately 500 bp. During lactation, the predominant Dab1 isoform changed to the variant that lacks exons 7, 8, 9b, and 9c, although several other Dab1 variants were also present (Figure 3.3A). To assess overall levels of reelin and Dab1 in MECs, we carried out qPCR analysis using primers to reelin, and the C-terminal region of *Dab1* common to all variants. *Dab1* mRNA levels are significantly reduced in MECs at all stages compared to *Dab1* levels in the E13.5 brain (Figure 3.3B). *Dab1* expression in lactating MECs is almost 3-fold higher than that in virgin MECs. *Reelin* is downregulated in

MECs at late gestation and during lactation (Figure 3.3B). Thus, upregulation of *Dab1* during lactation may be independent of reelin levels.

In summary, our data show that alternative splicing of Dab1 may be spatially and temporally regulated in mammary glands as MECs undergo proliferation and differentiation during puberty, pregnancy, and lactation. The switch in alternative splice variants of Dab1 during brain development occurs when proliferating neuroblasts differentiate into neurons, which require phosphorylation of Dab1 in response to the reelin signal for correct positioning. Our findings suggest that Dab1 alternative splice isoforms are differentially expressed in pregnant and lactating MECs. During pregnancy, intact reelin signaling and phosphorylation of Dab1 may be required for alveolar expansion. The alveoli in lactating mammary glands are fully differentiated and predominantly express the Dab1 variant that lacks exons 7/8. Further studies are needed to assess whether the requirement for Dab1 phosphorylation changes in MECs during pregnancy and lactation.

Materials and Methods

Mouse lines

Balb/C male and female mice were obtained from Charles River Laboratories, and maintained in a breeding colony at UCLA. For studies of spatial variations in Dab1 alternative splicing, inguinal mammary glands were dissected from 6 week-old virgin female mice. The position of the central lymph node was used to divide the mammary gland into proximal and distal sections. To generate pregnant and lactating mice, 8 week-old female mice were paired with male Balb/C mice. The day of appearance of the vaginal plug was marked as gestational day 0.5, and mammary glands were dissected at gestational days 12.5 (Pg 12.5) or 18.5 (Pg 18.5). For analysis of lactating mammary glands, pregnant female mice were allowed to give birth, and mammary glands were dissected 48 hours later. Embryonic brains were collected from embryos at 13.5 days of gestation (E13.5).

Mammary Epithelial Cell (MEC) Purification

MECs were purified as previously described (Ewald, 2013). Briefly, mammary glands were minced and incubated in DMEM/F12 (Corning) containing 5% FBS, 100 u/mL penicillin/streptomycin, 2 mg/mL collagenase IV (Sigma), 2 mg/mL trypsin (Sigma), and 5 µg/mL insulin (Life Technologies) on an orbital shaker at 100 RPM, 37°C, for 1 hr. Digested tissue was treated with 4 u/mL DNAse (Sigma), organoids containing MECs were purified by repeated pulse centrifugation, collected into 1 mL of TRI reagent (Sigma), and samples were stored in -80°C until ready for RNA isolation.

Reverse Transcription PCR (RT-PCR)

RNA from MECs was extracted using TRI reagent (Sigma), and the cDNA was generated using oligo(dT) primer and Superscript II reverse transcriptase (Life Technologies). Exons 2-7, 2-8, 2-9, or 5-11 of Dab1 were amplified using primers listed in Table 3-2. PCR

products were resolved on 1-2% Trevigel (Trevigen). For sequencing, PCR amplification products were cloned into pGEM-T Easy Vector System I (Promega).

Quantitative PCR (qPCR)

RNA from MECs was extracted using TRI reagent (Sigma), and the cDNA was generated using an iScript cDNA Synthesis kit (Bio-Rad). qPCR was carried out using the KAPA SYBR FAST master mix (KAPA Biosystems) on a Light Cycler 480 (Roche). Expression values were normalized to the housekeeping gene *36b4/RPLP0*. The following primers were used for qPCR analysis: *36b4/RPLP0*: forward – 5'-CTGTGCCAGCTCAGAACACTG-3', reverse – 5'-TGATCAGCCCGAAGGAGAAG-3'; *Dab1*: forward – 5'-GATGAAGTGTCCGCAGCTC-3', reverse – 5'GTGTTCTCCCTTGGAACGTG-3'; *reelin*: forward – 5'-GTCACGGTCTACCTGCCACT-3', reverse – 5'-TCAATAGCCCAGGAATCTGC-3'.

Figures

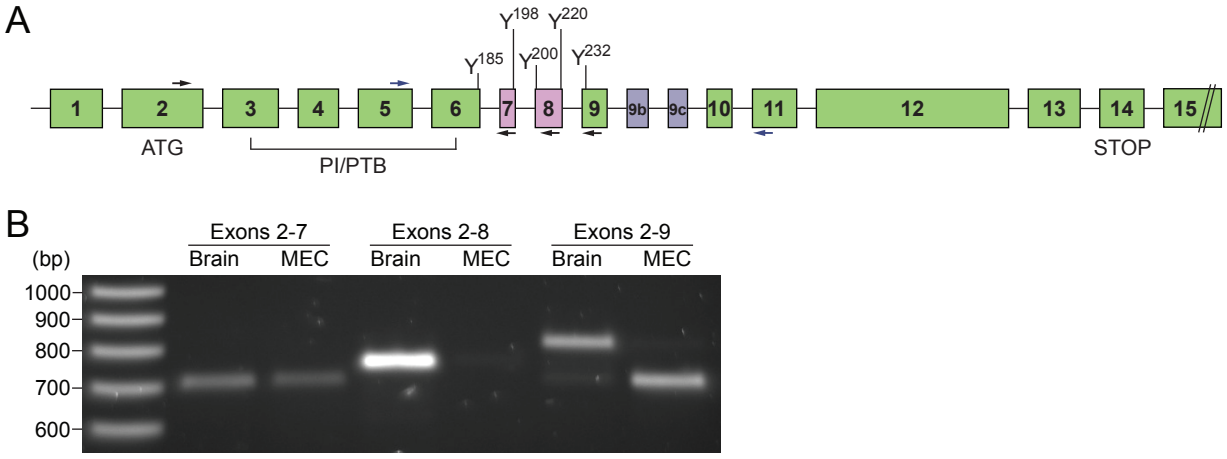

Figure 3.1. Alternative splicing of Dab1 in mammary epithelial cells.
(A) Schematic representation of *Dab1* gene structure (adapted from Bar et al., 2003). ATG, STOP - indicate the exons containing the beginning and the end of the coding sequence. The position of the PI/PTB domain-coding region is indicated with brackets. The positions of tyrosine residues encoded by exons 6-9 are shown. The constitutive exons are shown in green, and the alternatively spliced exons are shown in pink and purple. Arrows indicate the position of primers for amplification of Dab1 using RT-PCR. (B) RT-PCR analysis of Dab1 splice variants using RNA isolated from E13.5 brain and adult virgin MECs. Exon 2 forward primer and exon 7, 8, and 9 reverse primers were used.

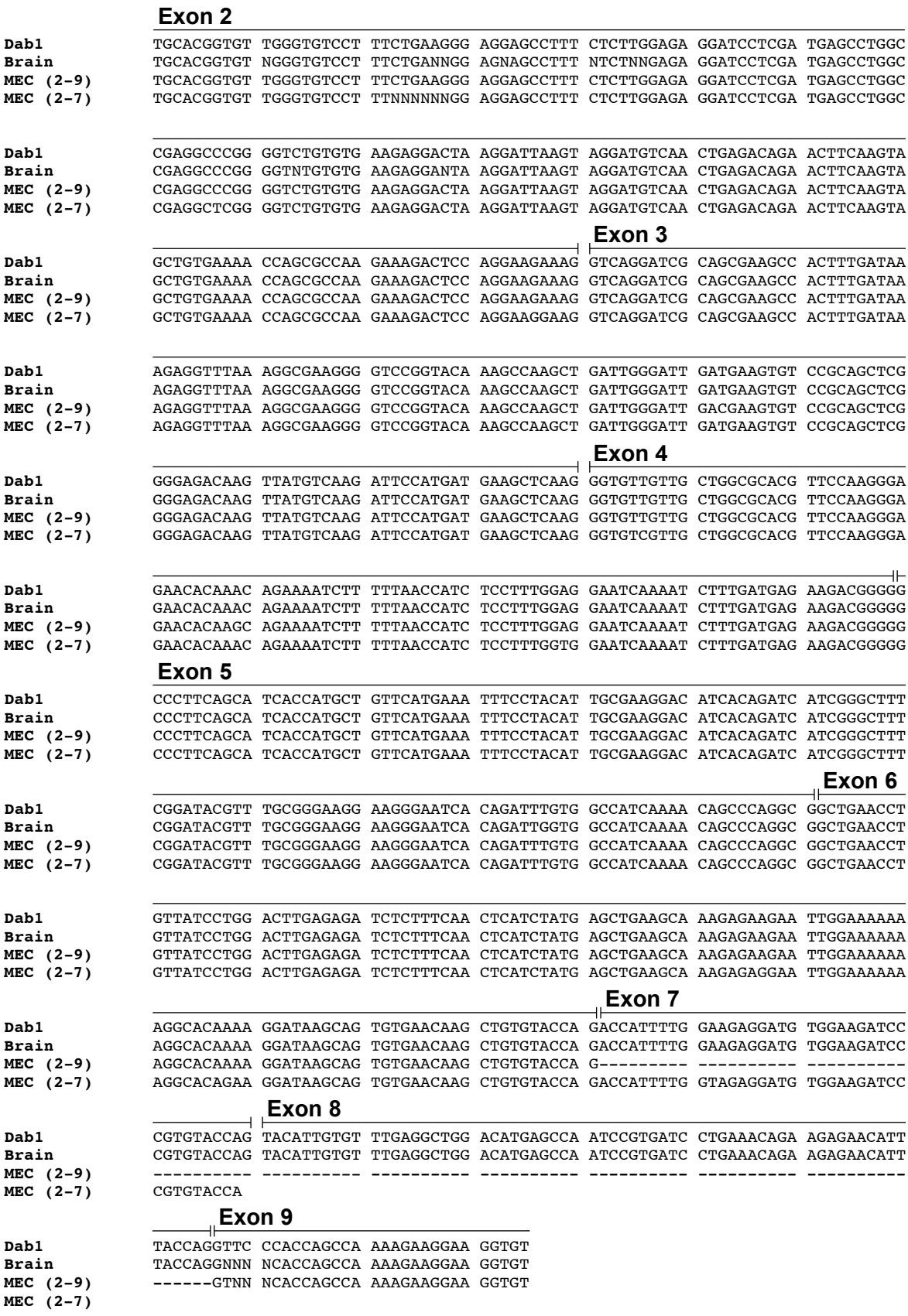
Exon 2
Dab1 TGCACGGTGT TGGGTGTCCT TTCTGAAGGG AGGAGCCTTT CTCTTGGAGA GGATCCTCGA TGAGCCTGGC
Brain TGCACGGTGT NGGGTGTCCT TTCTGANNGG AGNAGCCTTT NTCTNNGAGA GGATCCTCGA TGAGCCTGGC
MEC (2-9) TGCACGGTGT TGGGTGTCCT TTCTGAAGGG AGGAGCCTTT CTCTTGGAGA GGATCCTCGA TGAGCCTGGC
MEC (2-7) TGCACGGTGT TGGGTGTCCT TTNNNNNNGG AGGAGCCTTT CTCTTGGAGA GGATCCTCGA TGAGCCTGGC
Dab1 CGAGGCCCGG GGTCTGTGTG AAGAGGACTA AGGATTAAGT AGGATGTCAA CTGAGACAGA ACTTCAAGTA
Brain CGAGGCCCGG GGTNTGTGTG AAGAGGANTA AGGATTAAGT AGGATGTCAA CTGAGACAGA ACTTCAAGTA
MEC (2-9) CGAGGCCCGG GGTCTGTGTG AAGAGGACTA AGGATTAAGT AGGATGTCAA CTGAGACAGA ACTTCAAGTA
MEC (2-7) CGAGGCTCGG GGTCTGTGTG AAGAGGACTA AGGATTAAGT AGGATGTCAA CTGAGACAGA ACTTCAAGTA
Exon 3
Dab1 GCTGTGAAAA CCAGCGCCAA GAAAGACTCC AGGAAGAAAG GTCAGGATCG CAGCGAAGCC ACTTTGATAA
Brain GCTGTGAAAA CCAGCGCCAA GAAAGACTCC AGGAAGAAAG GTCAGGATCG CAGCGAAGCC ACTTTGATAA
MEC (2-9) GCTGTGAAAA CCAGCGCCAA GAAAGACTCC AGGAAGAAAG GTCAGGATCG CAGCGAAGCC ACTTTGATAA
MEC (2-7) GCTGTGAAAA CCAGCGCCAA GAAAGACTCC AGGAAGGAAG GTCAGGATCG CAGCGAAGCC ACTTTGATAA
Dab1 AGAGGTTTAA AGGCGAAGGG GTCCGGTACA AAGCCAAGCT GATTGGGATT GATGAAGTGT CCGCAGCTCG
Brain AGAGGTTTAA AGGCGAAGGG GTCCGGTACA AAGCCAAGCT GATTGGGATT GATGAAGTGT CCGCAGCTCG
MEC (2-9) AGAGGTTTAA AGGCGAAGGG GTCCGGTACA AAGCCAAGCT GATTGGGATT GACGAAGTGT CCGCAGCTCG
MEC (2-7) AGAGGTTTAA AGGCGAAGGG GTCCGGTACA AAGCCAAGCT GATTGGGATT GATGAAGTGT CCGCAGCTCG
Exon 4
Dab1 GGGAGACAAG TTATGTCAAG ATTCCATGAT GAAGCTCAAG GGTGTTGTTG CTGGCGCACG TTCCAAGGGA
Brain GGGAGACAAG TTATGTCAAG ATTCCATGAT GAAGCTCAAG GGTGTTGTTG CTGGCGCACG TTCCAAGGGA
MEC (2-9) GGGAGACAAG TTATGTCAAG ATTCCATGAT GAAGCTCAAG GGTGTTGTTG CTGGCGCACG TTCCAAGGGA
MEC (2-7) GGGAGACAAG TTATGTCAAG ATTCCATGAT GAAGCTCAAG GGTGTCGTTG CTGGCGCACG TTCCAAGGGA
Dab1 GAACACAAAC AGAAAATCTT TTTAACCATC TCCTTTGGAG GAATCAAAAT CTTTGATGAG AAGACGGGGG
Brain GAACACAAAC AGAAAATCTT TTTAACCATC TCCTTTGGAG GAATCAAAAT CTTTGATGAG AAGACGGGGG
MEC (2-9) GAACACAAGC AGAAAATCTT TTTAACCATC TCCTTTGGAG GAATCAAAAT CTTTGATGAG AAGACGGGGG
MEC (2-7) GAACACAAAC AGAAAATCTT TTTAACCATC TCCTTTGGTG GAATCAAAAT CTTTGATGAG AAGACGGGGG
Exon 5
Dab1 CCCTTCAGCA TCACCATGCT GTTCATGAAA TTTCCTACAT TGCGAAGGAC ATCACAGATC ATCGGGCTTT
Brain CCCTTCAGCA TCACCATGCT GTTCATGAAA TTTCCTACAT TGCGAAGGAC ATCACAGATC ATCGGGCTTT
MEC (2-9) CCCTTCAGCA TCACCATGCT GTTCATGAAA TTTCCTACAT TGCGAAGGAC ATCACAGATC ATCGGGCTTT
MEC (2-7) CCCTTCAGCA TCACCATGCT GTTCATGAAA TTTCCTACAT TGCGAAGGAC ATCACAGATC ATCGGGCTTT
Exon 6
Dab1 CGGATACGTT TGCGGGAAGG AAGGGAATCA CAGATTTGTG GCCATCAAAA CAGCCCAGGC GGCTGAACCT
Brain CGGATACGTT TGCGGGAAGG AAGGGAATCA CAGATTGGTG GCCATCAAAA CAGCCCAGGC GGCTGAACCT
MEC (2-9) CGGATACGTT TGCGGGAAGG AAGGGAATCA CAGATTTGTG GCCATCAAAA CAGCCCAGGC GGCTGAACCT
MEC (2-7) CGGATACGTT TGCGGGAAGG AAGGGAATCA CAGATTTGTG GCCATCAAAA CAGCCCAGGC GGCTGAACCT
Dab1 GTTATCCTGG ACTTGAGAGA TCTCTTTCAA CTCATCTATG AGCTGAAGCA AAGAGAAGAA TTGGAAAAAA
Brain GTTATCCTGG ACTTGAGAGA TCTCTTTCAA CTCATCTATG AGCTGAAGCA AAGAGAAGAA TTGGAAAAAA
MEC (2-9) GTTATCCTGG ACTTGAGAGA TCTCTTTCAA CTCATCTATG AGCTGAAGCA AAGAGAAGAA TTGGAAAAAA
MEC (2-7) GTTATCCTGG ACTTGAGAGA TCTCTTTCAA CTCATCTATG AGCTGAAGCA AAGAGAGGAA TTGGAAAAAA
Exon 7
Dab1 AGGCACAAAA GGATAAGCAG TGTGAACAAG CTGTGTACCA GACCATTTTG GAAGAGGATG TGGAAGATCC
Brain AGGCACAAAA GGATAAGCAG TGTGAACAAG CTGTGTACCA GACCATTTTG GAAGAGGATG TGGAAGATCC
MEC (2-9) AGGCACAAAA GGATAAGCAG TGTGAACAAG CTGTGTACCA G--------- ---------- ----------
MEC (2-7) AGGCACAGAA GGATAAGCAG TGTGAACAAG CTGTGTACCA GACCATTTTG GTAGAGGATG TGGAAGATCC
Exon 8
Dab1 CGTGTACCAG TACATTGTGT TTGAGGCTGG ACATGAGCCA ATCCGTGATC CTGAAACAGA AGAGAACATT
Brain CGTGTACCAG TACATTGTGT TTGAGGCTGG ACATGAGCCA ATCCGTGATC CTGAAACAGA AGAGAACATT
MEC (2-9) ---------- ---------- ---------- ---------- ---------- ---------- ----------
MEC (2-7) CGTGTACCA
Exon 9
Dab1 TACCAGGTTC CCACCAGCCA AAAGAAGGAA GGTGT
Brain TACCAGGNNN NCACCAGCCA AAAGAAGGAA GGTGT
MEC (2-9) ------GTNN NCACCAGCCA AAAGAAGGAA GGTGT
MEC (2-7)

Figure 3.2. Sequence alignment of RT-PCR amplification products.
Positions of exons 2-9 are indicated above the sequences. Dab1 – mRNA sequence of murine *Dab1* (accession number NM_177259.4). Brain – RT-PCR amplification product of Dab1 exons 2-9 from E13.5 brain RNA. MEC (2-9), MEC (2-7) – RT-PCR amplification products of Dab1 exons 2-9 and 2-7 from adult virgin MEC RNA.

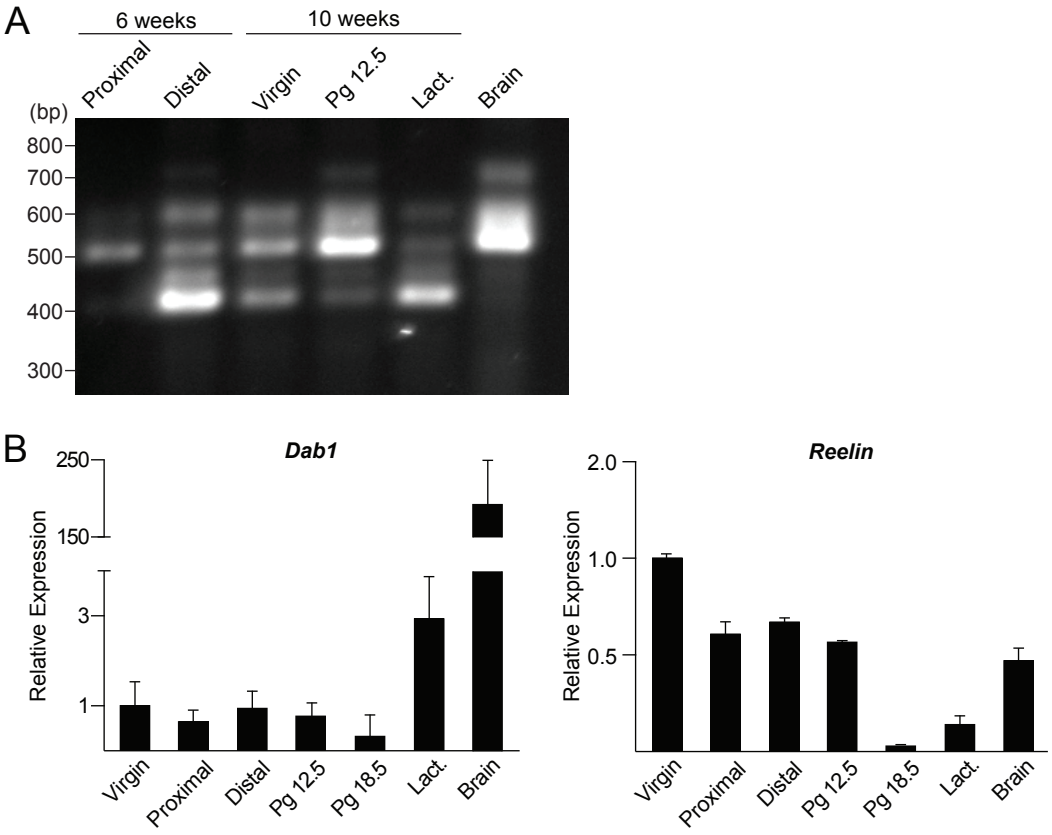

Figure 3.3. Alternative splicing of Dab1 during puberty, pregnancy, and lactation.
(A) RT-PCR analysis of alternatively spliced Dab1 variants using RNA from MECs and E13.5 brain. Proximal and distal – MECs isolated from proximal and distal portions of the mammary gland #4, 6 week-old mice. Virgin – MECs isolated from adult virgin mice. Pg 12.5 – MECs isolated from mammary glands at gestation day 12.5. Lact. – MECs isolated from lactating mammary glands. Adult virgin, pregnant, and lactating mice were 10 weeks old. Exon 5 forward and exon 11 reverse primers were used. (B) *Dab1* and *reelin* mRNA expression levels in MECs from 6 week-old mammary glands (Proximal, Distal), as well as MECs from adult virgin, gestation day 12.5 and 18.5, lactating mammary glands, and the E13.5 brain, analyzed by qPCR. Gene expression levels are relative to those in adult virgin MECs.

Exon 7	Exon 8	Exon 9b	Exon 9c	Predicted Size (bp)
-	-	-	-	403
+	-	-	-	442
-	-	+	+	502
+	+	-	-	508
+	+	+	+	607

Table 3.1. Possible Dab1 alternative splice variants present in MECs.
Presence or absence of alternatively spliced exons 7, 8, 9b, and 9c in each variant observed by RT-PCR analysis are indicated by "+" and "-", respectively. Our analysis precludes the distinction between the 502 bp and 508 bp variants, one or both of which may be present in MECs.

Dab1 amplification primers (5'-3')	
Exon 2 forward	TGCACGGTGTTGGGTGTCCTTTC
Exon 5 forward	CGGGCTTTCGGATACGTTTG
Exon 7 reverse	GGTACACGGGATCTTCCACATCCTC
Exon 8 reverse	CAGGATCACGGATTGGCTCATGTCC
Exon 9 reverse	ACACCTTCCTTCTTTTGGCTGGTGG
Exon 11 reverse	AGGGTACAGCAGCAGTGCCGAA

Table 3.2. Primers used for RT-PCR analysis.

References

Bar, I., Tissir, F., Lambert de Rouvroit, C., De Backer, O., Goffinet, A.M. (2003). The gene encoding disabled-1 (DAB1), the intracellular adaptor of the Reelin pathway, reveals unusual complexity in human and mouse. *J. Biol. Chem.* **278**:5802-5812.

Ewald, A.J. (2013). Isolation of mouse mammary organoids for long-term time-lapse imaging. *Cold Spring Harb. Protoc.* **2**:130-133.

Gao, Z., Poon, H.Y., Li, L., Li, X., Palmesino, E., Glubrecht, D.D., Colwill, K., Dutta, I., Kania, A., Pawson, T., et al. (2012). Splice-mediated motif switching regulates disabled-1 phosphorylation and SH2 domain interactions. *Mol. Cell Biol.* **32**:2794-2808

Hennighausen, L., Robinson, G.W. (2005). Information networks in the mammary gland. *Nat. Rev. Mol. Cell Biol.* **6**:715-725.

Herz, J., Chen, Y. (2006). Reelin, lipoprotein receptors and synaptic plasticity. *Nat. Rev. Neurosci.* **7**:850–859.

Howell, B.W., Lanier, L.M., Frank, R., Gertler, F.B., Cooper, J.A. (1999). The disabled 1 phosphotyrosine-binding domain binds to the internalization signals of transmembrane glycoproteins and to phospholipids. *Mol. Cell. Biol.* **19**:5179–5188.

Howell, B.W., Herrick, T.M., Hildebrand, J.D., Zhang, Y., Cooper, J.A. (2000). Dab1 tyrosine phosphorylation sites relay positional signals during mouse brain development. *Curr. Biol.* **10**:877–885.

Katyal, S., Godbout, R. (2004). Alternative splicing modulates Disabled-1 (Dab1) function in the developing chick retina. *EMBO J.* **23**:1878-1888.

Katyal, S., Glubrecht, D.D., Li, L., Gao, Z., Godbout, R. (2011). Disabled-1 alternative splicing in human fetal retina and neural tumors. *PLOS One* **6**:e28579.

Khialeeva, E., Lane, T.F., Carpenter, E.M. (2011). Disruption of reelin signaling alters mammary gland morphogenesis. *Development* **138**:767-776.

Morris, J.S., Stein, T., Pringle, M.A., Davies, C.R., Weber-Hall, S., Ferrier, R.K., Bell, A.K., Heath, V.J., Gusterson, B.A. (2006). Involvement of axonal guidance proteins and their signaling partners in the developing mouse mammary gland. *J. Cell. Physiol.* **206**:16-24.

Rice, D.S., Sheldon, M., D'Arcangelo, G., Nakajima, K., Goldowitz, D., Curran, T. (1998). Disabled-1 acts downstream of reelin in a signaling pathway that controls laminar organization in the mammalian brain. *Development* **125**:3719–3729

Rice, D.S., Curran, T. (2001). Role of the reelin signaling pathway in central nervous system development. *Annu. Rev. Neurosci.* **24**:1005–1039.

Sheldon, M., Rice, D.S., D'Arcangelo, G., Yoneshima, H., Nakajima, K., Mikoshiba, K., Howell, B.W., Cooper, J.A., Goldowitz, D., Curran, T. (1997). *Scrambler* and *yotari* disrupt the disabled gene and produce a *reeler*-like phenotype in mice. *Nature* **389**:730–733.

Yano, M., Hayakawa-Yano, Y., Mele, A., Darnell, R.B. (2010). Nova2 regulates neuronal migration through an RNA switch in disabled-1 signaling. *Neuron* **66**:848–858.

CONCLUSIONS

During organ development, a relatively small number of signaling pathways orchestrate a variety of functions that include cellular proliferation, differentiation, epithelial to mesenchymal transition (EMT), and migration. The studies completed in the last two decades identified the reelin signaling pathway as an important regulator of cellular migration in the central nervous system. However, more recent studies suggest a set of diverse functions for reelin in development of many other organs. We now know that the reelin signaling pathway is involved in migration, proliferation, and homeostasis of different cell types in multiple non-neuronal tissues. The energy expended by cells to produce and secrete the large reelin protein, and its ubiquitous expression in multiple organs implies strong likelihood of its functional relevance during developmental processes and in tissue homeostasis. Interestingly, alterations in reelin expression are observed in injury and pathologies of several tissues. One such example is seen in the liver, and since this organ has an ability to regenerate, it is likely that the pathways needed for development of the liver, including the reelin signaling pathway, are utilized for repair in order to return the tissues to their normal state.

Our results indicate that the reelin signaling pathway plays a prominent role in the development of the mammary gland. Reelin and its adaptor Dab1 are critical players in regulation of mammary gland morphogenesis and ductal elongation. One question that remains to be addressed is whether Reelin and Dab1 function via the canonical lipoprotein receptors ApoER2 ad VLDLR, or if alternative receptors for reelin are involved during mammary gland development. Studies of the mechanisms controlling neuronal migration identified integrins as additional receptors for reelin. Reelin can bind to α3β1 integrin via its N-terminal domain, leading to recruitment of Dab1 to the intracellular portion of β1 integrin (Schmid et al., 2005). Mice lacking β1 integrin fail to form a normal radial glial scaffold and display abnormalities in neuronal migration (Förster et al., 2002). Moreover, reelin controls terminal translocation of neurons and promotes neuronal adhesion to the extracellular matrix via activation of α5β1

integrin (Sekine et al., 2012). In the mammary gland, integrins regulate growth and differentiation of mammary epithelial cells and promote cell anchorage, survival and migration (Taddei et al., 2003). Given that reelin is expressed in the extracellular matrix of the mammary gland, and the absence of reelin leads to disorganized mammary epithelium and defects in ductal elongation, integrins may contribute to reelin signaling during mammary gland morphogenesis.

In addition, it is still not clear whether reelin signaling regulates proliferation and differentiation of mammary epithelial cells during pregnancy and lactation. Several alternatively spiced variants of Dab1 exist in the mammary gland, and the predominant Dab1 variants change in pregnant and lactating mice. However, we do not know whether these changes are functionally significant. The proliferation and differentiation of the alveolar cells during pregnancy and lactation is controlled by prolactin and placental lactogens (Hennighausen and Robinson, 2005). Alternative splicing of Dab1 may be modulated in response to changing hormone levels during pregnancy, providing a mechanism by which the mammary epithelial cells can fine-tune the response to the reelin signal.

Our studies showed that global deficiency in reelin is protective against tumor growth and metastatic progression of breast cancer. We found that reelin may regulate polarization of macrophages in the tumor microenvironment, and this effect of reelin seems to be independent of Dab1. It is likely that the impact of reelin on the tumor microenvironment via modulation of the innate immune cells is independent of the mechanisms by which reelin signaling regulates the development of the mammary gland. If this is the case, it will be interesting to examine whether reelin deficiency is protective against other solid cancers in which the innate immune cells of the host are employed for tumor cell survival, such as melanoma or lung cancer (Tham et al., 2014; Yuan et al., 2015).

The alteration in reelin expression levels in various cancers further strengthens the idea that the reelin signaling pathway is a broader regulator of development than assumed

previously. Similar to other developmental pathways, the reelin signaling mechanism may be used by cancer cells to promote their growth and migration, and to spread to distant organs. In fact, it is possible that the reelin pathway plays a dual role in cancer progression. Cancer cell growth may be promoted via activation of the PI3K/Akt signaling axis by reelin, while a decrease in reelin expression may be necessary to promote EMT and increase migratory properties of cancer cells and subsequent metastasis.

Although we now recognize the diversity of reelin, further studies are needed to address the exact mechanisms of reelin function, and to establish the non-canonical players in the reelin signaling cascade. In addition, it is still unclear how reelin functions in malignancies, and whether it could be used as a therapeutic target. The use of tissue-specific knockouts of the reelin signaling pathway components will be imperative to understanding the exact mechanisms by which reelin impacts tumor growth and metastasis.

References

Hennighausen, L., Robinson, G.W. (2005). Information networks in the mammary gland. *Nat. Rev. Mol. Cell. Biol.* **6**:715-725.

Schmid, R.S., Jo, R., Shelton, S., Kreidberg, J.A., Anton, E.S. (2005). Reelin, integrin and DAB1 interactions during embryonic cerebral cortical development. *Cereb. Cortex.* 15:1632-1636.

Sekine, K., Kawauchi, T., Kubo, K., Honda, T., Herz, J., Hattori, M., Kinashi, T., Nakajima, K. (2012). Reelin controls neuronal positioning by promoting cell-matrix adhesion via inside-out activation of integrin α5β1. *Neuron.* **76**:353-369.

Taddei, I., Faraldo, M.M., Teulière, J., Deugnier, M.A., Thiery, J.P., Glukhova, M.A. (2003). Integrins in mammary gland development and differentiation of mammary epithelium. *J. Mammary Gland Bio. Neoplasia.* **8**:383-394.

Tham, M., Tan, K.W., Keeble, J., Wang, X., Hubert, S., Barron, L., Tan, N.S., Kato, M., Prevost-Blondel, A., Angeli, V., et al. (2014). Melanoma-initiating cells exploit M2 macrophage TGFβ and arginase pathway for survival and proliferation. *Oncotarget.* **5**:12027-12042.

Yuan, A., Hsiao, Y.J., Chen, H.Y., Chen, H.W., Ho, C.C., Chen, Y.Y., Liu, Y.C., Hong, T.H., Yu, S.L., Chen, J.J., et al. (2015). Opposite Effects of M1 and M2 Macrophage Subtypes on Lung Cancer Progression. *Sci. Reports.* **5**:14273. doi:10.1038/srep14273.